

Faculdade de Engenharia da Universidade do Porto



Monitoring of Health by Means of Saliva Testing

Bárbara Marques

VERSION 1

Mestrado em Engenharia Biomédica

Supervisor: Professor José Machado da Silva

Co-supervisors: Professor Benedita Maia (FMDUP)
Professor António Rangel (UCP)
Professor Raquel Mesquita (UCP)

September 2018

A Dissertação intitulada

“Monitoring of Health by Means of Saliva Testing”

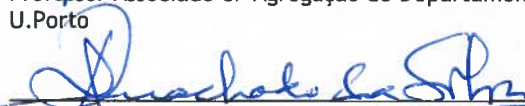
foi aprovada em provas realizadas em 24-09-2018

o júri

Presidente



Prof. Doutor João Manuel Ribeiro da Silva Tavares
Professor Associado c/ Agregação do Departamento de Engenharia Mecânica da FEUP -
U.Porto



Prof. Doutor José-Alberto Peixoto Machado da Silva
Professor Associado do Departamento de Engenharia Eletrotécnica e de Computadores - FEUP
- U. Porto



Prof.^a Doutora Filomena Maria Rocha Menezes Oliveira Soares
Professora Associada da Escola de Engenharia da U. Minho

O autor declara que a presente dissertação (ou relatório de projeto) é da sua exclusiva autoria e foi escrita sem qualquer apoio externo não explicitamente autorizado. Os resultados, ideias, parágrafos, ou outros extratos tomados de ou inspirados em trabalhos de outros autores, e demais referências bibliográficas usadas, são corretamente citados.



Autor - Bárbara Marques

Abstract

The presence of high urea levels in the human saliva has been reported has a possible biomarker for the detection of some diseases. Its hydrolysis process catalysed by urease enzyme in the oral cavity promotes the possibility of detecting its levels through the concentration of ammonium (NH_4^+), one of the products of this process. NH_4^+ can be converted in its volatile molecular form ammonia (NH_3), depending only on the sample pH value.

In this dissertation, a prototype of a NH_3 molecules sensor was developed that allows estimating the NH_4^+ concentration present in a sample of saliva, enabling the correlation of its value with saliva urea levels. This prototype is constituted by a multiwalled carbon nanotube (MWCNTs) based sensor film together with a flow-injection system, a gas diffusion unit (GDU) and an electronic impedance measurement circuit (IMC). Two type of MWCNTs-based sensor films were developed, a chemiresistive film and a capacitive film. It was observed that the chemiresistive sensor film is a better choice at this point of the project because the capacitive film's response does not present a clear relation with NH_4^+ concentration. Also, the chemiresistive film could detect NH_4^+ concentrations as low as 1 mg/l. It was also seen that a continuum flux of the sample allowed by the flow system used is a determinant condition for the prototype good performance.

The measurement of the relative variation of the sensor film's resistance and data recording are made with an impedance measurement circuit based on the AD5933 integrated circuit and an additional analogue circuit that allows enlarging its measurement range. The results achieved for the conceived prototype using synthetic saliva standard samples were encouraging for applying it in real human saliva samples.

Resumo

A presença de elevados níveis de ureia salivar tem sido reportada como um possível biomarcador para a deteção de algumas patologias. O processo de hidrólise deste composto feito pela enzima urease na cavidade oral promove a possibilidade de detetar os níveis de ureia salivar através da concentração de amónio (NH_4^+), um dos produtos desta reação. Dependendo do valor de pH da amostra, o NH_4^+ pode ser convertido na sua forma de molécula volátil amoníaco (NH_3).

Nesta dissertação, foi desenvolvido um protótipo de um sensor de moléculas de NH_3 que permite estimar a concentração de NH_4^+ existente em amostras de saliva, possibilitando a sua correlação com os níveis de ureia presentes. Este protótipo é constituído por um filme sensor baseado em nanotubos de carbono de parede múltipla (MWCNTs) em conjunto com um sistema de injeção de fluxo, uma unidade de difusão de gás (GDU) e um circuito de medição de impedância (IMC). Dois tipos de filmes sensores de MWCNTs foram desenvolvidos, um filme quimiorresistivo e um filme capacitivo. Nesta fase do projeto, foi observado que o filme quimiorresistivo apresenta uma melhor opção uma vez que não foi verificado uma clara relação entre a resposta do filme capacitivo e a concentração de NH_4^+ . Para além disso, a resolução de deteção do filme quimiorresistivo foi de 1 mg/l de NH_4^+ . Foi também demonstrado que o fluxo contínuo da amostra, permitido devido ao sistema de fluxo utilizado, é determinante para o bom funcionamento do protótipo.

A medição da variação relativa da resistência do filme sensor e a gravação dos dados é feita por um sistema eletrónico de medição de impedância baseado no circuito integrado AD5933 e num circuito analógico adicional que permite aumentar a sua gama de medição. Os resultados obtidos para o protótipo desenvolvido com amostras padrão de saliva sintética foram encorajadores para a sua aplicação em amostras de saliva real humana.

Acknowledgements

First of all, I would like to thank Professor José Machado da Silva, my supervisor, for the permanent availability demonstrated throughout the project. All the meetings with him and recommendations were crucial for the realization of this dissertation. Secondly, I would like to thank to Professor Benedita Maia, Professor António Rangel and Professor Raquel Mesquita for all the advices and help, and for making available the necessary conditions for the realization of this work. I would also want to leave here a very a special thanks to Mónica Afonso, Pedro Alves, Bruno Guedes and Tiago Mendes for their unconditional help. Last but not least, I would like to thank to my relatives and close friends for all the support and for never letting me give up.

Contents

1 Introduction.....	1
1.2 - Motivation and Main Objectives	3
1.3 - Structure of the Dissertation	3
2 Saliva Urea Levels as Pathology Biomarker	5
2.1 - Renal Insufficiency	5
2.1.1 - Chronic kidney disease	6
2.1.2 - Acute kidney injury	7
2.2 - Diabetes Type II	7
2.3 - Dental Caries	8
2.4 - Halitosis	9
2.5 - Stomach Cancer	9
2.6 - Conclusion	10
3 Ammonia Detection Methods	11
3.1 - Spectroscopy.....	12
3.1.1 - Flow-based methodologies	13
3.1.1.1 - Gas diffusion method	14
3.2 - Gas Chromatography	15
3.2.1 - Gas chromatography-mass spectrometry	16
3.3 - Electronic Nose.....	16
3.3.1 - Metal oxide semiconductor sensors	17
3.3.2 - Conductive polymer-based sensors	18
3.4 - Organic Field Effect Transistors	18
3.5 - Carbon Nanotubes as Ammonia Sensor Material.....	22
3.5.1 - Chemiresistive sensors	23
3.5.2 - Capacitive sensors	25
3.5.3 - Field effect transistors.....	26
3.6 - Conclusion.....	26

4 Development of the Sensor Prototype and Impedance Measurement Circuit	29
4.1 - General Prototype Operation	29
4.2 - Adaptations made in GDU	30
4.3 - Development of MWCNTs-based Sensor Films	32
4.3.1 - Chemiresistive sensor film	32
4.3.2 - Capacitive sensor film.....	34
4.4.1 - Impedance measurement with the AD5933	35
4.4.2 - Additional analogue circuit	36
4.5 - Final Apparatus and Experimental Procedure	42
4.5.1 - Reagents and Solutions	43
4.5.2 - Synthetic Saliva	43
5 Performance of the Sensor Prototype and Discussion	45
5.1 - Characterization of the Multiwalled Carbon Nanotubes-based Films.....	45
5.1.1 - Chemiresistive sensor film	45
5.1.1.1 - Measurement of the initial resistance.....	45
5.1.1.2 - Relative variation of resistance, response and recovery times	46
5.1.1.3 - Comparison with the Flow Analysis Spectrophotometric Technique	50
5.1.1.4 - Influence of the sensor film's length on the relative variation of its resistance	51
5.1.1.5 - Performance of the sensor film within a static flux	52
5.1.2 - Capacitive sensor film.....	53
5.1.2.1 - Initial capacitance measurement	53
5.1.2.2 - Relative variation of capacitance and recovery time	53
5.2 - Measurements with the Impedance Measurement Circuit.....	55
5.2.1 - Chemiresistive sensor film	55
5.2.2 - Capacitive sensor film.....	57
5.3 - Sensor Prototype Operation with Synthetic Saliva.....	58
5.4 - Conclusions	59
6 Conclusions and Future Work.....	63
6.1 - Conclusions	63
6.2 - Suggestions for Future Work	64
Appendix A	67
References	71

List of Figures

Figure 3.1 - Experimental setup developed in [22]. Ion pair-doped beads contained Cresol Red-quaternary ammonium ion paired sensible to dissolved CO ₂ , and Zinc tetra-phenylporphyrin (Zn(TPP)) doped beads are used to detect NH ₃	12
Figure 3.2 - System developed in [30]. PP1 and PP2 represent peristaltic pumps	14
Figure 3.3 - Block diagram of the GC system developed in [32]	15
Figure 3.4 - Basic block diagram of the electronic nose system (adapted from [36])	17
Figure 3.5 - Basic organic field-effect transistor structure	19
Figure 3.6 - Organic field-effect transistor structure developed in [41].....	20
Figure 3.7 - Operation principal of IL-gate GFET (ILGFET) proposed in [44]	21
Figure 3.8 - Scheme of an (a) individual SWCNT and (b) MWCNT (adapted from [49]).	22
Figure 3.9 - A one atom thick layer of graphite demonstrating the vector that defines the direction in which the sheet is rolled up (adapted from [51])	23
Figure 3.10 - The three factors responsible for the change in the conductivity of the CNTs: (a) CNT electrode junction, (b) charge transfer between the CNTs and the analyte and (c) intertubes junction	24
Figure 3.11 - Schematic of a chemiresistive CNTs-based sensor, functionalized with Pt and Pd particles, developed in [53].	25
Figure 3.12 - (a) Schematic of the capacitive sensor based on carbon nanotubes and titanium dioxide, and (b) equivalent circuit, developed in [55].	26
Figure 4.1 - Basic block diagram of the implemented system in the present work	30
Figure 4.2 - (a) Lateral view of the GDU developed in [30], in which the channels have 2mm of inner diameter and 1mm of depth. (b) Channels' top view	30
Figure 4.3 - Top view of the additional piece for the GDU with the correspondent dimensions	31
Figure 4.4 - Assemble of the GDU with the new adaptations made	31
Figure 4.5 - Top view of the configuration of the developed MWCNTs-based chemiresistive sensor film	32

Figure 4.6 - Format of sensor films developed with their respective dimensions.....	33
Figure 4.7 - Lateral view of the configuration of the developed MWCNTs-based capacitive sensor film	34
Figure 4.8 - The Real component (R) and imaginary component (X_c) of the vector impedance Z	35
Figure 4.9 - Functional block diagram of the AD5933	35
Figure 4.10 - Impedance as a function of frequency for a resistor of 100 Ω with a $R_{FB}=100 \Omega$	37
Figure 4.11 - Impedance as a function of frequency for an equivalent resistance of 101 Ω with a $R_{FB}=100 \Omega$	38
Figure 4.12 - Impedance as a function of frequency for a 30 k Ω resistor with different values of R_{FB}	38
Figure 4.13 - Impedance as a function of frequency for 100 k Ω resistor with a $R_{FB}=1k\Omega$	39
Figure 4.14 - Impedance as a function of frequency for 1 k Ω resistor with a $R_{FB}=10k\Omega$	40
Figure 4.15 - Impedance as a function of frequency for a RC series combination	40
Figure 4.16 - Impedance as a function of frequency for a RC parallel combination.....	41
Figure 4.17 - Final apparatus of the experimental set-up.....	42
Figure 5.1 - Relative variation of the 4L-film's resistance as a function of various NH_4^+ concentrations (1-5 mg/l) at room temperature	47
Figure 5.2 - Relative variation of the 4L-film's resistance as a function of various NH_4^+ concentrations (0.1-0.5 mg/l) at room temperature.	50
Figure 5.3 - Relative variation of the resistance of the three sensors of different lengths as a function of the mass of NH_4^+ diffused.....	51
Figure 5.4 - Measured response of the 4L-film to various NH_4^+ concentrations (1-5 mg/l) at room temperature, in a static flux	52
Figure 5.5 - Relative variation of the film's capacitance to various NH_4^+ concentrations (1-5 mg/l) at room temperature for a frequency of 1 kHz.....	54
Figure 5.6 - Comparison of 2L-film response using a digital multimeter and the developed IMC	56
Figure 5.7 - Carbon nanotubes deposited in the membrane (red circles) after the disassemble of the GDU	57
Figure 5.8 - Impedance as a function of frequency for a resistance of 560 k Ω with a $R_{FB}=33 k\Omega$	58
Figure 5.9 - Comparison of 2L-film response using deionized water and synthetic saliva samples, both with different NH_4^+ concentrations (1-5 mg/l).....	58
Figure A.1 - Additional analogue circuit connected to AD5933 (scheme design on Eagle)	69

List of Tables

Table 1.1 - Electrolyte concentration and total concentration of proteins in non-stimulated saliva and plasma (adapted from [3])	2
Table 2.1 - Pathologies related to levels of urea concentration in saliva	6
Table 3.1 - Summary of advantages and disadvantages of MOX and CP sensors, modified from [36]	17
Table 3.2 - Summary of advantages and disadvantages of various NH ₃ detection methods	27
Table 4.1 - Quantity of MWCNTs deposited in each film	33
Table 5.1 - Initial resistance values of the three chemiresistive sensor films	46
Table 5.2 - Linear fitting curves for the three measurements made with the 4L-film for an ammonium concentration range of 1-5 mg/l	48
Table 5.3 - Response time of the 4L-film for the ammonium concentration range of 1-5 mg/l	48
Table 5.4 - Recovery time of the 4L-film for the ammonium concentration range of 1-5 mg/l ..	49
Table 5.5 - Recovery time of the 2L-film and 1L-film sensors for the ammonium concentration range of 1-5 mg/l	52
Table 5.6 - Recovery time of the capacitive sensor film with ammonium concentration in the range of 1-5 mg/l	55

Abbreviations, Acronyms and Symbols

ADC	Analogue-to-Digital Converter
AKI	Acute Kidney Injury
BUN	Blood Urea Nitrogen
CCVD	Catalytic Chemical Vapour Deposition
CNTs	Carbon Nanotubes
CNTFETs	Field Effect Transistors based on Carbon Nanotubes
CKD	Chronic Kidney Disease
CP	Conductive Polymers
CVC	Current-to-Voltage Converter
DAC	Digital-to-Analogue Converter
DFT	Discrete Fourier Transform
DNTT	Dinaphtho[2,3-b:2',3'-f]Thieno[3,2-b]Thiophene
e-nose	Electronic Nose
FET	Field Effect Transistor
FIA	Flow-Injection Analysis
GC	Gas Chromatography
GC-MS	Gas Chromatography-Mass Spectrometry
GDU	Gas Diffusion Unit
GLDH	Glutamate Dehydrogenase
GFET	Graphene Field Effect Transistor
IC	Integrated Circuit
IL	Ionic Liquid
IL-GFET	Graphene Field Effect Transistor with an Ionic Liquid gate
ITO	Indium Tin Oxide
IUC	Impedance Under Test
MOX	Metal Oxide
MWCNTs	Multi-walled Carbon Nanotubes
NAD	Nicotinamide Adenine Dinucleotide
OFETs	Organic Field Effect Transistors
PANI	Polyaniline

PGA	Programmable Gain
PMMA	Poly(methyl methacrylate)
PPy	Polypyrrole
PS	Polystyrene
PT	Polythiophene
PVA	Poly(vinyl alcohol)
PVC	Poly(vinyl chloride)
PVP	Polyvinyl pyrrolidone
ROMP	Ring-Opening Metathesis Polymerized Materials
SFA	Segmented Flow Analysis
SIA	Sequential Injection Analysis
SWCNTs	Single-walled Carbon Nanotubes
s-sWCNTs	single-Single-walled Carbon Nanotubes
SUN	Saliva Urea Nitrogen
SPME	Solid Phase Microextraction
VSCs	Volatile Sulfuric Compounds
4L-film	MWCNTs- based chemiresistive sensor film with 40 mm of length
2L-film	MWCNTs- based chemiresistive sensor film with 20 mm of length
1L-film	MWCNTs- based chemiresistive sensor film with 10 mm of length
μ	Charge carrier mobility in an OFET
Ω	Ohms
ρ	Resistivity
A	Structure area
Au	Gold
C	Electrical capacitance
Ca^{2+}	Calcium ion
C_{CNT}	Initial film capacitance
Cl^-	Chloride ion
C_{NH_3}	Film capacitance in the presence of ammonia
CO_2	Carbon dioxide
Cr	Chromium
CuPc	Copper phthalocyanite
CVC_{ext}	CVC external to the AD5933 IC
eV	Electron volts
f	Frequency
H^+	Hydron
HCO_3^-	Bicarbonate ion
HNO_3	Nitric acid
H_2O	Water

H_3O^+	Hydronium
I_{DS}	Source-drain current of a FET
I_z	Imaginary part of the impedance measured with AD5933
K^+	Potassium ion
$k\Omega$	Kiloohms
L	Structure length
L_o	OFET's channel width
Mg^{2+}	Magnesium ion
mg/l	Milligrams per litre
mm	Millimetres
Na^+	Sodium ion
NaOH	Sodium hydroxide
$(NH_2)_2CO$	Urea
NH_3	Ammonia
NH_4^+	Ammonium ion
NH_4OH	Ammonium hydroxide
NO_2	Nitrogen dioxide
OH^-	Hydroxide ion
Pt	Platinum
Pd	Palladium
R	Electrical Resistance
R_{CNT}	Initial film resistance
R_{FB}	Feedback resistance used in the calibration of the electronic circuit
R_{NH_3}	Film resistance in the presence of ammonia
R_{out}	AD5933 output resistance
R_z	Real part of the impedance measured with AD5933
Si	Silicon
TiO_2	Titanium dioxide
V	Volts
V_C	Relative variation of the film's capacitance
V_{DS}	Source-drain voltage of a FET
V_G	Gate voltage of a FET
V_{pp}	Volts peak-to-peak
V_R	Relative variation of the film's resistance
V_T	Threshold voltage of a FET
V_{out}	Excitation voltage generated by AD5933
X_C	Reactance
W	OFET's channel length
$ Z $	Impedance magnitude
$Z(\omega)$	Unknown impedance

Z_{cal}	Known resistance used in the calibration of the electronic circuit
V_{CVCext_min}	Signal minimum amplitude value at the output of the CVCext
V_{CVCext_max}	Signal maximum amplitude value at the output of the CVCext

Chapter 1

Introduction

1.1 - Background

Health is considered a basic and essential right in the lives of populations, as well as a fundamental component in modern societies and a prime factor for a better quality of life. The diagnostics field is immediately associated to this idea since it assists health professionals in the identification of a pathology in a patient. In the literature, there are many parameters related to the diagnostics process, which are critical for its outcome, since an incorrect assessment of a disease can lead to a denial of an effective and timely therapy or even the administration of the wrong medicine [1,2]. Thus, it is understandable the high influence of diagnostics in the healthcare improvement and on the quality of life given to the patients.

Saliva is a body fluid formed essentially from three salivary glands (parotid, submandibular and sublingual glands) and small accessory glands, playing a key role in maintaining the oral homeostasis [3,4]. This fluid acts in the digestion of food, due to the presence of some enzymes in its composition, helps in the formation of food bolus and protects the oral mucosa against mechanical damage and pathogenic microorganisms. Although its composition is essentially water, saliva also contains inorganic compounds, of which some ions (Na^+ , K^+ , Cl^- and HCO_3^-) and proteins/polypeptides whose concentrations are shown in Table 1.1. In its constitution there are also non-protein organic compounds, like uric acid, which is one of the most important antioxidant components present in saliva, and hormones (e.g. steroids) [4].

Urea is an organic compound of chemical formula $(\text{NH}_2)_2\text{CO}$, whose concentration in plasma may be an indicative of certain pathologies. In a healthy subject, the concentration of this compound in plasma is around 2-7 mmol/l (Table 1.1), however this value can change in the presence of some diseases. Chronic kidney disease is associated with the accumulation of metabolism products in the blood that would be filtered by the kidney. The increased presence of these products, denominated uremic compounds, can change the normal functioning of the organism. Uremic compounds include, among others: creatinine, a substance measured to assess the toxic effects associated to renal insufficiency; uric acid, present in urine in small amounts; and urea [5,6]. In [7], urea is described as a small molecule that diffuses from the blood into the saliva through the salivary glands and is distributed homogeneously in the body

Table 1.1 – Electrolyte concentration and total concentration of proteins in non-stimulated saliva and plasma (adapted from [3]).

	Plasma	Non-stimulated Saliva
Na ⁺ (mmol/l)	145	5
K ⁺ (mmol/l)	4	22
Ca ²⁺ (mmol/l)	2.2	1-4
Cl ⁻ (mmol/l)	120	15
HCO ₃ ⁻ (mmol/l)	25	5
Phosphate (mmol/l)	1.2	6
Mg ²⁺ (mmol/l)	1.2	0.2
SCN ⁻ (mmol/l)	<0.2	2.5
NH ₃ (mmol/l)	0.05	6
(NH ₂) ₂ CO(mmol/l)	2-7	3.3
Proteins (g/l)	70	3

fluids. Taking this mechanism into account, some studies were made to investigate the possibility of salivary urea levels reflect the levels of urea in blood. In [8], saliva urea nitrogen (SUN) was evaluated as means for diagnosing renal diseases. In this study, it was found a positive correlation between blood urea nitrogen (BUN) and SUN through time, and it was concluded that the salivary urea levels reflect the levels of urea in blood. This result was also obtained in other investigation [7]. There are more pathologies that can be detected trough the levels of this compound in saliva which will be presented in the next chapter in more detail.

Once a strong correlation of the levels of urea present in the two fluids has been proved, the next step imposed is how to detect it. In previous studies, the saliva urea levels were determined through its hydrolysis [8]. This method consists in the utilization of two enzymes, urease and glutamate dehydrogenase, that hydrolyze urea into ammonium (NH₄⁺) and carbon dioxide (CO₂). In [9], a process was developed for detecting urea and ammonium ion based in an amperometric determination of NAD(P)H and in the use of the two enzymes previously mentioned. In this investigation, a linear relationship between the current and the analyte concentration was observed. Two platinum electrodes were developed, one for ammonium detection and the other for urea detection, both covered by a polymeric membrane where the enzymes were immobilized. However, it was mentioned that, comparing with carbon electrodes, the sensitivity of the platinum electrodes was lower. Subsequently, this procedure was also applied to several saliva samples, and comparing the obtained results with the spectrophotometric reference results, a good correlation was obtained. In other investigations, the urea hydrolysis principle was also applied with the main of accomplish a correlation between the saliva urea levels and the presence of caries in children [10].

1.2 - Motivation and Main Objectives

The use of blood for diagnostic purposes is an invasive process, which is often accompanied by stress and anguish of the patients [5]. Besides, specialized professionals are needed to collect the samples of this fluid, who may be exposed to non-negligible risks of contamination. In this sense, the availability of a diagnostics tool that can overcome these disadvantages, with minimal risk and with the capacity of providing accurate and reliable results would be important for both health professionals and patients.

Over time, saliva has seen an increased interest from the scientific community as a means for the diagnosis of some pathologies, since its analysis presents several advantages when compared to conventional blood tests. Saliva is a fluid whose collection does not need needles neither specialized people, which makes it a simple and safer method to obtain several samples. Additionally, it requires less manipulation in diagnostics procedures [11-13].

Besides the limitations already associated to blood tests, there are other pathologies whose detection requires the utilization of expensive equipment, complex processes and promote the discomfort of the patients (e.g. endoscopy). The main goal of this dissertation is to develop a device capable of detecting the presence of urea in human saliva in values that can be correlated with the presence of pathological conditions. Furthermore, the objective is to make it user friendly, portable and prone to be automated in order to allow the development of point-of-care units easy to implement in clinical environments and in places with minimal medical conditions (e.g. developing countries.).

As it was already mentioned, one of the products originated by the urea hydrolysis process is the ammonium ion (NH_4^+), which is present in the saliva due to the presence of bacterial originated urease enzyme. The pH is a factor that influences the acid-base balance of a solution, and, depending on its value, NH_4^+ can be present in its volatile molecular form, ammonia (NH_3). Assuming this principle, it is intended to develop a device sensible to NH_3 molecules to estimate the concentration of NH_4^+ in a sample of saliva. Therefore, knowing the concentration value of this compound will make it possible to correlate it with saliva urea values, becoming then easy and simple to promote the diagnosis of certain pathologies. The sensor prototype developed in the present work is constituted by a multiwalled carbon nanotubes (MWCNTs) based film, together with a flow-injection system, a gas diffusion unit (GDU) and an electronic impedance measurement circuit.

1.3 - Structure of the Dissertation

This dissertation is organized in six chapters, being the present one the first where the background and motivation for this project are presented together with the description of the main goals.

Chapter 2 reviews the main pathologies that can be detected by analysis of saliva urea levels. A brief explanation of each pathology is presented, and the need of alternative diagnostic procedures is reinforced. It is also detailed the reason why saliva urea levels can be related to the presence of each disease.

Chapter 3 presents the methods that can be employed to detect ammonia. It starts with the description of some conventional methods, and then more advanced approaches based on different ammonia sensor technologies are presented. Also, flow-based methodologies are described. In this chapter, the advantages and the disadvantages of each method are reviewed,

ending with the comparison among them and with the reasons behind the adoption of the method used in this project.

The operation principle of the developed sensor prototype is presented in Chapter 4. The development details of all components built for the conceived prototype are presented as well as the description of the solutions and reagents prepared for testing its operation.

Chapter 5 presents and discusses the results obtained from the experimental trials carried out with the developed prototype. It starts with the characterization of the developed sensor films and ends with the evaluation of the prototype performance using synthetic saliva standard samples.

Each one of the mentioned chapters ends with a conclusion which summarizes the main aspects to be retained in each one to allow a better reading and understanding of this dissertation. Nevertheless, the final conclusions are presented in Chapter 6. A vision of future research is also presented aiming at designing an optimized device.

Chapter 2

Saliva Urea Levels as Pathology Biomarker

Saliva urea levels appear to correlate with blood urea levels [5], suggesting that saliva urea levels can be a valuable biomarker of blood urea levels.

Many investigations were performed to evaluate the possibility of using salivary urea as a biomarker for some diseases, like renal insufficiency or even the incidence level of dental caries in the oral cavity [3,11,13]. This chapter describes the main pathologies that may be detectable after the evaluation of saliva urea levels. The concentration values of this molecular compound and their correlation with the specific pathological conditions are presented, considering the results published in papers that address this approach.

Table 2.1 lists several pathologies for which information was obtained in this domain. The case of stomach cancer is not included because it is not a cause, but a consequence associated with the presence of NH_3 levels, the product of a process which involves the bacterium *Helicobacter pylori*. Some examples of the obtained values for saliva urea concentration taken healthy subjects as control and as result of the pathological condition are presented.

2.1 - Renal Insufficiency

Renal insufficiency is a medical condition that evidences a deficiency in the renal filtration process of the metabolites present in the blood. There are two types of renal insufficiency: chronic kidney disease and acute kidney injury.

In advance stages of the disease, patients are exposed to renal replacement therapies, namely hemodialysis, peritoneal dialysis or renal transplantation. The diagnosis method of this pathology includes the analysis of uremic blood compounds. Considering the disadvantages of blood tests mentioned in the previous chapter, it becomes necessary to search for alternative or complementary methods [5].

Table 2.1 – Pathologies related with levels of urea concentration in saliva. These values are presented in the mean \pm standard deviation form, such as presented in the original publications, except for the first case that is in the form of the median value with interquartile range. All the values were converted into mg/l.

Pathologies	Salivary urea concentration used as control	Salivary urea concentration related to the pathology	Reference
Chronic Kidney Disease	205.0 (80.0) mg/l	920.0 (1390.0) mg/l	[5]
Acute Kidney Injury stage 1		282 \pm 245 mg/l	
Acute Kidney Injury stage 2		340 \pm 266 mg/l	
Acute Kidney Injury stage 3	111 \pm 48 mg/l	530 \pm 326 mg/l	[8]
Chronic Kidney Disease		375 \pm 284 mg/l	
Diabetes Type II	197 \pm 14 mg/l	290.5 \pm 38.1 mg/l	[14]
Dental Caries	439.64 \pm 62.09 mg/l	279.28 \pm 34.83 mg/l	[10]
Halitosis	26.0 \pm 18.4 mg/l	37 \pm 18.9 mg/l	[15]

2.1.1 - Chronic kidney disease

The number of patients with chronic kidney disease (CKD) is increasing. This pathology consists in the failure of the renal function over time, being associated with accumulation of metabolic products that are no longer filtered by the kidneys, named uremic toxins. Elevation of the blood levels of these compounds are biomarkers of CKD. The most common uremic toxins used as CKD biomarkers are creatinine and urea [5].

The composition of saliva in patients with CKD may be affected by the conditions of the disease, in a way that the changes in creatinine and urea levels, usually assessed in blood samples, may also be identified in saliva. The study presented in [5] was developed with the main of analyzing the urea and creatinine content in patients with CKD in an advanced stage. Samples of non-stimulated saliva were collected from participants with and without the disease. These samples were collected during the day (between 9h00 am and 4h00 pm), with the condition that the patients remained without eating for at least two hours prior to collection. In addition to the positive correlation obtained for the levels of urea both in blood and saliva, the investigators could also observe that patients with CKD had higher levels of salivary urea in comparison to the healthy ones (Table 2.1). These results are supported by the fact that an

increase of the concentration of this compound in blood creates a concentration gradient that facilitates the increase of urea diffusion from blood to the oral fluid.

It is important to highlight that in patients with CKD, a breath with a more ammoniacal smell (uremic factor) is noticeable. This is exactly caused by the reported excess of salivary urea which subsequently is transformed into ammonia [5].

2.1.2 - Acute kidney injury

Acute kidney injury (AKI) can be caused by a reduction of blood flow to the kidneys, a blockage of the urine flow or even a damage caused by infections. With proper medication, this condition may be reversible. However, if not timely diagnosed, it can cause high morbidity and mortality [8].

In the work published by Evans et al. [8], a clear correlation between saliva urea nitrogen (SUN) and blood urea nitrogen (BUN) was reported, motivating the development of a diagnostic method capable of detecting renal insufficiency, including AKI and CKD, by means of observation of the saliva urea levels. The simplicity of the procedure would make it prone to be used in developing countries to address the lack of resources and health professionals in these places. In this study, saliva samples were collected on day 0 for the measurements of SUN levels, on day 1 (after 24 hours), and then each 48h for SUN and BUN measurements, for a period of 7 days. The researchers considered that the results obtained at day 0 were the most important ones, and therefore were the only ones considered in this work. SUN collection was made using a plastic cup, with the imposed condition of the patients having not eaten at least 15 minutes prior to the collection of unstimulated saliva. They reported that the levels of SUN in patients with AKI were higher when compared with those of healthy subjects. It was also verified that the more advanced the disease stage the higher the SUN level (Table 2.1). In this study, higher values of SUN were also observed in patients with CKD when compared with those of healthy subjects. However, for lower levels of BUN, it was noticed that the efficacy of SUN as a diagnostic mean showed a lower level of accuracy. Nevertheless, salivary urea can still be considered as a good biomarker for diseases related to renal insufficiency, since, as previously mentioned, this type of pathologies is always associated to high concentrations of urea in bloodstream.

2.2 - Diabetes Type II

Diabetes *mellitus* is an endocrine disease associated to the insufficient production of insulin. It can be divided in two types: type I and type II.

Diabetes type II is the most common metabolic disease, which usually affects the population over the age of 40 years. It is a pathology in which a cellular dysfunction related to the insulin resistance of the peripheral tissues occurs, provoking disturbances in glucose metabolism that will affect the normal assimilation process [14,16].

Biochemical changes in patients' saliva with diabetes type II have been the subject of many investigations. In [16], Carda et al. developed a study with the goal of comparing the unstimulated saliva biochemical composition of patients with and without the disease. The increased levels of saliva urea concentration were one of the changes observed in patients with diabetes type II. This result was also reported in [14], where the levels of sodium, potassium, calcium, phosphorus and urea in patients with the disease were measured (Table 2.1).

This biochemical deficiency detected in the saliva of patients with diabetes type II can be related to changes previously observed in parotid glands. Data reported in the literature point to the fact that the permeability of acinar cells of the parotid gland is increased in patients with this disease. Consequently, this issue increases the ultrafiltration process of blood components to saliva, including urea. Thus, it is believed that this is the main reason for the high levels of salivary urea associated to this pathology, making this compound a good biomarker for its diagnosis [17].

2.3 - Dental Caries

One of the conditions that most affects oral health is the presence of dental caries, being “the most widespread noncommunicable disease” according to the World Health Organization [18]. A dental caries can be characterized as a chronic disease that particularly affects children, reaching values of 60-90% prevalence worldwide. If this pathology is not treated, it can have consequences related to chronic oral infection, dentition pain and even malnutrition [19].

Usually, the detection of this pathology occurs only in advanced stages of caries, with the manifestation of pain. In this sense, the early detection of caries or the detection of caries risk profile would be favorable, since procedures could be taken to prevent the pathology and avoid the discomfort and pain caused by it, as well reduce significantly associated cost.

Saliva plays an important role in oral health. Investigations on its biochemical components have been performed aiming at finding some correlation with caries incidence. The work presented in [10] had as purpose the determination of saliva urea values in adolescents with different indexes of dental caries. The saliva samples were collected in three distinct periods of the day: 5, 30 and 60 minutes after the daily meal, having as baseline values the samples collected in the morning, before the intake of any kind of food and implementation of oral hygiene. Focusing on the baseline values, since these are the most significant ones and reflect the same behaviour of salivary levels in the other three periods, it was verified that in adolescents with a lower cariogenic index, saliva urea values were higher when compared to those which have a higher incidence of pathology (Table 2.1).

One of the most significant properties of saliva in the incidence of dental caries is its buffer capacity. Urea plays an important role in this field, since it affects directly the neutralization of acids in the oral cavity, maintaining the acid-base balance of saliva, and consequently, the pH value in a certain level. In this way, it is clear the relationship between the saliva urea concentration and the incidence of caries.

In order to prevent and plan appropriate and preventive measures for the disease, saliva urea levels can be defined as a parameter for determining dental caries risk.

It is also important to highlight the low dental caries activities reported in patients with CKD. The incidence state of caries in children undergoing hemodialysis is investigated in [20]. It was observed that patients undergoing hemodialysis had both a lower incidence of dental caries and a higher concentration of salivary urea. High pH values, common in patients with CKD and consequently high values of urea, were reported as the possible cause of dental protection against the incidence of dental caries.

2.4 - Halitosis

Halitosis, or bad breath, affects 30% of the population. This condition can origin some social problems. It is caused by the microbial putrefaction that takes place in the oral cavity, resulting in the presence of volatile sulfuric compounds (VSCs) [21].

Normally, the methods used for halitosis diagnostic involve organoleptic tests, sulfide monitoring and gas chromatography, each of which presents some limitations [15]. This motivates the need for a method capable of combining simplicity and precision to detect this condition. The hypothesis that ammonia produced by oral bacterial microbiota reflects the level of halitosis has been a target in different researches. The results published in [21] suggest that the determination of ammonia produced from urea in the oral cavity can be useful to assess halitosis levels.

The study reported by Khozeimeh et al. [15] compares the concentrations of urea and uric acid in patients with and without halitosis. For that purpose, samples of unstimulated saliva were collected, after patients rinsed their mouths with water. From the obtained results, it could be observed that in patients with the disease, the saliva urea concentration levels were higher than those found in people without halitosis (Table 2.1), and that this compound is an important factor in the disease etiology. It was also concluded that the etiological perception of halitosis may be useful for the correct diagnosis of other adjacent diseases, such as chronic kidney disease, which is also associated with a higher concentration of salivary urea and a breath with an ammoniacal smell as already reported.

2.5 - Stomach Cancer

Stomach cancer is one of the most common causes of cancer death in the world. In Europe, the 5-year survival is below 5%. The main methods used in the detection of this type of cancer involve endoscopy with biopsy and histopathological evaluation, techniques that provide a high level of precision in its diagnosis. However, some of these methods present disadvantages, namely the fact of being invasive making them unsuitable for rapid detection, and the need for specialized professionals to perform them. In addition, in the case of endoscopy, individuals whose results are shown to be normal/mild are not adequately analyzed by professionals, who in this case fail to perform biopsies, making the disease impossible to detect [22,23].

Moreover, stomach cancer is a disease closely associated with the presence of bacteria *Helicobacter pylori* in the stomach walls. Therefore, early *H.pylori* infection detection will reduce the likelihood for the patient to develop cancer [22].

In the sense of neutralizing the acidic environment of the stomach, the *H.pylori* secretes urease enzyme which converts urea in carbon dioxide (CO₂) and ammonia (NH₃). One of the alternative methods purposed for the disease diagnosis is the detection of NH₃ in gastric juice as a potential biomarker of the bacterial presence. The use of an infrared spectroscopy detection process is advanced in [23], where the detection of NH₃ is made through its fingerprints absorption bands in the infrared spectrum. Nevertheless, in addition to the complexity of the method, considering the practicality factor required for the implementation of the process in clinical settings, the collection of gastric juice is not an easy or simple procedure.

NH₃ and CO₂ are both volatile compounds founded in expired air that are related to stomach cancer. These compounds exhaled from the oral cavity are also present in saliva, becoming potential biomarkers for the diagnosis of this type of cancer [22]. The NH₃ concentration in

gastric juice of healthy subjects is around 50 mg/l, while those affected by the disease have an NH_3 value that is around 200 mg/l. Since the concentrations of this molecule in expired air are only in the range of 0.002 mg/l-2 mg/l, this alternative becomes less reliable. In this way, saliva analysis has been proposed as an alternative method for the early detection of stomach cancer, since NH_3 saliva concentrations are only slightly lower than those relative to gastric juice, varying in a range of only 20 mg/l. Thus, the development of a method capable of detecting high levels of NH_3 in saliva may be a good alternative for the diagnosis of this pathology.

2.6 - Conclusion

Saliva analysis can be a good alternative to the means usually employed for the diagnosis of several pathologies, since saliva presents a significant change of its biochemical components in these situations. The salivary biomarker focused on this project is the concentration of urea, which normally presents higher levels in patients who develop one of the previously presented pathologies, except for the higher incidence of caries that is related to low levels of salivary urea.

It was demonstrated by Cardoso et al. [24] that the concentration of salivary urea was comparable in the morning and afternoon periods, suggesting that this compound does not have a significant change during the day and its concentration is independent of the saliva volume. However, although the correlation between the saliva urea levels and the presence of presented pathologies is obtained in many researches, it is observed a variation between the values in each study, as well as the values taken as control. This issue is also exposed in the literature [5]. The fact of not existing a standard method for the analysis and collection of saliva could be one of the reasons for the differences between the values.

In the various researches mentioned throughout the chapter, it is possible to notice that both sample collection times and established conditions vary, reason that may influence the levels obtained for urea in the oral fluid. It was reported in one of the studies that the time interval between meal and salivary sample collection, although not altering the correlation between urea levels and the occurrence of the disease, it may influence urea concentration values [5]. There are other limitations in the accuracy of salivary tests which may be related to salivary flow rate and composition in terms of the circadian rhythms of the salivary glands, the varying degrees of hydration of the patient and the potential interference of the oral microbiota with the degradation of urea, as well as age which also affects the levels of urea in saliva [10].

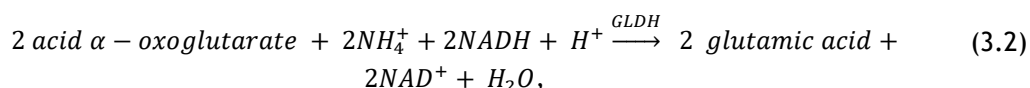
There is another issue associated to the type of saliva collected. In general, the reported investigations use unstimulated saliva, but there are other studies where stimulated saliva is used [20]. These two types of saliva present some differences in their constitution, beyond that the second type mentioned still differs in its characteristics (volume, viscosity, protein concentration, mucines concentration) depending on the nervous stimulus. This can influence salivary urea concentration which may vary according to the stimulation of salivary glands [3,8].

These variations of the oral fluid constitute the disadvantage of using saliva as a mean of diagnosis. Currently, salivary tests may not yet replace the conventional methods in all diagnostic applications. However, with the growing interest of the scientific community around this theme, it is believed that analysis of saliva may become a good alternative for the detection of diseases where early diagnosis is critical [25].

Chapter 3

Ammonia Detection Methods

The methods for salivary urea detection are usually based in its hydrolysis process, catalyzed by the urease enzyme which is present in the oral cavity. From this process, carbon dioxide (CO_2), ammonium ions (NH_4^+) and hydroxide ions are obtained (equation 3.1). Posteriorly, NH_4^+ reacts with acid α -oxoglutarate and NADH (reduced form of nicotinamide adenine dinucleotide (NAD)) due to the catalytic effect of glutamate dehydrogenase (GLDH) originating glutamic acid and NAD (equation 3.2). The presence of ammonium released from urea is proportional to the fall of absorption resulting from the oxidation of the reduced NAD [10,17].



The most widely used method for detecting salivary urea through the reactions (3.1) and (3.2) is spectrophotometry, which will be reviewed in this chapter. However, the ammonium released in the urea hydrolysis process can easily be converted into its ammonia volatile molecule form, depending only on the pH value of the sample, factor that influences the acid-base balance (equation 3.3). Thus, saliva urea concentration values can also be detected by methods capable of determining the concentrations of ammonia present. In this chapter, the various techniques used for detecting this gas, including more conventional procedures such as spectroscopy and gas chromatography, will be reviewed. Also, flow-based methodologies are used for ammonia detection and reported here.

The manufacture of NH_3 sensitive devices, as are the cases of the electronic nose and field effect transistors, will also be approached. One of the important factors in this type of systems is the material chosen for the sensor matrix. Carbon nanotubes have been capturing the attention of the scientific community in cases where their implementation in electronic systems promotes the detection of ammonia. For this reason, the many mechanisms of detecting this gas using these nanostructures will be reported in this chapter, too.

3.1 - Spectroscopy

The main optical method used for the detection of urea and NH_3 in saliva described in the literature is spectroscopy. Colorimetric methods can be associated to this technique, being referred to as spectrophotometry, which will also be described.

Spectroscopic analysis is based on the interaction between matter and electromagnetic radiation, being widely used as a method for gas detection. The light spectrum which crosses the air and reaches the detector is influenced by the gas composition. In the literature, the possibility of NH_3 being distinguished from a gas mixture through its absorption spectrum is reported [26].

In [22], it was developed a microfluidic optoelectronic platform with the goal of detecting NH_3 and CO_2 saliva concentrations, as a way of identifying possible situations of infection by *H.pylori* bacteria. The developed device is based on a microfluidic platform and a sensor system that included organic pH-sensitive dyes in the form of microspheres with the ability to detect CO_2 and NH_3 . This platform included also an optoelectronic part that consisted in a LED as light source. Light is transmitted through the sensor and guided by an optical fiber until a portable spectrometer which is responsible for recording the transmittance values in visible region (Figure 3.1). Afterwards, diluted saliva samples were used for the preparation of solutions with higher levels of NH_3 and CO_2 to understand if the developed system could be sensible to these compounds. Indeed, the achieved results were good in a way that the difference in the responses of collected saliva from healthy subjects and those with higher levels of NH_3 and CO_2 were notorious. In addition, the developed sensor showed sensitivity to different concentrations of the two gases at ppm level. Both factors were essential to potentiate their platform for the diagnostic of stomach cancer.

For the detection of this type of cancer, in another investigation, it was developed an infrared spectroscopy method with the goal of detecting NH_3 in gastric juice, which was based on the typical absorption bands of the infrared spectrum of this gas [23].

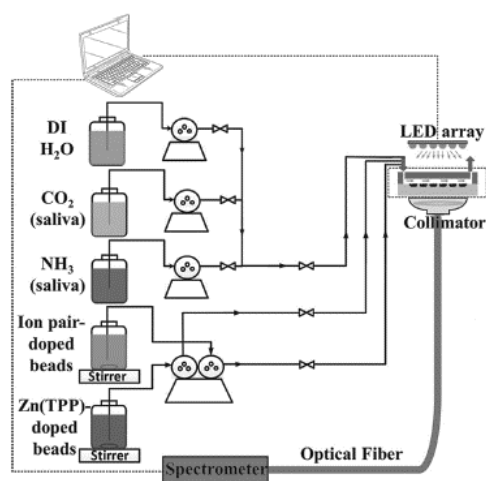


Figure 3.1 - Experimental setup developed in [22]. Ion pair-doped beads contained Cresol Red-quaternary ammonium ion paired sensible to dissolved CO_2 , and Zinc tetraphenylporphyrin (Zn(TPP)) doped beads are used to detect NH_3 .

Although the high sensitivity and selectivity that spectroscopy analysis presents for NH_3 detection, there are some disadvantages associated to this method. The sensitivity of the absorption spectroscopy is determined, in part, by the quantity of gas between the light source and the detector. A correct analysis depends on the measuring system which normally has large dimensions, making its miniaturization a difficult process. For this purpose, the lower detection limit does not support very small concentrations, making it unviable for applications such as breathing analyzers. Moreover, the necessary equipment is expensive, a problem that has been tried to be overcome with the use of laser diodes. However, this solution resulted in a decrease of the sensitivity [26,27].

Spectroscopic analysis is usually combined with colorimetric methods where a specific reaction causes the coloring of an analyte. This combination is usually referred as spectrophotometric analysis.

The best-known example of a colorimetric method is the pH paper which colors a solution according to its pH value [27]. In a study comparing saliva urea levels between patients with some type of renal impairment and healthy individuals, the detection of this compound was performed using a pH-indicating substance. This substance changes the color of a test pad due to the presence of OH^- ions resulting from urea hydrolysis. The determination of urea concentration is made by finding the best approximation of this color to those of six standard test pads [8].

Another colorimetric reaction used in the literature for the quantification of the saliva urea levels involves the utilization of the diacetyl monoxime reagent. This reagent produces labile diacetyl in the presence of hydrolyzed acid, colouring the solution into yellow. In the research made by Shirzaiy et al. [14], this reagent was used to estimate the concentration of urea in patients with diabetes type II, together with the atomic absorbance spectrophotometry technique. This reagent was as well used in another investigation to determine the concentration of salivary urea in patients with halitosis [15].

Although this technique has a high sensitivity, to perform a spectrophotometric analysis it is necessary to use equipment capable of measuring and comparing the amount of light absorbed, transmitted or reflected by a given sample. A spectrophotometer is used in many investigations to determine the levels of salivary urea [15,20]. Nevertheless, this type of equipment is generally expensive making it difficult to implement in underdeveloped countries, where generally the need for simpler procedures is greater because of the lack of conditions. Besides that, colorimetric reactions which are associated to this technique also require the consumption of reagents and are dependent on the speed of their reaction with the analyte, influencing the cost and speed of the process of salivary urea detection.

3.1.1 - Flow-based methodologies

Flow-based methodologies can be associated to spectrophotometric analysis. It was reported that these methodologies are usually used to detect low concentrations of ammonia in estuarine and marine waters [28]. The most commonly used flow systems include flow-injection analysis (FIA) and sequential injection analysis (SIA). Another approach is the segmented flow analysis (SFA) but this technique is already considered as an outdated technique [29].

SFA is characterized by a “continuous, flowing stream segmented by air bubbles” with problems related to the expensive cost and air-bubble segmentation which involve slower start-up times and higher reagent use [28,29].

FIA is described in [28] as a “non-segmented stream, where the sample is inserted in a carrier/reagent stream through an injection valve, in a reproducible fashion and with controlled dispersion”. Compared to SFA, this is a more attractive technique since its operation is simpler and the cost is lower. The portability is also possible when using this methodology. However, there are some issues related to it, namely when using peristaltic pumps. The tubes used with these pumps imply the recalibration of the system every time they are changed due to tube squashing. They are also vulnerable to aggressive reagents which can damage the tubes [28,29].

In SIA, the sample and reagent plugs are sequentially aspirated through a selection valve toward a holding coil. Then, the plugs are directed to the detector by flow reversal. The main advantages associated to sequential injection analysis are the versatility, the reagent saving, easy automatization due to the possibility of computer control and robustness. The main disadvantage of this technique is the analysis frequency. SIA aspirates sample and reagents one after the other which introduces a considerable decrease of sampling rate when compared to FIA and a more difficult mixture of the sample and reagents [28,29].

Usually, there are analytical methods that are employed together with these flow-based methodologies. One of these methods involves the gas-diffusion method that has been reported for the determination of ammonia [28,30], and so it will be described next.

3.1.1.1 - Gas diffusion method

One of the processes also used to cause gas separation is the application of a gas diffusion unit (GDU). In the literature, this method is associated to the spectrophotometric technique, and it was reported in the separation of chloride and ammonia [31].

GDU is usually employed in flow systems, where it improves the selectivity by separating the analyte from the interferences. In [30], it was developed a sequential injection system which include a GDU to determine ammonium concentrations in coastal and transition waters (Figure 3.2). The system involves the conversion of the NH_4^+ into NH_3 through the addition of sodium hydroxide (NaOH) in the samples at the GDU donor channel. Subsequently, the NH_3 diffuses through a hydrophobic membrane into its acceptor channel. In this channel, a blue bromothymol solution (acid-base indicator) is injected, which change its color in the presence of the gas. This system encompasses spectrophotometry as a detection method to measure the change in indicator's absorbance and consequently determine the concentration of NH_4^+ . In this study, the lower detection limit obtained was 0.027 mg/l.

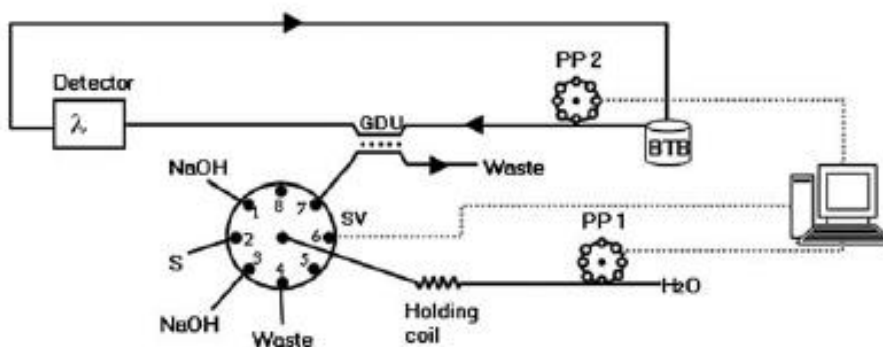


Figure 3.2 - System developed in [30]. PP1 and PP2 represent peristaltic pumps.

Since spectrophotometric analysis is used in this method, its already mentioned disadvantages are also associated to it. However, in the study mentioned above, it was accomplished a null consumption of the colorimetric reagent per determination due to its recirculation incorporated in the system.

The disadvantage of using a GDU can be related to interferences which may impair the correct operation of the system. In the reported study, since the detection of NH_3 includes the NaOH addition into the samples, the formation of insoluble calcium (Ca^{2+}) and magnesium (Mg^{2+}) hydroxides may occur. These interferences can block the flow channels, and even the GDU membrane pores, compromising the accuracy, sensitivity and transfer rate. However, the formation of these precipitates can be reduced by the addition of a chelating agent (e.g. citrate) to the NaOH stream. Although in small amounts, saliva also contains Ca^{2+} and Mg^{2+} , and thus, if this method is used in the detection of salivary urea or NH_3 , it may be necessary to consider this fact [4].

3.2 - Gas Chromatography

Gas chromatography (GC) is an important tool in the detection of gaseous compounds. It is a technique widely used in areas such as environmental analysis and for diagnostic purposes through analysis of expired air [32].

A conventional GC system comprises five principal components: i) the carrier gas, also known as mobile phase, is a highly pure gas (e.g. hydrogen or helium) which transports the gas sample through the column; ii) sample injector that introduces a finite and precise volume of sample in the carrier gas which continuously flow through the column; iii) the column that is coated with the stationary phase which interacts chemically with the injected gas sample, and where physical separation of the sample individual constituents takes place; iv) the detector, localized at the column exit; and v) the data processing system [32].

Kolesar et al. [32] developed a miniaturized gas chromatography system with a structure based on the components described above (Figure 3.3) for detecting nitrogen dioxide (NO_2) and ammonia (NH_3). Helium gas was used as gas carrier and the sample injection system involved the incorporation of a commercial injection valve. The column was considered the most critical component of the system and it was configured as two interconnected spirals. The detector was constituted by a primary detector which consisted in a chemical resistance based on copper phthalocyanite (CuPc) that is sensible to the gas of interest, and by a secondary detector constituted by a thermal conductivity detector. Regarding the system response in the presence of NH_3 , they found that it only operated correctly at concentrations greater than 3 mg/l and that the maximum duration of each measuring cycle was 85 minutes.

Despite the good sensitivity associated with this technique, GC-based systems are usually quite bulky and fragile, making them unsuitable for operating in non-laboratory environments. The cost and time required to carry out the process are also disadvantages of this method [32].

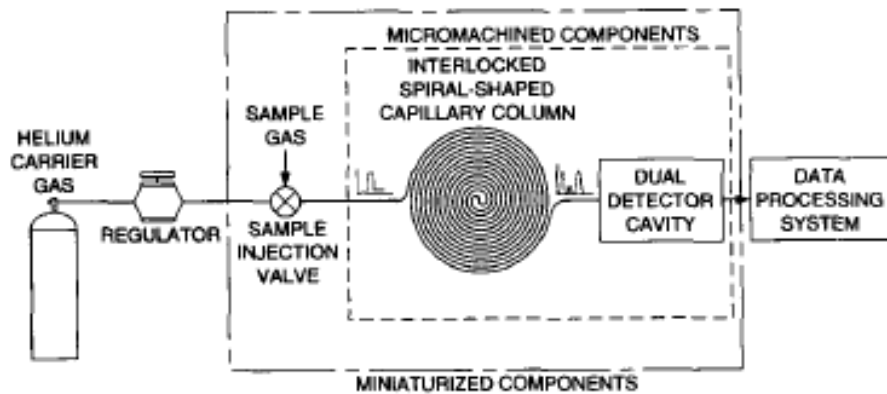


Figure 3.3 - Block diagram of the GC system developed in [32].

3.2.1 - Gas chromatography-mass spectrometry

There are other techniques that can be used together with gas chromatography for the detection of volatile samples. Compound detection based on gas chromatography-mass spectrometry (GC-MS) is done according to the mass/charge of atoms or ionized molecules ratio to analyze the desired compounds [33]. In [34], it was developed a method for the quantification of NH_3 levels in explosive compounds, based on GC-MS technique. In that investigation, they used a derivatized solid phase microextraction fiber (SPME). This type of fiber is derived from alkylchloro-reformate which directly converts the samples of gaseous or dissolved NH_3 in solution into a high molecular weight product, increasing gas separation and detectability. However, the system showed a high sensitivity to moisture, which introduced oscillations in the system response when exposed to ammonia.

This type of technique requires very complex and time-consuming sample preparation methods. The high cost and the need of expert knowledge for the data interpretation are some of the factors that make GC-MS a limited method for applications in the clinical diagnosis field [33].

3.3 - Electronic Nose

The electronic nose (e-nose) is a device capable of measuring and characterizing volatile aromas from many sources for multiple applications. This type of system aims to mimic the olfactory system of mammals and it is used in several scenarios in diagnostic field (e.g. in the analysis of expired air) [35].

Systems based on electronic nose are constituted by three fundamental parts, including the sensor matrix, the signal transducer and a pattern recognition mechanism (Figure 3.4). The sensors selected to form the sensor matrix are responsible for detecting the odor. Posteriorly, the chemical signal is transformed by the transducer in a detectable electrical signal. The pattern recognition mechanism uses principal component analysis algorithms or artificial neural-network.

When compared with the traditional gas analysis methods, as GC-MS and infrared spectroscopy, the e-nose has a simpler structure gathering the advantage of having a smaller size and a lower cost. Moreover, it is much faster and adequate for non-expert users becoming suitable

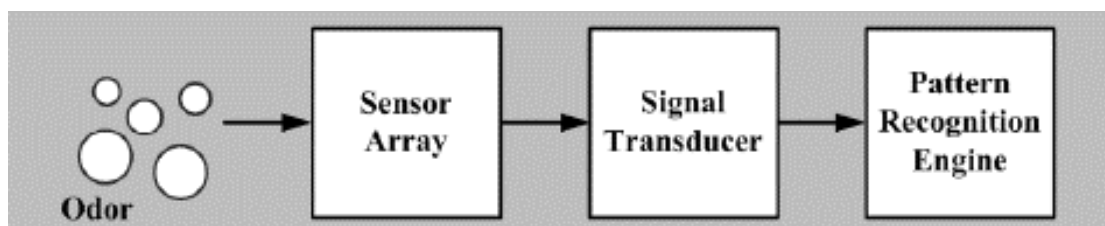


Figure 3.4 - Basic block diagram of the electronic nose system (adapted from [36]).

for daily applications. However, commercial e-noses do not have these characteristics. Indeed, the devices that exist in the market have a very large size and can only be used in a laboratory environment [36].

There are many types of e-nose sensors available in the market, including conductive sensors (metal oxide semiconductors (MOX) and conductive polymers (CP)), piezoelectric sensors, field effect transistor sensors, optical sensors and spectroscopy-based sensors. Due to the problems associated to this technology already reported, a hypothesis of developing a e-nose capable of overcome these disadvantages has been investigated by using integrated circuit technology to reduce size and energy consumption. In this field, the more used sensors are the conductive sensors due to their electric properties and simple interface circuit [35].

Table 3.1 shows the main advantages and disadvantages presented by the MOX and CP sensors, with respect to their behavioural characteristics in electrical and thermal terms which will be explored next.

Table 3.1 – Summary of advantages and disadvantages of MOX and CP sensors (modified from [36])

Sensor Type	Advantages	Disadvantages
Metal-Oxide Semiconductor (MOX)	Very high sensitivity	High temperature operation
	Rapid response and recovery time	High power consumption
Conductive Polymer (CP)	Ambient temperature operation	Sensitive to humidity and temperature
	Sensitive to many gases	Sensors can overload by certain analytes
	Short response time	Limited lifetime
	Low cost	

3.3.1 - Metal oxide semiconductor sensors

Metal oxide semiconductor (MOX) sensors are usually constituted by three layers, including a silicon semiconductor, a silicon oxide insulator and a catalytic metal [35]. The interaction between the gas and the metal causes changes in its characteristics. In [37], it was developed

a prototype capable of being integrated in a e-nose system, with the goal of detecting NH_3 in expired air for clinical diagnostic applications. In this prototype, a MOX sensor of tin dioxide was used. The sensor operating principle is based on the decrease of its resistance due to the interaction of the NH_3 with tin dioxide, resulting in a change on the device conductivity.

This type of sensors has a high sensitivity and a rapid response time regarding the gas detection, however they only work properly with high temperatures. This feature demands the use of heating machines and a high energy consumption (Table 3.1).

MOX sensors can be integrated in a unique microchip sensor for e-nosed based systems, and the size and consumption energy conditions can be improved. Nevertheless, the energy consumption is still a limitative factor. However, although a large number of MOX sensors are required in the e-nose systems, they remain the most favorable choice for this type of integrated and miniature systems [36].

3.3.2 - Conductive polymer-based sensors

Conductive polymer-based sensors (CP) usually consist of a substrate (e.g. silicon), two interdigitated electrodes and an organic polymer as sensor material. The most used polymers are polyaniline (PANI), polypyrrole (PPy) and polythiophene (PT) [35].

This type of sensors is also frequently used in gas detection (e.g. NH_3). Their performance is based on the interaction of the gas with the polymer. This mechanism can reflect changes in the polymer conductivity due to the electrons transferred for or from the analyte. Seesaard et al. [38] manufactured an amine sensor embroidered on a substrate based on polymers/carbon nanotubes and applied it as an e-nose system. In this work, four types of polymers were used, including polyvinyl chloride (PVC), cumene terminated polystyrene-co-maleic anhydride (cumene-PSMA), poly (styrenecomaleic acid) partial isobutyl/methyl mixed ester (PSE) and polyvinylpyrrolidone (PVP). The sensors were tested for four types of gas, one of them the ammonium hydroxide (NH_4OH) with concentrations of 50, 200, 500 and 1000 mg/l. It was found that the different polymers exhibited notable variations in their resistance values in a way that the percentage of the change in their resistance increased as the gas concentration increased. It was also verified that the most sensible polymer to NH_4OH was the PSE.

Indeed, this type of polymeric materials presents a good performance at room temperature and a high energy consumption is not required. In addition, they are easily manufactured and can display different sensitivity and selectivity. The major disadvantage of CP-based sensors is their sensitivity to humidity, which can jeopardize their proper operation (Table 3.1).

3.4 - Organic Field Effect Transistors

Field effect transistors have as basic principle the modulation of electric current intensity that flows between source and drain electrodes through an electric field applied to a third electrode called gate [39].

There are several types of field effect transistors, however organic field effect transistors (OFETs) are the most promising as gas sensing elements in areas such as health monitoring. They are low cost and portable devices that can detect multiple analytes through an organic semiconductor. They also have fast response times and can be integrated into complex circuits with embedded signal processing, e.g. electron-nose [40,41].

Usually, OFETs have the structure shown in Figure 3.5. This type of devices operates in an accumulation regime. This means that when a voltage is applied between the gate (V_G) and source, the electric field induces majority carriers in the organic semiconductor (more precisely in the semiconductor/dielectric interface) forming a conduction channel. The voltage applied between the source and drain (V_{DS}) is responsible for draining these charge carriers from the conducting channel.

OFETs have gained considerable visibility as ammonia sensing elements. In the investigation lead by Werkmeister et al. [42], they explored the use of OFETs for urea detection. The operation principle of the developed device is based on urea hydrolysis process. They manage to detect concentrations of NH_3 in the range of 45.01-450.45 mg/l. The detection process involves a functionalized parylene-C membrane with urease enzyme used as a semipermeable upper gate dielectric, where the NH_3 diffusion to the organic semiconductor layer (dinaphtho[2,3-b:2',3'-f]thieno[3,2-b]thiophene (DNTT)) occurred. The charge carrier concentration in the transistor channel is manipulated by capacitive coupling, resulting in a current change through the device. In this study, it was verified a quick current decrease with increasing NH_3 concentrations.

There are two operation states for OFETs: linear state and saturation state. The linear region occurs when $V_{DS} < (V_G - V_T)$, being V_T the threshold voltage (minimum voltage that must be applied so that there will be accumulation of charge carriers in the channel). Saturation region occurs when $V_{DS} > V_G - V_T$, with no more drainage of charge carriers than those being injected. The current between the source and drain I_{DS} , in this second case is given by equation (3.4), and usually it is the one being measured [42]. W and L_0 correspond to the channel width and length, respectively, while C represents the capacitance of the dielectric and μ the mobility of the majority carriers in the conductor channel formed in the semiconductor.

$$I_{DS} = \frac{W}{2L_0} \times C \times \mu \times (V_G - V_T)^2. \quad (3.4)$$

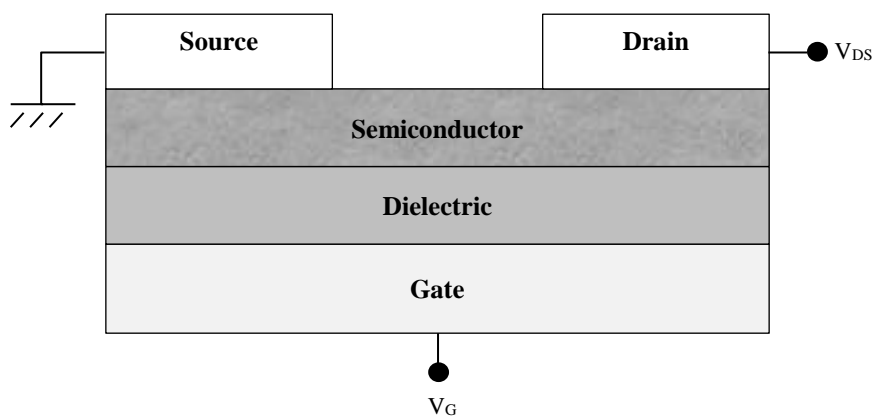


Figure 3.5 - Basic organic field-effect transistor structure. V_{DS} is the voltage applied between the drain and source electrodes, and V_G is meant as the voltage applied at the gate electrode.

According to [42], these parameters could change depending on the analyte concerned. V_T may change due to changes in electrostatic field (e.g. different pH values or charged molecules absorption); capacity C may also change thanks to the analyte binding. The alterations of μ can occur, for example, due to the interface morphologic effects. This way, for characterizing an OFET is necessary to consider its characteristic curves, the mobility of the charge carriers, the ON/OFF ratio (ratio between the two output signals, one with the device ON and the other in the OFF state), and the threshold voltage.

In [41], it was developed a NH_3 sensor based in an OFET, with a semiconductor layer of pentacene and polymethyl methacrylate (PMMA) as dielectric. The device characterization was done through the study of changes in threshold voltage, saturation current and charge carriers' mobility according to different concentrations of NH_3 . The structure of the developed OFET is presented in Figure 3.6. The researchers detected that the device exhibited a behaviour characteristic of p-type transistors. They observed a decrease of I_{DS} current with the increase of NH_3 concentration, which was confirmed by the results obtained for the device's current in the OFF state. In relation to the threshold voltage, they verified that it decreases (becoming more negative) when the NH_3 concentration increased. They attributed this phenomenon to the interaction of the gas molecules (dipole molecules) adsorbed in the pentacene film, since these act as "traps" for the charge carriers which moving at the interface between the organic film and the dielectric. In this study, it was also identified that the charge carriers' mobility decreased with increasing concentration of the analyte, causing a decrease in the transistor's conductivity. However, pentacene-based OFETs present a disadvantage characterized by their sensitivity to water vapor that can drastically decrease the good performance of the device, undermining their sensing characteristics.

Another disadvantage which may also affect the use of OFETs as a gas sensor mechanism is related to the high voltage required for their stable operation [43]. To overcome this problem, in [44], Inaba et al. developed a low-voltage graphene field-effect transistor (GFET) electrochemically gated by an ionic liquid (IL). IL consisted in organic salts molten at room temperature. In the proposed sensor, the IL and the graphene act as a mean for gas adsorption and sensor material, respectively. The truth is that, due to the double layer formed at the graphene/IL interface, the developed IL-GFET (ILGFET) could be activated by a voltage approximately 100 times lower. When ILGFETs are used as gas sensors, the gas molecules can diffuse through the IL to reach the graphene/IL interface, modifying the electrical properties of the device (Figure 3.7). In this research, they used ammonia concentrations in the range of 9-2400 mg/l, applying a constant V_{DS} of 10 mV and a variable V_G . Under these conditions, they observed a decrease in the I_{DS} current as the NH_3 concentration increased.

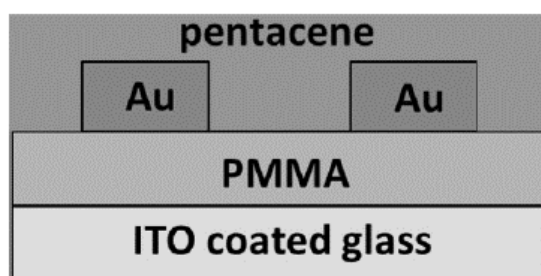


Figure 3.6 - Organic field-effect transistor structure developed in [41]. They used indium tin oxide (ITO) as substrate as well as gate electrode. PMMA was spin coated on the ITO, and subsequently gold (Au) source and drain electrodes were thermally evaporated on the dielectric.

In OFETs, it is usually the interaction of the analyte with the organic semiconductor layer that causes the change of the electrical properties of the device. However, in [40], it was approached the idea of a sensitive gate dielectric to NH_3 concentrations. The researchers presented a new concept of OFET which was based on the application of an organic ion-conducting dielectric material chemically adapted for changing its electronic properties after the contact with the analyte. This interaction will generate an electrically detectable response. The dielectric also strongly affects the operation of the device in a FET. The application of this ion-conducting component can be a solution for solving problems related to the high operating voltages needed for OFETs operation by generating large charge carrier densities in the channel's device through ions moving to the interface or even into the semiconductor. Furthermore, a further advantage of having an active-sensitive gate dielectric involves the annulation of the oxygen and/or humidity effect on the organic semiconductor, which is often detrimental to the OFET's performance. In the mentioned research, this annulation was achieved by using a structure in which the dielectric is deposited over the organic semiconductor layer. The dielectric sensor was constituted by ring-opening metathesis polymerized (ROMP) materials, and it was directly in contact with NH_3 through an aluminum electrode. When exposed to an alkaline analyte as NH_3 , the -OH polymer groups (organic dielectric constituents) are deprotonated, thus creating the mechanism responsible for the sensor response which involves mobile NH_4^+ ions and counterions.

In [45], Huang et al. also focused on the role of the dielectric in the operation of OFETs, since an improvement in the semiconductor/dielectric interface may benefit the device performance. The goal of their investigation was to compare various types of polymeric materials in pentacene-based OFETs to see with which one the device achieves the best performance. Among them, they studied the polystyrene (PS), poly(vinyl alcohol) (PVA), poly(methyl methacrylate) (PMMA) and poly (4-vinylphenol) (PVP). The one which presented the best results was the PS, since its use allowed a detection limit below 1 mg/l of NH_3 and presented good recovery properties. In this study, the researchers also verified that the molecule structure of the dielectrics has a more important role than morphology in their sensor properties, since the larger the grain the more grain boundaries will exist, a factor that may reduce the electrical characteristics, especially the mobility in OFETs.

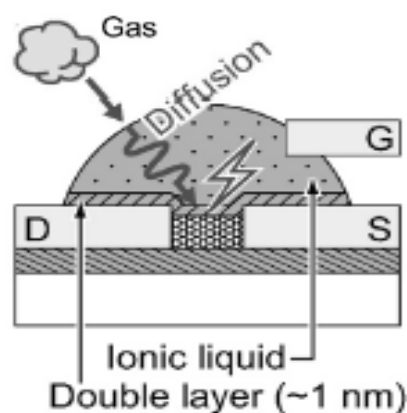


Figure 3.7 - Operation principal of IL-gate GFET (ILGFET) proposed in [44]. D, S and G represent drain, source and gate electrodes, respectively.

3.5 - Carbon Nanotubes as Ammonia Sensor Material

To produce devices capable of detecting ammonia, it is necessary to have a component where its interaction with the gaseous molecules causes some change in its properties capable of being measured. In OFETs, it was verified that pentacene or graphene semiconductor layers exhibited electronic changes according to their exposure to the concerned analyte. In fact, it is their interaction with the gas molecules that will trigger the system's response. Therefore, it is understandable that the choice of this material is the key point to build a system that works correctly.

Conductive polymers have also gained a huge visibility as NH_3 sensor materials [46]. Polyaniline (PANI) is a polymeric material that presents a high or low electric conductivity in a reversible way by alternating its exposure to acidic or basic solutions, respectively. In [47], the researchers studied the performance of ultrathin polyaniline films for controlling their exposure to NH_3 in a range of 0-20 mg/l, based on impedance spectroscopy technique. Here, it was verified that ammonia has an effect of increasing the electrical resistivity of PANI films at low frequencies. However, some disadvantages related to this kind of material as sensor film were also reported, namely its low electrical stability and its high response time.

Another type of materials with increasing interest by researchers in the creation of gas sensor devices is the field of nanotechnology. The utilization of nanomaterials is becoming interesting due to their size which offers many advantages, like surface/volume ratio. Increasing the surface area of nanomaterials provides highly active interfaces, thereby increasing sensitivity and decreasing response and recovery times. In addition, its use in gas sensors allows the development of low cost detection systems, portable and easy to use devices [33].

Carbon nanotubes (CNTs) are among the most widely used nanomaterials for the detection of NH_3 . The structure of these nanocomposites provides them with unique chemical, physical and electrical properties. Due to its C-C binding, CNTs are the strongest and most rigid fibers currently known, in addition to the great thermal stability that they exhibit both in vacuum and in air. The dielectric properties of these nanotubes revealed that these are highly anisotropic structures. This feature together with the ballistic transport through the tube axis allow them to transport high currents with a minimum effect of heating. In this sense, the utilization of these nanomaterials as sensor material becomes ideal for compact, portable and low-power detection devices [48-50].

There are two types of CNTs, single-walled CNTs (SWCNTs) and multi-walled CNTs (MWCNTs) (Figure 3.8). The first ones can be considered as a layer of a graphite rolled into a cylinder with a diameter of several nanometers and length in the order of 1-100 micrometers (Figure 3.8 (a)). SWCNTs can be metallic or semiconductors, depending the direction in which the graphite sheet is rolled up to form the cylinder. This direction can be characterized by the vector (n,m) , being n and m integers. This vector defines the structure of the nanotube (Figure 3.9). If $n=m$, the configuration of the nanotube will be armchair. If $n=0$ or $m=0$, it will adopt a zig-zag configuration. Other values for n and m conceive a chiral configuration to the nanotube. All the armchairs and the ones in which $n-m=3k$ (being k a non-zero integer) are metallic [50,51]. With respect to MWCNTs, these consist in multi layers of graphite rolled together in form of a tube, sharing the same central axis (Figure 3.8 (b)). Both SWCNTs and MWCNTs have already been used in the NH_3 detection [52,53].

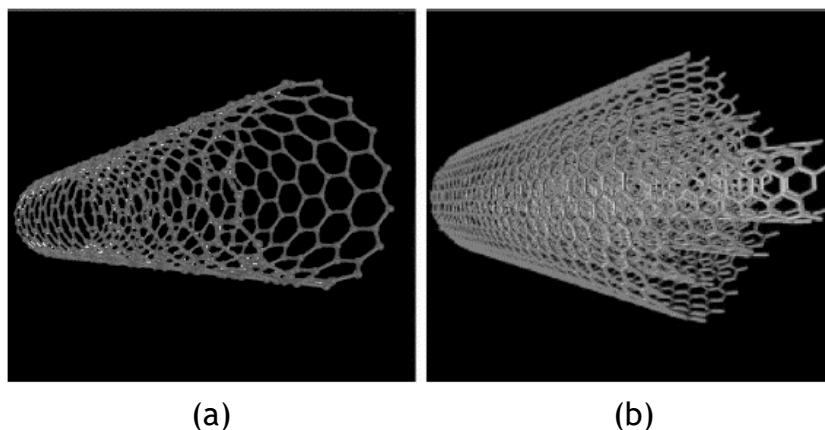


Figure 3.8 - Scheme of an (a) individual SWCNT and (b) MWCNT (adapted from [49]).

CNTs can be encompassed in several types of sensors, each with its respective detection mechanism [48,54]. However, in this work, it will be reported the most commonly used sensor types, which include chemiresistive, capacitive and field effect transistors based on CNTs.

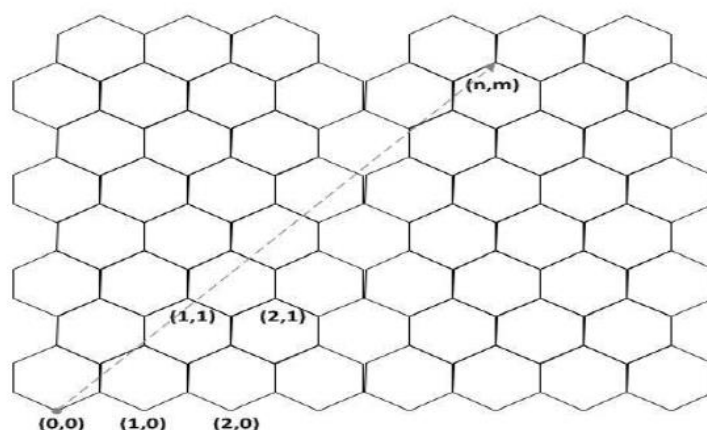


Figure 3.9 - A one atom thick layer of graphite demonstrating the vector that defines the direction in which the sheet is rolled up (adapted from [51]).

3.5.1 - Chemiresistive sensors

Since sensors whose operating principle relies on the resistance's change are easy to build, test and calibrate, they are those whose architecture is most used in the implementation of gas sensors based on CNTs [48].

In chemiresistive sensors, CNTs are used as a conductor channel. This type of nanostructures is almost entirely composed by surface atoms. In this way, a small alteration in the chemical environment that surrounds the CNTs results in a change of the conductivity capable of being measured.

Analyte adsorption in CNTs surface can change its conductivity based on three factors (Figure 3.10): i) modulation of Schottky barrier in electrode-CNT junctions (Figure 3.10 (a)), ii) charge transfer between CNTs and the analytes (Figure 3.10 (b)), and iii) the distance increasing in the intertube junction (Figure 3.10 (c)). Relative to the first factor, if an analyte is adsorbed

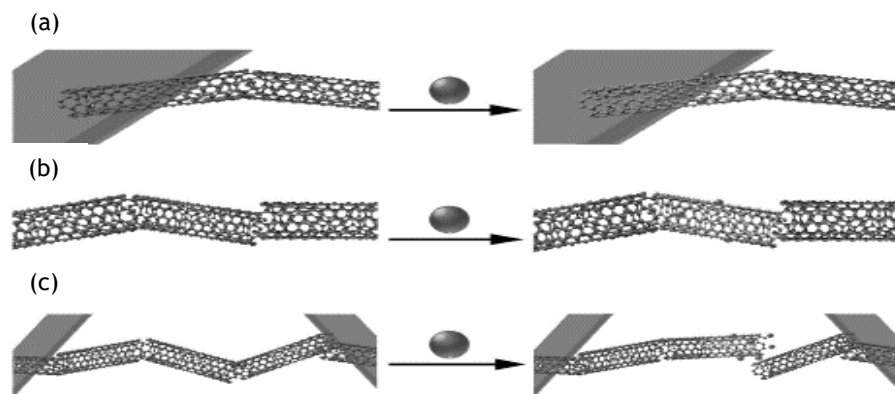


Figure 3.10 - The three factors responsible for the change in the conductivity of the CNTs: (a) CNT electrode junction, (b) charge transfer between the CNTs and the analyte, and (c) intertubes junction. The plates represent the electrodes, whereas the CNTs and the analyte are represented by the network structures and spheres, respectively (adapted from [49]).

in the CNT-metal interface, the conductivity may change due to the change in the Schottky barrier. On the other hand, CNTs are type-p semiconductors at ambient conditions. This means that the electrons donated to the CNTs valence band due to the adsorption of the analyte cause a decrease in their conductivity. Finally, since an individual CNT is not long enough to form conductive channels, these are formed through the connection between several CNTs. If the analytes are adsorbed at the intertube junctions, the conductivity of the nanostructures can also be altered by the perturbation of these junctions [49].

This type of sensors is very used in NH_3 detection. In [52], Author et al. developed a NH_3 CNT-based sensor on cotton textile. The sensor described in the investigation consists in a SWCNTs network as resistive element which changes its resistance value when exposed to the gas molecules considering the concentration range of 10-100 mg/l. Here two types of sensor were fabricated. The first has a structure of gold electrode/CNT-based sensor/gold electrode, and the second one had a structure all based in CNTs, composed by conductor/sensor/conductor. In both types, it was verified that exposing the sensor to the NH_3 molecules caused an increase in its resistance. However, it is important to notice that in the sensor with the gold electrode/CNT-based sensor/gold electrode structure there are different physical and chemical properties between CNTs and gold. Therefore, the contact cross-points between these two compounds can result in a Schottky contact, which degrades the sensor performance.

CNTs, depending on the analyte concerned, may show a weak response and low selectivity to the gas molecules due to the weak interaction between the two. Thus, the process of functionalization of CNTs arises to overcome this difficulty. The functionalization of these nano-materials can be done by using organic polymers or metal nanoparticles. In [53], a chemiresistive MWCNTs-based sensor for gas detection (including the NH_3) was fabricated. In this study, the nanotubes network was functionalized with platinum (Pt) and palladium (Pd) particles. The fabricated sensor was developed on an alumina substrate where two chromium (Cr) and gold (Au) metal strips were vacuum evaporated in the MWCNTs films for making the electrical contacts (Figure 3.11). The electrical resistance of MWCNTs increased when they were exposed to NH_3 molecules.

As it was previously mentioned, chemiresistive sensors are easy to implement. However, many improvements are still needed in the sensitivity, selectivity and anti-interference capability of these CNTs-based sensors.

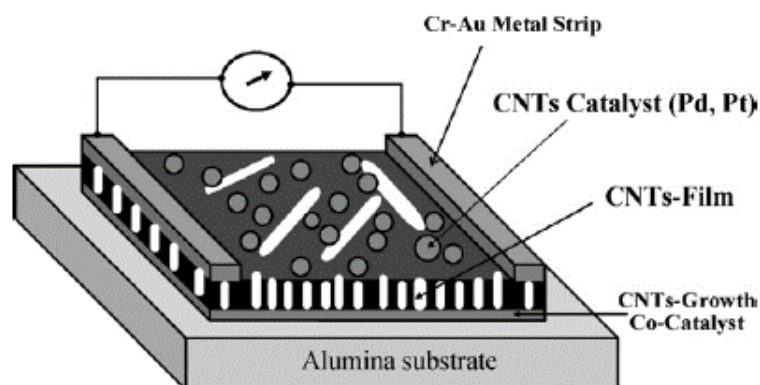


Figure 3.11 - Schematic of a chemiresistive CNTs-based sensor, functionalized with Pt and Pd particles, developed in [53].

3.5.2 - Capacitive sensors

In this type of sensors, its operation principle is based in capacity change of the CNTs when they are exposed to the gas of interest.

In [55], the researchers presented the performance of composite materials based on MWCNTs and titanium dioxide (TiO_2) tested as resistive and capacitive sensors for the detection of ammonia. Here, they verified that the variations in capacity were much higher than the changes in resistance. In that study, the CNTs network was functionalized with many concentrations of nitric acid (HNO_3). The structure of the capacitive sensor developed is presented in Figure 3.12 (a) and is based on an indium tin oxide (ITO) substrate, with a layer system of TiO_2 /CNT/ TiO_2 and a contact made of silver. The equivalent circuit of this structure is presented on Figure 3.12 (b), where R_0 represents the resistance due to the external connectors, R_1C_1 represents the grain boundaries of TiO_2 (in air only) at high frequencies, and R_2C_2 represents the carbon nanotubes for low frequencies. The variation of the capacity was studied by

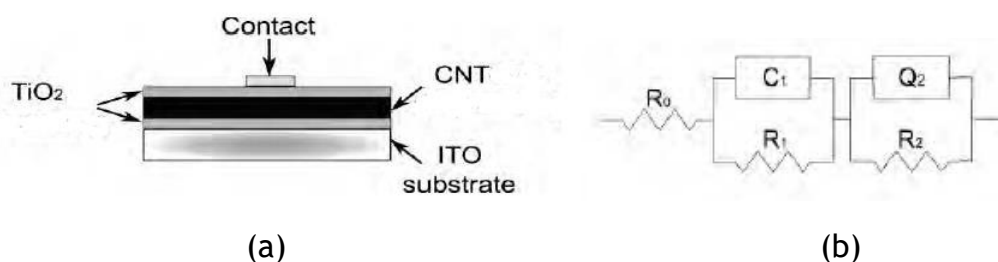


Figure 3.12 - (a) Schematic of the capacitive sensor based on carbon nanotubes and titanium dioxide, and (b) equivalent circuit, developed in [55].

the electrochemical impedance spectroscopy technique. The sensor whose exhibited a better response was the one functionalized with a HNO_3 concentration of 2.5 M. The obtained results showed that, during ammonia exposure, what dominates is the process at low frequencies. In this sense, an increase of R_2 and C_2 was obtained when the sensor was exposed to the gas.

In another investigation reported on the literature [56], a capacitor based on SWCNTs was developed on a silicon substrate (Si) highly doped in two plates. When an excitation voltage is

applied between the plates, an electric field is created at the end of nanotubes. This results in polarization of the adsorbed molecules and in the increase of the capacity value. Based on this principle, this sensor showed a high sensitivity to a variety of gases.

Although capacitive sensors are more stable than resistive sensors, their main disadvantage lies in their longer response time.

3.5.3 - Field effect transistors

Usually, SWCNTs are used for developing CNTs-based field effect transistors (CNTFETs) [57].

If two metal contacts are connected to each end of an individual SWCNT (s-SWCNT), the metal/s-SWCNT/metal device exhibits characteristics of a transistor. This way, the response based on the CNTs resistance change to gas adsorption may be detected by a field effect transistor [48].

NH_3 is an example of gas that can be detected through this type of sensor. In [58], a transistor with a s-SWCNT semiconductor for nitrogen dioxide (NO_2) and ammonia detection was developed. It was used a silicon/silicon dioxide substrate with a polysilicon layer as the transistor gate. When exposed to NH_3 , it was verified that the current-voltage characteristic curve (I-V) has been displaced by -4V. In addition, it was also observed a decrease of the device's conductivity, explained by the depletion of holes in the semiconductor resulting from the fact that NH_3 is a reducing agent. The investigators also verified that, when the device was exposed to 1% of the concerned gas, its response time was 1-2 min, a value that increased as the concentration decreased.

CNTFETs are compact devices, effective at room temperature and with a low manufacturing cost. They are detection systems that require a low power consumption, exhibiting a fast response time coupled with a low recovery time. However, its operation process can be affected by the humidity of atmospheric air, due to the interaction between water molecules and CNTs. To this disadvantage, it is added the problem of sensor stability during over long periods of time and the low selectivity when compared to other gas detection technologies [57].

3.6 - Conclusion

In table 3.2, a comparison between the various methods enunciated here for NH_3 detection is presented. As it is possible to be verified, the most conventional ones (optical methods and gas chromatography) usually have a higher sensitivity. However, they are associated to very large equipment, which makes them very difficult to use in environments other than laboratories. Another common aspect of these methods is the cost, which due to their operation conditions, is very high. In this way, alternatives to these techniques have been idealized. Most of them are based in platforms capable of being sensitive to the concerned gas.

The electronic nose has been one of the researchers' approaches, since it can be adapted for a wide range of areas, such as in the field of pathology diagnosis through the analysis of expired air [35]. In fact, it is a system with a simple structure, easy to use and it can include many types of sensors. However, this type of product requires a high-power consumption and, commercially, it remains expensive. Nevertheless, it is still a promising choice as a gas detection system, since these disadvantages can be overcome by choosing the right sensor array together with the incorporation of integrated circuit technology.

Organic field effect transistors can also be a good choice for NH₃ detection systems. They have a good sensitivity when exposed to the gas molecules, and its manufacturing is not expensive, becoming possible to use them in many electronic systems. However, depending on the

Table 3.2 – Summary of advantages and disadvantages of various NH₃ detection methods.

Method	Advantages	Disadvantages
Optical Methods	High sensitivity High selectivity Good precision in the results	Large and expensive equipment It does not support very low detection limits Reagent consumption when associated with colorimetric assays
Gas Chromatography	Very high sensitivity	Large and expensive equipment Time-consuming process Trained personnel for result interpretation
Electronic Nose	Simple structure Cheap and fast sampling technique Suitable for non-expert users	High power consumption Commercially expensive
Organic Field Effect Transistors	Applicable structure for electronic devices Good sensitivity Low production costs	High power consumption Sensitive to humidity
CNTs-Based Chemiresistive Sensors	Easy to build, test and calibrate Rapid response time	Low selectivity
CNTs-Based Capacitive Sensors	High stability	High response time
Transistors based on CNTs	Compact devices Low power consumption Rapid response time	Sensitive to humidity Low selectivity

organic semiconductor material, their operation may be affected by the humidity of the environment and may require a high energy consumption.

The chosen material for detecting the concerned gas is an important factor for the good performance of the device. In this area, carbon nanotubes have been widely explored for NH₃ detection systems. The most used types of CNTs-based sensors are the chemiresistive, the capacitive and FETs, each one with their own advantages and disadvantages. While chemiresistive sensors are easier to implement and have a lower response time than capacitive sensors, they exhibit lower stability. In turn, the capacitive sensors have a higher response time. For FETs based on carbon nanotubes, they are compact devices that require low power consumption. However, this last type of sensor can be affected by the humidity of the atmosphere and, when compared to other technologies (e.g. conventional methods of gas detection), it presents a low selectivity.

It can be understood that there are many techniques for NH₃ detection. However, the aim of the present work is the development of a portable and easy-to-use device adapted to the analysis of saliva urea concentration that gathers the characteristics of easy automatization and possible to be operated by anyone. Conventional methods present some gaps concerning

these impositions. Another goal of this project is also the construction of a device that needs a low energy consumption, so that it can be easily implemented. In this sense, neither electronic nose neither OFETs are good alternatives which obey to this characteristic.

Carbon nanotubes are entirely composed by superficial atoms where the adsorbed gas molecules can change their electrical properties at room temperature. Also, the ballistic electronic transport through the axis of the tube gives them an excellent transmission of the electrical signal for the external contact. Another important feature of these structures that makes them a good option is their long-term performance since the sensors based on CNTs presents a good stability due to their chemically robust graphitic surface [51]. To conclude, in this project, attending to the available resources and their characteristics, the NH_3 detection process being considered is based on the use of CNTs as sensing material. It will be also implemented a gas-diffusion unit together with FIA for developing a prototype sensor capable of detecting the NH_3 concentration in saliva samples. The system that was implemented is presented in the next chapter.

Chapter 4

Development of the Sensor Prototype and Impedance Measurement Circuit

As it was previously mentioned, the main objective of this dissertation is the development of a device capable of detecting pathologies after the analysis of the concentration of urea in saliva. This salivary compound can be detected by its hydrolysis product, ammonium which could be transformed into ammonia. Among the various methods for the detection of this gas, the one used in this project is based on carbon nanotubes for reasons already mentioned in the previous chapter.

The device purposed here combines a flow-injection technique together with a gas diffusion unit (GDU) and a CNTs-based sensor film to detect the ammonia present in saliva. The operation principle of the purposed system is presented in this chapter. The NH_3 detection method being employed is based on a previous work [30]. However, some changes were made to introduce carbon nanotubes as the sensing material. These changes will also be mentioned as well as the development process of the CNT-based sensor film.

In order to achieve a system capable of being portable, automatic and easy to use, an electronic circuit based on the AD5933 integrated circuit (IC) was also developed. The operation of this IC and the roll of the additional analogue circuit needed to implement the impedance measurement circuit will be explained. The calibration of the circuit and results obtained within the measurement of different known resistors and RC circuits are presented as well.

The preparation of reagents, solutions and saliva samples will also be described. In the end, the final apparatus and procedure will be presented.

4.1 - General Prototype Operation

The developed prototype relies on four fundamental aspects: i) the process of converting salivary urea into NH_3 by its hydrolysis in the oral cavity, ii) the separation of NH_3 from the oral fluid, iii) the gas detection process, and iv) the estimation of NH_4^+ concentration with an electronic circuit. The system was built based on a previously developed gas diffusion system for the determination of ammonium [30].

The basic block diagram of the prototype is shown in Figure 4.1. The initial idea involves the injection of a saliva sample in the donor channel of the GDU. NH_3 separation from the oral fluid occurs due to the incorporation of a hydrophobic membrane in the GDU, which allows its diffusion. In this project, the gas detection process involves the use of a CNT-based sensor film, since the interaction between the gas and these nanomaterials causes a change in CNTs' electrical properties (resistance and capacitance) capable of being measured. In turn, this sensor film could be connected to an electronic circuit capable of measuring the variation of its impedance, and through the connection with a microcontroller, these values may be recorded and shown on the PC. After the correlation between the obtained impedance variation and NH_4^+ concentration present in the saliva sample, it is possible to estimate the concentration of the salivary urea.

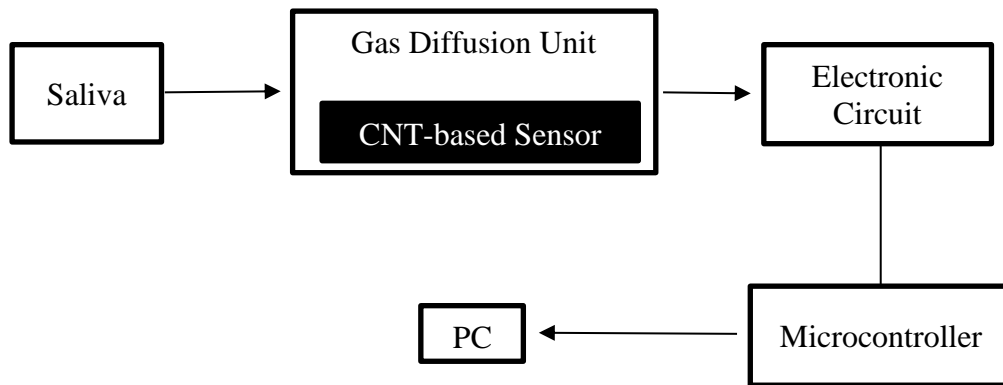


Figure 4.1 - Basic block diagram of the implemented prototype in the present work.

4.2 - Adaptations made in GDU

In the previously developed system [30], the NH_3 detection is based on the spectrophotometric technique. Thus, the GDU comprises two symmetric pieces, as shown in Figure 4.2, of which one incorporates the donor channel where the sample flows, and the other, the acceptor channel, where the colorimetric assay changes its colour due to the NH_3 concentration diffused from the hydrophobic membrane.

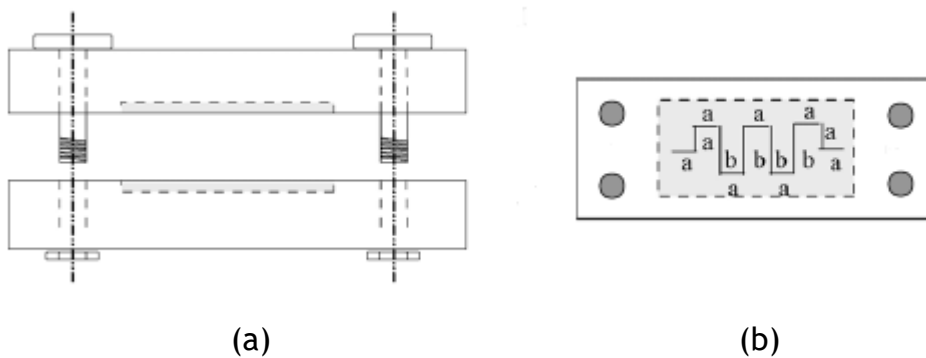


Figure 4.2 - (a) Lateral view of the GDU developed in [30], in which the channels have 2mm of inner diameter and 1mm of depth. (b) Channels' top view whose length is shown as $a = 0.5$ cm and $b = 1$ cm.

In the present work, only the donor channel is used because the detection method does not include the colorimetric reaction used in the previous work. Instead, an additional piece was developed to place the sensor film in the GDU and to create a gap, which allows the gas accumulation, and posteriorly, the interaction of its molecules with the film. This additional piece is made of Perspex® acrylic, a non-toxic pure material with a long service life [59]. It has a center cavity with the same dimensions of the CNTs-based film. Since the length of the film will be a variable in the study of the variation of the sensor resistance, three additional pieces with different cavity dimensions were developed (Figure 4.3). Each piece also has two holes of 1.8 mm diameter in both extremities where two needles are inserted in order to gain access to the cavity for cleaning purposes. To keep the sensor film in a closed environment and to prevent the gas from escaping, a cover was developed. The assemble of the GDU with the sensor film, the additional piece and the cover is shown in Figure 4.4.

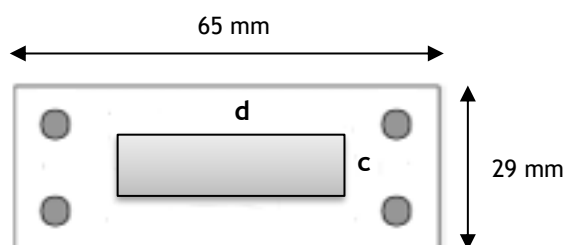


Figure 4.3 - Top view of the additional piece for the GDU with the correspondent dimensions, where $c = 10$ mm and d varies depending on the length of the sensor films, being able to adopt values of 40 mm, 20 mm or 10 mm. All the three pieces have a thickness of 3.5 mm.

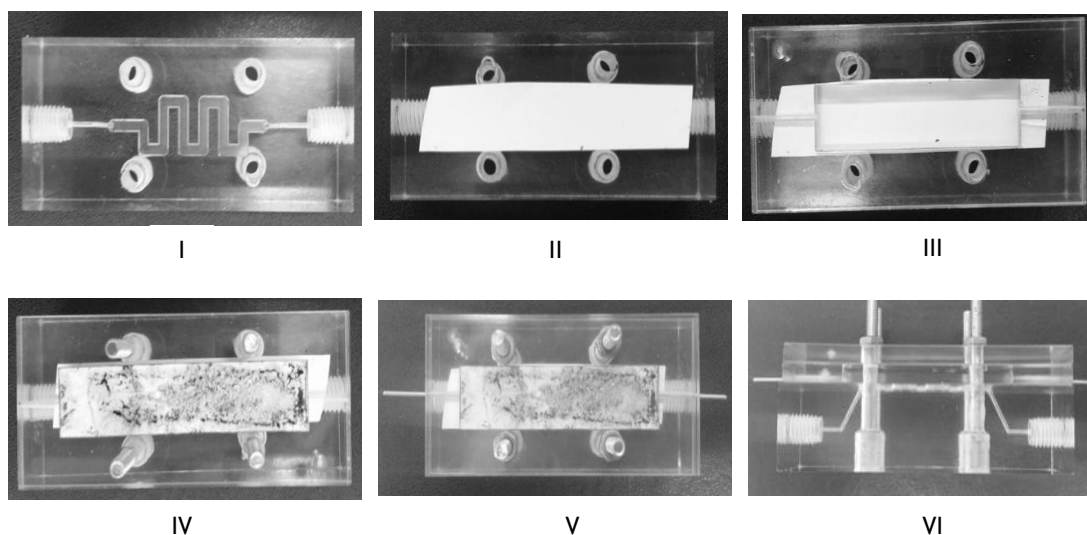


Figure 4.4 - Assemble of the GDU with the adaptations made: I - the donor channel where the sample will pass (top view); II - the hydrophobic membrane which will allow the gas diffusion (top view); III - the additional piece made for create a gas accumulation (top view); IV - the sensor film with the surface covered by nanotubes turned to the side where the gas is accumulated (top view); V - the cover developed for keeping the system isolated and the two needles incorporated into the additional piece for cleaning purposes (top view); VI - side view of the completed system.

4.3 - Development of MWCNTs-based Sensor Films

Chemiresistive sensor films are the simplest configuration for a CNTs-based sensor, being easy to calibrate and test. These reasons have made this type of gas sensor based on CNT the first option to be considered for the detection of the targeted gas molecules. In the literature, this is the most used type of sensor. However, capacitive sensors have been also developed to detect NH_3 molecules since it was reported that the capacitance of the CNTs can change with their exposure to certain gases [55]. To understand which one of the CNTs electrical properties presents a higher variation when exposed to the gas, a capacitive sensor film was also developed in this project.

4.3.1 - Chemiresistive sensor film

The configuration of the developed chemiresistive sensor film involves a substrate, a carbon nanotube ink and two electrical contacts in both extremities allowing the measurement of its resistance value (Figure 4.5). To better understand if the film's length influences its response, three sensor films with different lengths were developed (Figure 4.6).

Initially, three different options were thought for the substrate which include acetate paper, cellulose paper and photographic paper. Acetate paper was the first option to be considered due to, not only the ease with which it can be acquired, but also because it is suitable for printing. However, when in contact with the CNT ink, it proved to be a bad option since, contrary to the expectations, it did not permit a good adhesion of the CNTs based ink. Besides that, it was verified that these nanostructures did not have a uniform distribution on this material.

Cellulose is a simple chain polymer with multiple hydroxyl groups (OH^-), that can form strong hydrogen bonds with the carboxyl and hydroxyl end groups of the CNTs, thereby conferring good adhesion of these nanostructures to cellulose substrates [52]. In this way, the hypothesis of cellulose paper was thought based on the good adhesion that CNTs can establish with this material, besides that it can be easily acquired. However, the cellulose paper used in this work showed some obstacles when used as substrate, since it had a very fibrous structure. Although cellulose could prove to be a good option, a larger amount of carbon nanotube ink would be needed.

The idea of using photographic paper as substrate was based on [60], where this type of material was utilized for the development of organic electrochemical transistors. Indeed, it was verified that this paper is the best option as substrate, since it promoted a good adhesion and a good homogeneous deposition of CNTs.

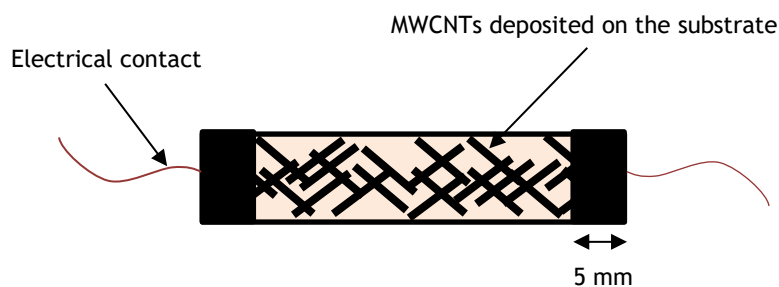


Figure 4.5 - Top view of the configuration of the developed MWCNTs-based chemiresistive sensor film. 5 mm were added to each end of the films to make the electrical contacts.

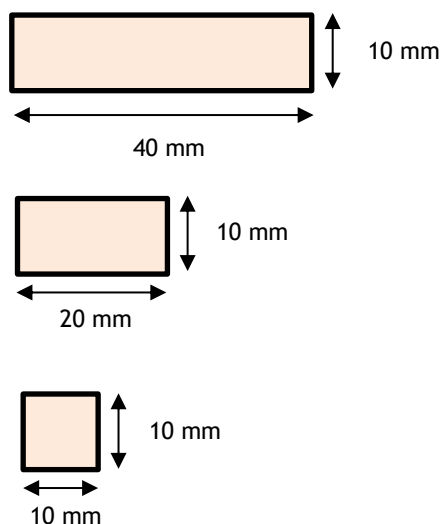


Figure 4.6 - Format of sensor films developed with their respective dimensions.

Usually, the researches which involve the development of a gas sensor based on carbon nanotubes use SWCNTs as sensing material. Nevertheless, MWCNTs can be produced in large scale and the production cost is much lower [50,57]. Here, the type of CNTs used are multi-walled carbon nanotubes commercially available from NANOCYL® (NC3100TM series). These nanostructures were grown by catalytic chemical vapour deposition method (CCVD) and are characterized by their high electrical conductivity and high level of purity (95%). The average length of these MWCNTs is around 1.5 μm .

To achieve a good adhesion between the MWCNTs and photographic paper, an ink containing the nanostructures was prepared. Its optimized composition consists in 0.220 g of MWCNTs in a 64 μL of nafion perfluorinated resin dispersion (Aldrich) mixed with a solution of water/ethanol (4/1, V/V) for 30 minutes in an ultra-sonic bath, to form a homogeneous ink. The method of deposition of the ink in the substrate comprised three steps. First, the sensor film was submerged in the ink to wet the surface, predisposing it for a homogeneous deposition of the ink. Then, drops of ink were placed with a Pasteur pipette in the film and spread equally across the surface until it was totally covered. In the final step, the films underwent a drying process in the air, with subsequent exposure to a hot air jet in which the immobilized samples went through periods of mechanical agitation. The amount of carbon nanotubes deposited in the film extension was determined by weighing the samples before and after the deposition of the ink (Table 4.1).

The electrical contacts were made in the extremities of the film after it was dry. They are made of two thin copper wires connected to the nanotubes with a conductive silver ink. In

Table 4.1 - Quantity of MWCNTs deposited in each film.

Length (mm)	MWCNTs mass (mg)
40	17.6
20	13.3
10	11.1

order to prevent the gas from interfering with the electrical contacts, these were covered with insulating tape (Figure 4.5).

4.3.2 - Capacitive sensor film

The configuration of the capacitive sensor film developed in this work is shown in Figure 4.7. The deposition method of the MWCNTs on the photographic paper was the same used in the development of the chemiresistive sensor films. The film has 20 mm of length and 10 mm of width. The quantity of MWCNTs deposited is 13.6 mg.

After the nanotubes were deposited, the opposite side of the substrate was covered with conductive silver ink. This configuration is similar to a capacitor, where the carbon nanotubes and the silver ink behave like the two parallel plates of a capacitor and the photographic paper behaves like its dielectric. The electrical contacts were also made in the same way as those made in the previous sensor film. However, in this configuration they are in the same extremity of the film to measure the change of the capacitance of MWCNTs when they are exposed to NH_3 gas molecules.

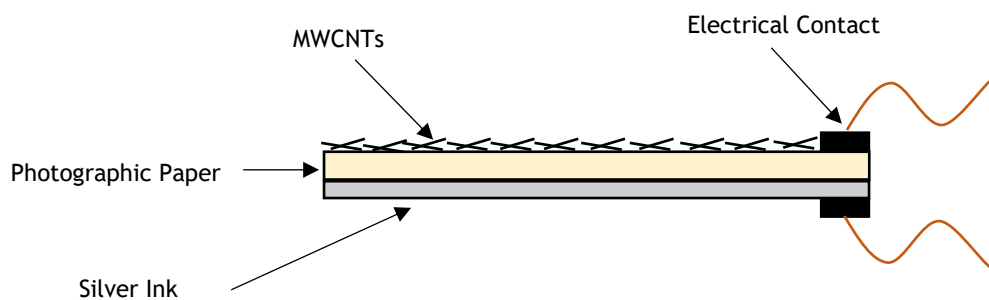


Figure 4.7 - Lateral view of the configuration of the developed MWCNTs-based capacitive sensor film.

4.4 - Impedance Measurement Circuit

An impedance measurement circuit (IMC) was used to measure the change in the electrical characteristics of the MWCNT-based sensor films in response to the NH_3 molecules diffused through the hydrophobic membrane. This circuit is connected to an ArduinoUno platform, which supplies it with a voltage of 5 V, and that in turn is connected to a computer enabling the recording of the data.

This IMC is based on the AD5933 IC from Analog Devices and an analogue additional circuit [61], capable of compensating some of the limitations associated to the IC. The AD5933 is described as a high precision instrument that can measure unknown impedances [62]. This IC can communicate with the microcontroller through an I^2C interface.

An impedance value is conventionally represented by a complex number in which its real component corresponds to resistance (R) and its imaginary component corresponds to reactance (X_C or X_L) (Figure 4.8) [63].

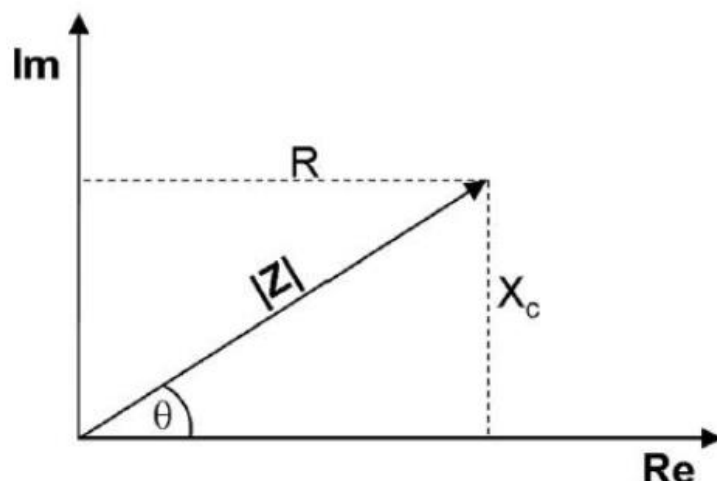


Figure 4.8 - Real component (R) and imaginary component (X_c) of the vector impedance Z . θ corresponds to the phase angle (adapted from [63]).

4.4.1 - Impedance measurement with the AD5933

The operation of the AD5933 IC can be divided in two principal stages: transmission and reception stages. The functional block diagram of this IC is shown in Figure 4.9.

The transmission stage is composed by a 27-bit phase accumulator DDS core, a digital-to-analogue converter (DAC) and an amplifier with a programmable gain (PGA_1) (Figure 4.9). The clock defined for the DDS can be determined by an external reference or by the internal oscillator of the AD5933 as defined for this work. The DDS generates an excitation voltage (V_{out}) amplified by the PGA_1 , which will be applied on the unknown impedance ($Z(\omega)$). The AD5933 can generate four different values of V_{out} , each one with a corresponding DC bias. Despite these values are defined for a power supply of 3,3 V, it is possible their conversion to a 5 V supply [62].

The AD5933 IC allows performing a frequency sweep in the 1 kHz to 100 kHz range, in which

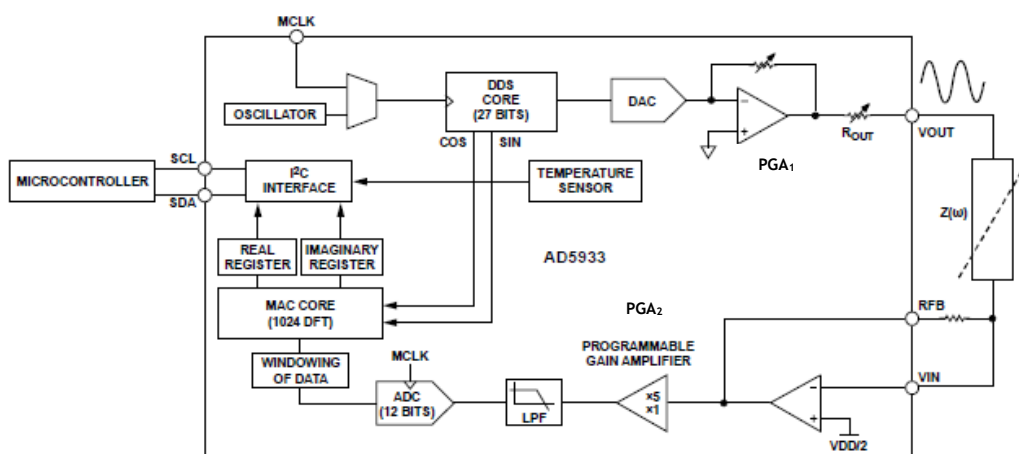


Figure 4.9 - Functional block diagram of the AD5933. $Z(\omega)$ corresponds to the unknown impedance and R_{out} is the output resistance whose value varies according to the V_{out} signal (adapted from [62]).

the user can choose the initial frequency, the increment and the number of increments.

The current signal that passes in $Z(\omega)$, in response to the applied V_{out} , is captured by the AD5933 at the reception stage. This stage is composed by a current-to-voltage converter (CVC), an amplifier with a programmable gain (PGA_2), a low-pass filter and a 12-bit analogue-to-digital converter (ADC). The digital captured values are processed with a discrete Fourier transform (DFT) that allows the AD5933 to provide the real (R_Z) and imaginary (I_Z) parts of the measured impedance as a function of frequency (Figure 4.9). With these values, the IC calculates the magnitude of the $Z(\omega)$ (equation 4.1).

$$|Z(\omega)| = \sqrt{(R_Z)^2 + (I_Z)^2}. \quad (4.1)$$

The calibration process of the AD5933 is a critical step to ensure its proper operation. The feedback resistance (R_{FB}) represented in Figure 4.9 is the reference resistance for the impedance range intended to be measured and can be selected by the user. According to [62], this process involves the use of a known resistance (Z_{cal}) in the place of the $Z(\omega)$ with the same value of R_{FB} . In the calibration process, a gain factor is calculated (equation 4.2). After this, the unknown impedance can be calculated using equation (4.3).

$$\text{Gain Factor} = \frac{\left(\frac{1}{Z_{cal}}\right)}{|Z_{cal}|}. \quad (4.2)$$

$$Z(\omega) = \frac{1}{\text{Gain factor} \times |Z(\omega)|}. \quad (4.3)$$

It is important to mention that the R_{FB} used in the calibration process is maintained during the impedance measurement process. The value of this resistance and the one defined for the PGA_2 will determine the achieved measurement accuracy.

4.4.2 - Additional analogue circuit

The AD5933 IC can measure the value of an unknown impedance in the 1 k Ω -10 M Ω range. The limitation of these values is due to the effect of R_{out} in the transmission stage (Figure 4.9). Carbon nanotubes do not present a specific impedance range. Therefore, to enable the application of this circuit in a wider range of values, an analogue circuit is needed to create an appropriate interface between the IC and the impedance to be measured [62]. The analogue circuit developed for this purpose is based on the work published in [61]. This additional circuit allows the measurement of impedance values in the of 10 Ω -10 M Ω range. The schematic of this circuit is presented in Appendix A-Figure A.1. It is based on peak detectors (IC1 and IC3 for positive peaks and IC2 and IC4 for negative peaks) followed by a voltage divider to detect the mean value of the AD5933 output signal, which corresponds to the DC bias. The amplitude of the signal at the IC5 output is 10 times decreased and its DC bias level is shifted to $AVCC/2$ in the IC6 stage. As a result, V_{out} will have the same DC bias as the CVC in the AD5933 reception stage. IC7 is used as an impedance buffer ensuring that the signal applied to the impedance

under test (IUT) is as low as the signal at the output of IC5. In Figure A.1, the IUT is represented by a connector (JPG_1).

The current signal generated in the IUT in response to V_{out} will pass through an external current-to-voltage converter (CVC_{ext}) composed by an amplifier and a connector (JPG_2) which represents the R_{FB} . This feature allows to change the R_{FB} according to the impedance range of interest. The internal CVC of the AD5933 is not used and its value was fixed at 4.7.

4.4.3 - Operation of the Impedance Measurement Circuit with Resistors

To ensure that the impedance measurement circuit can be used to measure the changes in the resistance value of the chemiresistive MWCNT-based sensor film, its operation was verified with different known resistor values.

For these tests, a AC V_{out} of 3 Vpp with a DC bias of 2.24 Vpp was chosen, and the values of PGA_1 and PGA_2 were established with a unit gain to ensure that ADC of the receiving stage not saturates. The measurements were made in the 10-100 kHz frequency range.

A resistor of 100 Ω was used to verify if the developed system can measure impedances lower than 1 k Ω . The calibration of the system was made with a 100 Ω resistor as well. The results are presented in Figure 4.10. As it can be observed, the values measured by the IMC are in agreement with the expected resistor value, with an average error of 0.025%. This proved that the additional analogue circuit can really enlarge the AD5933 IC lower limit of the impedance range that the IC can measure.

The main goal of this impedance measurement circuit is to detect the variations of the resistance value of MWCNTs-based sensor film when exposed to NH_3 gas molecules. To understand if the IMC can detect small changes, the resistance of a 100 Ω resistor in series with a 1 Ω resistor was measured with a calibration of a 100 Ω resistor. Figure 4.11 shows that the IMC can correctly detect resistance variations as low as 1 Ω with an average error of 0.1%, making it suitable for using in low resistance change measurements.

For a better understanding of the influence that the calibration process has in the performance of the IMC, the impedance of a 30 k Ω resistor was measured with a calibration of a

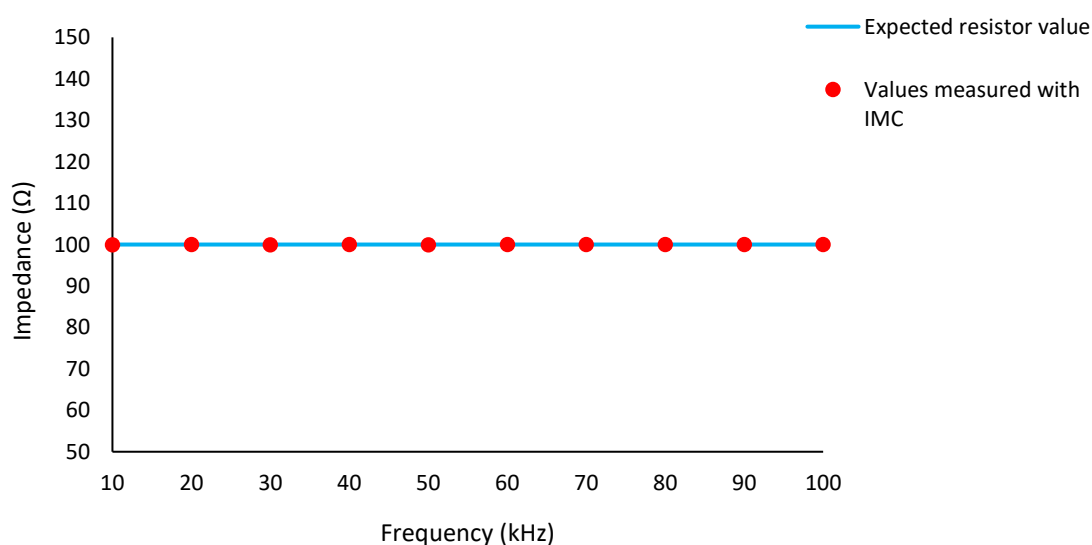


Figure 4.10 - Impedance as a function of frequency for a resistor of 100 Ω with a $R_{FB}=100 \Omega$.

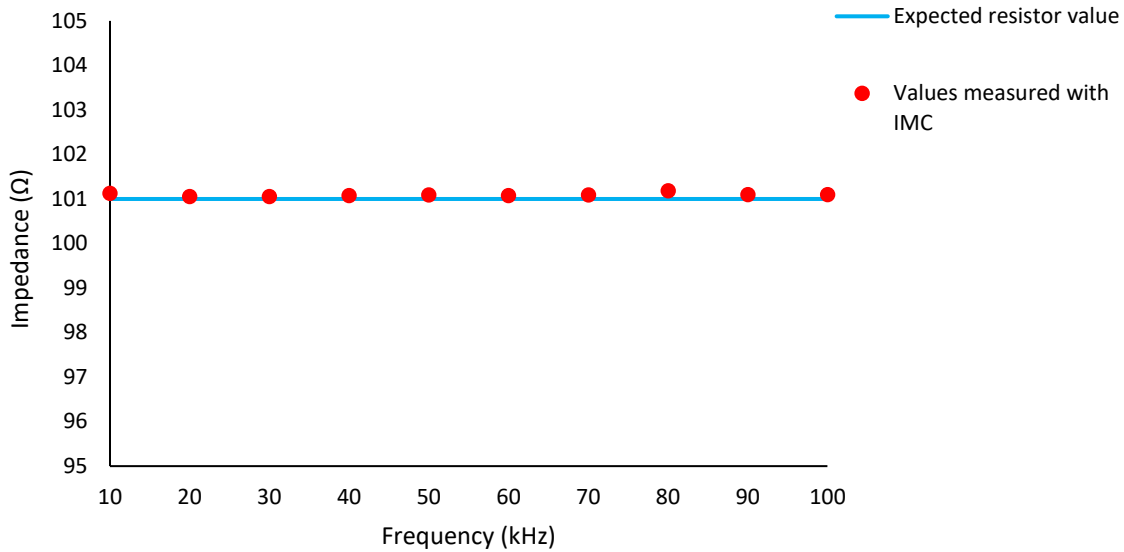


Figure 4.11 - Impedance as a function of frequency for an equivalent resistance of 101 Ω with a $R_{FB}=100 \Omega$.

30 k Ω and 1 k Ω resistors. The results present in Figure 4.12 show that for measuring an impedance of 30 k Ω , it is better to calibrate the system with a R_{FB} of the same value (average error = 0.5%). In fact, when measuring an impedance of 30 k Ω with a calibration of 1 k Ω , the value of the measured impedance starts to diverge from the expected resistor value (average error = 1.9%). This means that the value of R_{FB} plays an important role on the good performance of the impedance measurement circuit. If the value of R_{FB} is too far from the unknown impedance, the error will increase, and this can lead to an erroneous judgement.

In Figure 4.13, a calibration of 1 k Ω was made for the measurement of a 100 k Ω resistor.

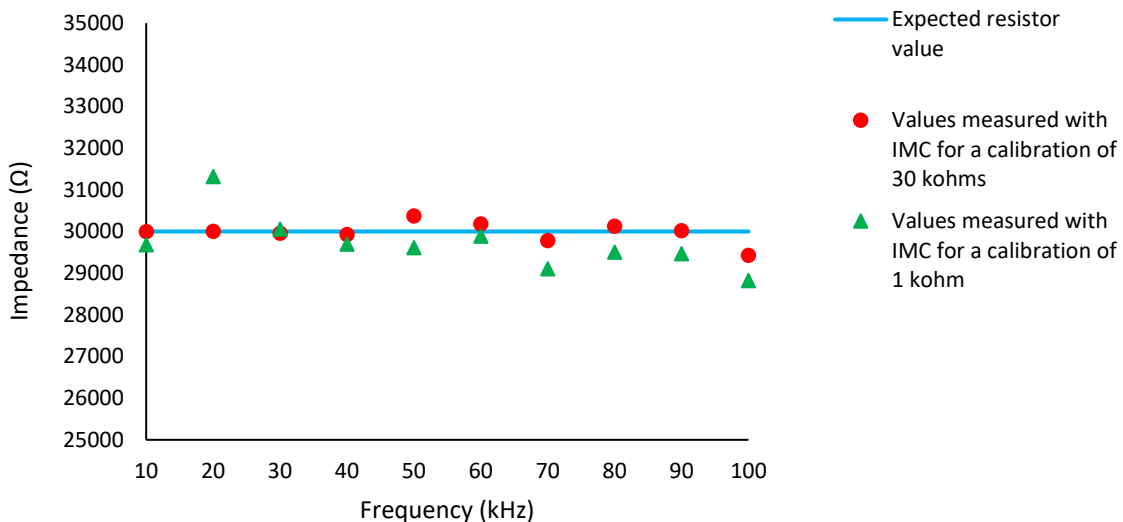


Figure 4.12 - Impedance as a function of frequency for a 30 k Ω resistor with different values of R_{FB} . Red circles represent the values obtained for a $R_{FB}=30 \text{ k}\Omega$ and green triangles represent the values obtained for a $R_{FB}=1 \text{ k}\Omega$.

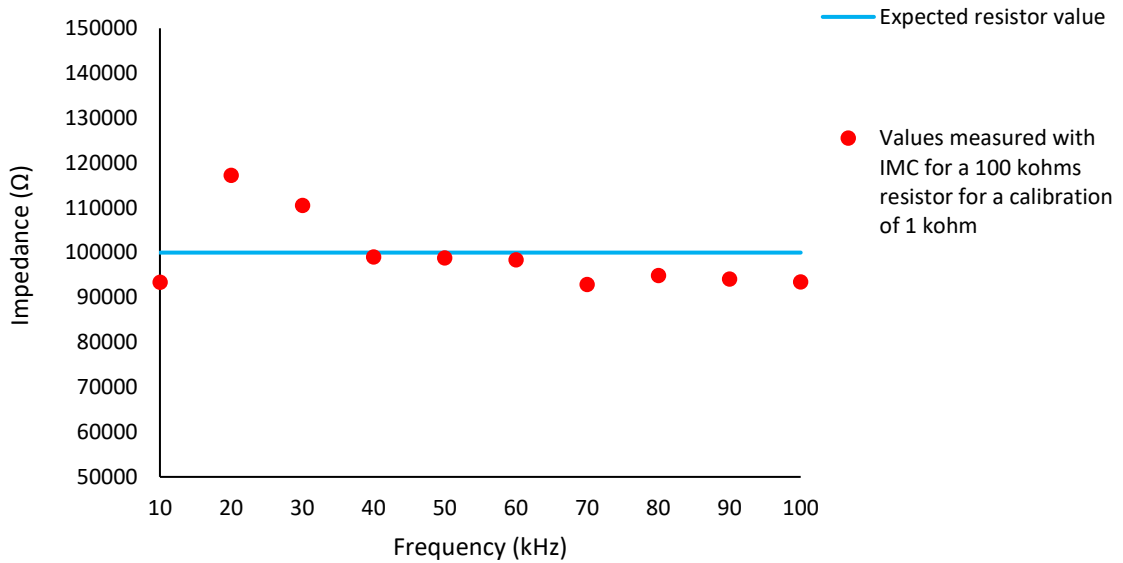


Figure 4.13 - Impedance as a function of frequency for 100 kΩ resistor with a $R_{FB}=1k\Omega$.

The obtained average error obtained is 6.3%. In [64], Seoane et al. developed a system based on AD5933 for a biomedical application context. As expected, the results obtained from that research indicate that an appropriate operation of the system is achieved when the value of the measuring impedance is close to the value of R_{FB} .

In this work, the maximum impedance value that the IMC could read is established by the relation given by equation (4.4):

$$|Z_{max}| = \frac{V_{out} \times R_{FB}}{V_{CVC_{ext_min}}}, \quad (4.4)$$

where V_{out} is 0.3 V (due to a 10 times decrease of the signal in IC5 stage), $V_{CVC_{ext_min}}$ corresponds to the minimum amplitude value that the signal should take at the output of the CVC_{ext} . In [61], it was experimentally verified that the amplitude of the signal at the input of the ADC, in the reception stage of AD593, should be greater than 15 mV because of its limited dynamics. Thus, the signal at the output of the CVC_{ext} should have an amplitude greater than 3 mV due to its amplification gain of 4,7 and the PGA_2 unit gain programmed.

Similarly, the minimum impedance value that the system could read can be calculated with equation (4.5):

$$|Z_{min}| = \frac{V_{out} \times R_{FB}}{V_{CVC_{ext_max}}}, \quad (4.5)$$

where $V_{CVC_{ext_max}}$ corresponds to the maximum amplitude value that the signal should take at the output of the CVC_{ext} (same value that V_{out}). This means that the system cannot read impedances with values lower than the value established for R_{FB} . Figure 4.14 was obtained for the measurement of a 1 kΩ resistor with a calibration resistance of 10 kΩ. Indeed, it is shown that the measured values do not correspond to the real value. It was also verified that if the impe-

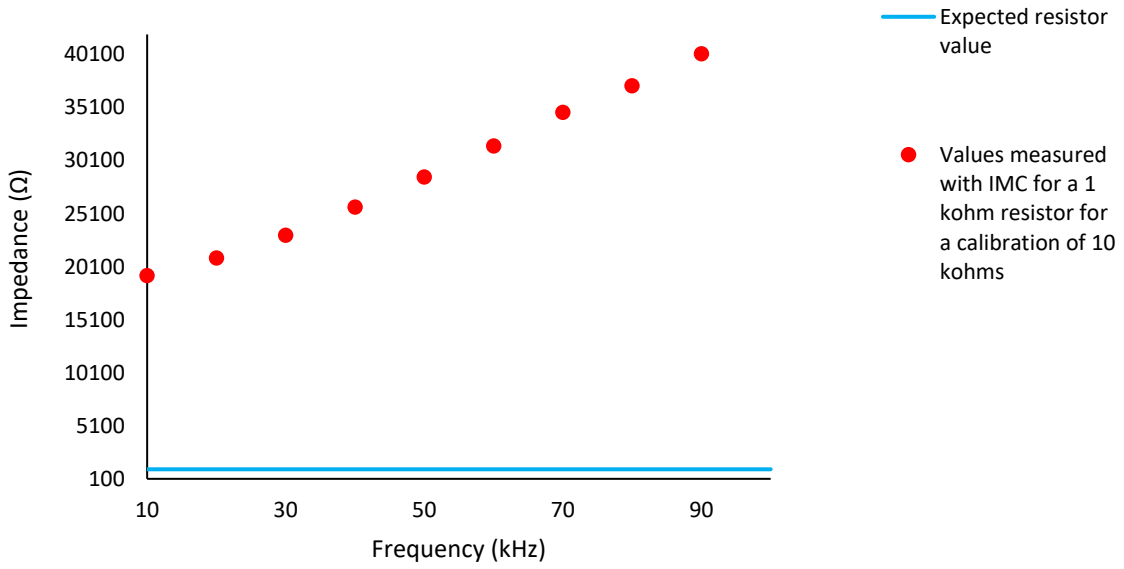


Figure 4.14 - Impedance as a function of frequency for 1 kΩ resistor with a $R_{FB}=10k\Omega$.

dance under measurement is lower than the R_{FB} value, the signal at the output of the CVC_{ext} multiplied by the 4.7 gain, fixed at the internal CVC of the AD5933, will exceed half of the supply voltage. This will cause the saturation of the ADC compromising the performance of the overall system.

4.4.4 - Operation of the Impedance Measurement Circuit with RC Circuits

To ensure that the impedance measurement circuit can be used to measure the changes in the capacitance value of the capacitive MWCNT-based sensor film, its operation was verified with different known RC circuits.

Figure 4.15 shows the response of the IMC to the measurement of an impedance formed by

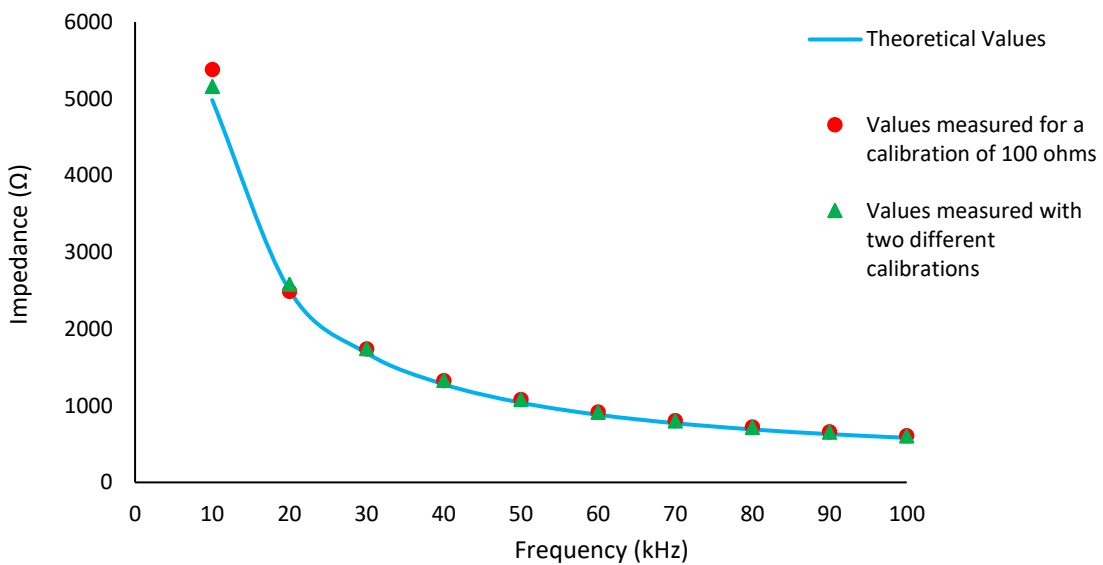


Figure 4.15 - Impedance as a function of frequency for a RC series combination. Values measured after a one-time calibration with a resistor of $R_{FB}=100\ \Omega$ and with two different calibrations with resistors of $R_{FB}=1\ k\Omega$ and $R_{FB}=100\ \Omega$.

the series combination of a $300\ \Omega$ resistor and a $3.3\ \text{nF}$ capacitor. First, the measurements were taken with a calibration resistor of $100\ \Omega$ for all the frequencies in the $10\ \text{kHz}$ - $100\ \text{kHz}$ range. As it can be seen, the measured values are close to the expected ones, with an average error of 4.4% . Nevertheless, the obtained error is higher compared to the results obtained in resistance measurements. In order to decrease this error and considering the important role that the R_{FB} value has in the system performance, the impedance measurements were made with two different calibrations: a resistor of $1\ \text{k}\Omega$ for frequencies between $10\ \text{kHz}$ and $50\ \text{kHz}$, and a resistor of $100\ \Omega$ for frequencies between $60\ \text{kHz}$ and $100\ \text{kHz}$. Indeed, this leads to a lower average error of 3.8% .

The same was made for a RC parallel circuit formed by a $330\ \text{k}\Omega$ resistor and a $10\ \text{nF}$ capacitor. Figure 4.16 shows the impedance values obtained for this configuration. Likewise, first a calibration of $100\ \Omega$ resistor was made and an average error of 10% was obtained. Then, the values were measured with a two-time calibration: a resistor of $1\ \text{k}\Omega$ for the frequency of $10\ \text{kHz}$ and $100\ \Omega$ for the others. This process reduced the average error to 8.9% .

This two-time calibration process may be a better alternative for this type of circuits. It is true that the reduction of the errors percentage may not seem very high, but this is because the impedance of each circuit does not vary in a wide range. When considering IUTs that have a wider range of frequency dependent impedance values, this two-time calibration process can lead to a more reliable reading. Again, the closeness of the R_{FB} value and the IUT proved to be an important aspect for the good performance of the impedance measuring circuit.

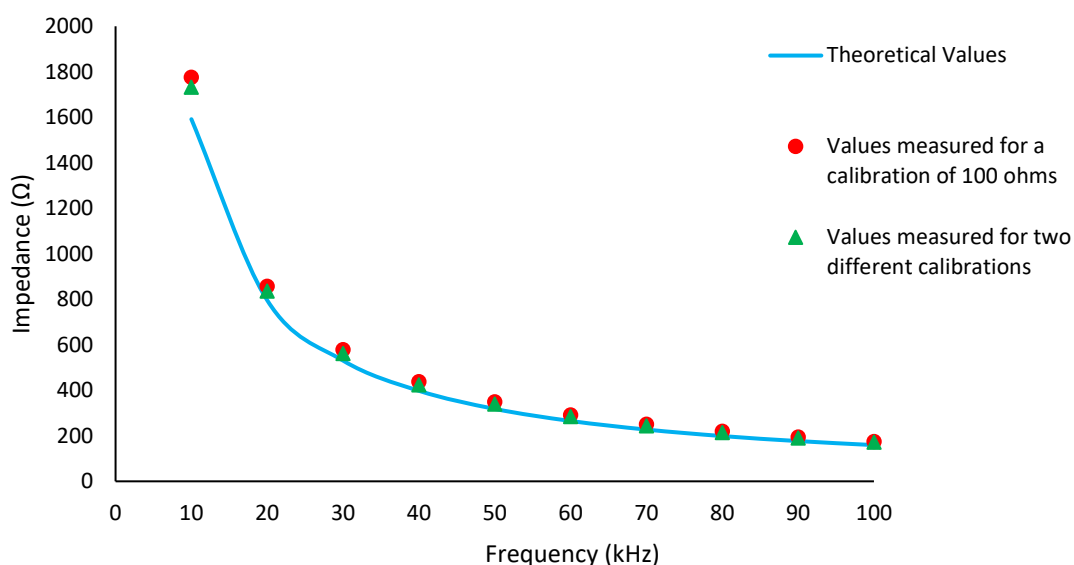


Figure 4.16 - Impedance as a function of frequency for a RC parallel combination. Values measured after a one-time calibration with a resistor of $R_{\text{FB}}=100\ \Omega$ and with two different calibrations with resistors of $R_{\text{FB}}=1\ \text{k}\Omega$ and $R_{\text{FB}}=100\ \Omega$.

4.5 - Final Apparatus and Experimental Procedure

The final aspect of the experimental set-up is shown in Figure 4.17. It includes a pump from Ismatec® which aspirate the sample and the NaOH solution to a confluence with a caudal of 3.25 ml/min and 2.8 ml/min, respectively. At the confluence, the two solutions are mixed for converting the dissolved NH_4^+ into gaseous NH_3 allowing the diffusion of the gas through a Milipore Durapore® membrane filter (ref.HVHP09050). After passing in the donor channel of the GDU, the mixing ends at a waste container. The impedance measurement circuit is directly connected to the contacts of the sensor film and the data recording is made on the PC while the mixing is passing in the GDU's donor channel. To clean the sensor film after each measurement, the GDU is also connected to a dry nitrogen (N_2) conduct through the cleaning system already mentioned in the subsection 4.2.

The characterization of the prototype performance involves the characterization of the MWCNT-based sensor films together with a better understanding of the flow system. For this purpose, the prototype was first tested with standard solutions of NH_4^+ . Then, standard solutions of synthetic saliva with known NH_4^+ concentrations were prepared to evaluate the urea detecting system in conditions closer to those of the foreseen final application. The preparation of all used reagents and solutions used is described next.

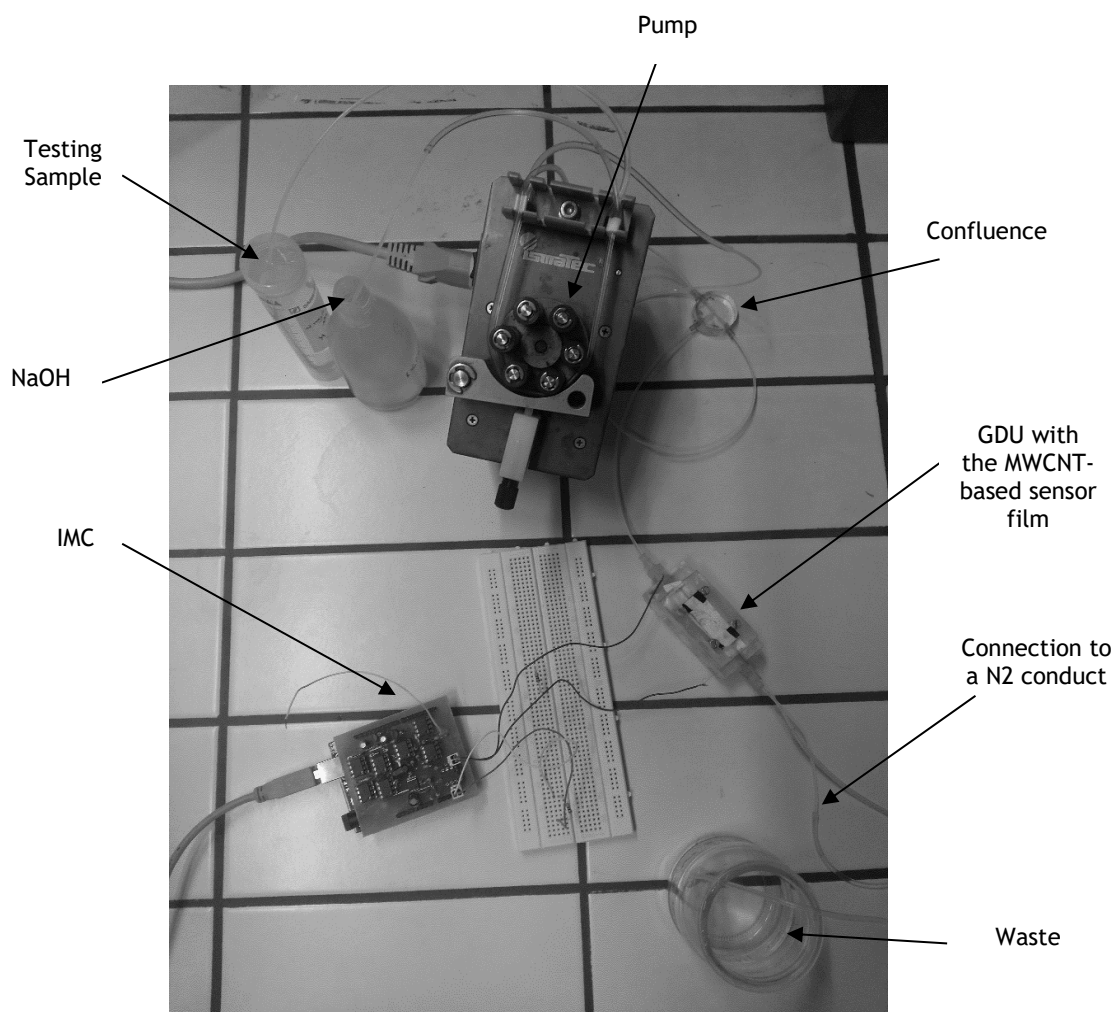


Figure 4.17 - Final apparatus of the experimental set-up.

4.5.1 - Reagents and Solutions

The reagents and solutions used for testing the sensor prototype were sodium hydroxide reagent and ammonium solutions with different concentrations. The working solution of NaOH (0.025 M) was prepared weekly by appropriate dilution of the stock solution (0.1 M) in a volume of 100 ml.

Ammonium stock standard solution with a concentration of 500 mg NH_4^+ per l was prepared by dissolving 148,58 mg of ammonium chloride in 1000 ml of deionized water and stored in the refrigerator. A second stock solution of 50 mg NH_4^+ per l was prepared from the previous standard in a volume of 50 ml of deionized water. The working standards were prepared weakly by appropriate dilution, involving two different ranges: 0.1-0.5 mg NH_4^+ per l and 1-5 mg NH_4^+ per l.

4.5.2 - Synthetic Saliva

A volume of 200 ml of synthetic saliva was prepared [65]. This preparation involved 448,3 mg of potassium chloride (KCl), 108,872 mg of monopotassium chloride (KH_2PO_4), 953,24 mg of 4-(2-hydroxyethyl)-1-piperazineethanesulfonic acid (HEPES) and 540 mg of mucine. All the components were first dissolved in deionized water. After this, they were all mixed in the same goblet and deionized water was added to achieve the final volume.

Standard solutions of NH_4^+ were prepared following the procedure stated previously. However, instead of deionized water, the working standards were dissolved in synthetic saliva.

4.6 - Conclusions

This chapter describes a method and a system capable of detecting the NH_4^+ concentration present in saliva samples, that comprises a flow-injection system together with a gas diffusion unit, a MWCNTs-based sensor film and an impedance measuring system. It can convert the NH_4^+ present in saliva (product of urea hydrolysis) into NH_3 , separate it from the oral fluid, detect its concentration and record the data. It also presents the possibility of being portable having only the limitation of the cleaning system. As explained, dry nitrogen is injected in the GDU through a needle placed in the extremity of the developed additional piece. However, this cleaning gas is provided by a conduct in the laboratory. To make the system completely portable, this feature should be replaced by a nitrogen gas bottle, for example.

MWCNTs-based chemiresistive and capacitive sensor films were developed. Their connection with the impedance measurement circuit gives the advantage of making the application of the device even simpler for the users since the results can be shown and recorded on the PC. As it was demonstrated, the calibration of the circuit is crucial for the good performance of the device. This leads to the need of making a careful choice of the R_{FB} value to make a proper calibration and, consequently, a good analysis of the results.

To study the performance of the device and to evaluate if it is suitable for saliva measurements, synthetic saliva standards with different concentrations of NH_4^+ were prepared. Next chapter presents the results obtained with the developed sensor prototype.

Chapter 5

Performance of the Sensor Prototype and Discussion

This chapter presents the results obtained with the developed sensor prototype. Since the detection method is based on MWCNTs-based sensor films, their characterization was made in first place. After the characterization of the films, it was tested if variations of their electrical characteristics (resistance and capacitance) could be detected by the IMC, in standard samples with different concentrations of NH_4^+ . A comparison between the NH_3 detection method developed here and that described in [30] is also made in this chapter. Finally, it is presented the performance of the overall prototype making use of standard samples of synthetic saliva that mimic its targeted final application.

5.1 - Characterization of the Multiwalled Carbon Nanotubes-based Films

5.1.1 - Chemiresistive sensor film

5.1.1.1 - Measurement of the initial resistance

In the development of the chemiresistive sensor film, the length was considered a variable to understand if its value could influence the resistance of the film. Thus, three sensor films with different lengths were fabricated, as already mentioned in the previous chapter (subsection 4.3). For an easier understanding and writing, the three sensor films are named according to their lengths: 4L-film (length = 40 mm), 2L-film (length = 20 mm) and 1L-film (length = 10 mm).

The initial resistance of each film was measured with a Protek 506 digital multimeter and the results are in Table 5.1. When comparing the 4L-film and the 2L-film, it is verified that

Table 5.1 – Initial resistance values of the three chemiresistive sensor films.

Length (mm)	MWCNTs mass (mg)	Resistance (Ω)
40	17.6	506
20	13.3	236
10	11.1	817

there is a decrease of the resistance with the length decrease. Resistance (R) is an electric parameter that can be defined by equation (5.1) [52]:

$$R = \rho \times \left(\frac{L}{A}\right), \quad (5.1)$$

where ρ is the material resistivity, L the length and A the area of the structure. Since the resistance is directly proportional to the length, the obtained result is explained. In [66], the behaviour of individualized SWCNTs with SWCNTs arrays is compared for the development of FETs, in which the channel length was a variable. In that study, it was also verified that the conductivity of the device with individualized SWCNTs increased inversely with the channel length.

However, when analyzing the initial resistance of the 1L-film, the obtained value does not follow the same reasoning. Indeed, the resistance of this sensor film is higher than the other two. The reason for this may be associated to the quantity of MWCNTs deposited in the 1L-film. This sensor film has a smaller area, and so the quantity of MWCNTs that covers the surface of the film is lower. A smaller quantity of the nanostructures can be the motive for the obtained result. Since carbon nanotubes are structures that allow the conduction of electric current, the fact of existing in small quantities can influence the conductivity of the sensor film, and consequently its resistance. Equation (5.1) also demonstrates the inverse proportionality between resistance and the area of the structure. These two facts may lead to the conclusion that there is a trade-off between the length and the quantity of MWCNTs in determining the resistance value of the sensor films in which the MWCNTs mass may be the governing parameter.

5.1.1.2 - Relative variation of resistance, response and recovery times

The first tests were carried out using the 4L-film. These were done according to the procedure described in the previous chapter. The sample of NH_4^+ and a NaOH solution are aspirated and mixed at a confluence. This promotes the conversion of NH_4^+ into NH_3 . After, the standard follows to the GDU's donor channel where the NH_3 gas molecules diffused through the hydrophobic membrane into the gap created by the additional piece and where the sensor film is placed. To characterize the response of the sensor film to the target gas, a Protek 506 digital multimeter was connected to the electrical contacts of the film. After each measurement, the sensor film went to a cleaning process.

The first range of ammonium concentrations considered to see if the sensor film responds to the target gas was 1-5mg/l. The resistance values for each concentration were taken in the moment when the sensor film resistance stabilized under a continuum flux of the sample through the donor channel, at room temperature. In this work, the relative variation of the film's resistance (V_R) was calculated with equation (5.2):

$$V_R(\%) = \frac{R_{NH_3} - R_{CNT}}{R_{CNT}} \times 100, \quad (5.2)$$

where R_{NH_3} corresponds to the film resistance in the presence of ammonia and R_{CNT} is the initial resistance of the MWCNT sensor film.

This procedure was repeated three times, in three different days, to prove the sensor repeatability. Figure 5.1 shows the relative variation of the film's resistance plotted as a function of NH_4^+ concentration. The respective fitting curves are presented in table 5.2.

When analyzing Figure 5.1, it is observed that the V_R increases with the NH_4^+ concentration in all the three measurements. This relation demonstrates the increase of the resistance value with the increase of NH_3 concentration, and is in agreement with the results presented elsewhere [65-67]. The NH_3 molecule presents a lone electron pair which can be donated to other species (NH_3 behaves like an electron donor). When the film sensor is exposed to the gas molecules, NH_3 donates these electrons to the valence band of MWCNTs increasing the resistance of the sensor film. This result also demonstrates that the film presents a p-type semiconductor behaviour which is also in agreement with the literature [50,52,66,67]. With the decrease of holes concentration (positive charge carriers), due to the electrons donated to the carbon nanotubes, the resistance of sensor film increases.

The best linear fit was obtained for the second measurement (Table 5.2), where the R^2 value is closer to 1. The three measurements were made in three different days, which implies the reassemble of the GDU including the placement of the membrane, the additional piece, the sensor film and the cover. This assemble process could influence the performance of the prototype since a wrong placement of the sensor film on the additional piece could lead to a

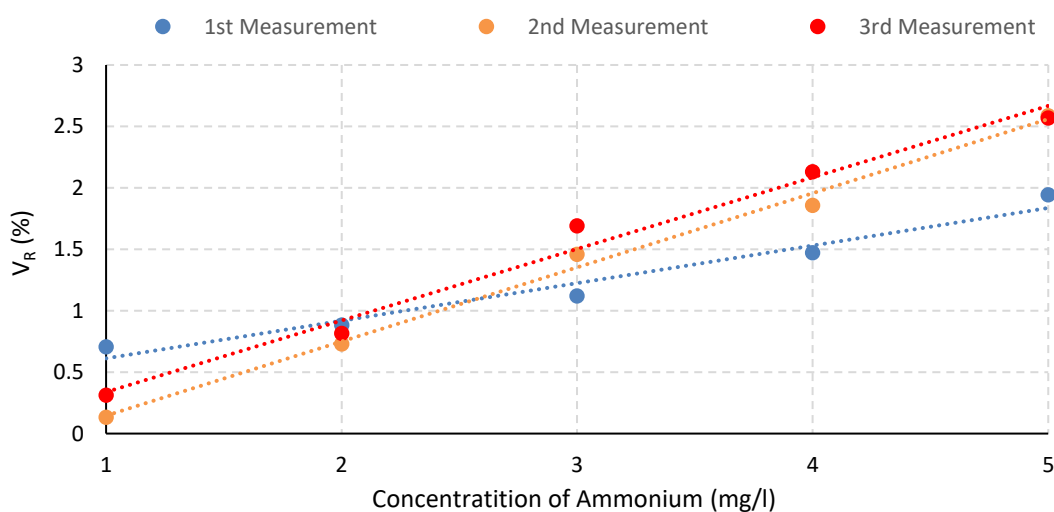


Figure 5.1 - Relative variation of the 4L-film's resistance as a function of various NH_4^+ concentrations (1-5 mg/l) at room temperature. The dashed lines correspond to the linear fitting curves of each measurement.

Table 5.2 - Linear fitting curves for the three measurements made with the 4L-film for an ammonium concentration range of 1-5 mg/l.

Measurement	Equation curve	R ² value
1	$y = 0.3061x + 0.3061$	0.963
2	$y = 0.6034x - 0.4576$	0.9939
3	$y = 0.5823x - 0.2442$	0.9828

no exposure of the total area covered by MWCNTs. This reduces the number of MWCNTs active sites for interacting with NH₃ molecules influencing the relative variation of the film's resistance in the first and third measurements.

To be certain that the obtained response is due to the interaction between NH₃ molecules and the MWCNTs, deionized water was passed through the donor channel and no resistance variation was obtained.

When the MWCNTs-based sensor film is exposed to NH₃ molecules, the V_R is in the range of 0.2%-2.6% which can be considered a small variation range. Nevertheless, the concentration range considered in this work is lower than the NH₃ concentration values considered in some of the reviewed literature presented in chapter 3 for sensing mechanisms (including electronic nose and FETs). Even so, for a future optimization, the functionalization of the MWCNTs could be a solution to increase the relative variation of the sensor film's resistance.

In the first measurement (blue circles in Figure 5.1), the response time of the film was measured for each concentration, given by the time elapsed between starting the exposure to the flux and the instant when the resistance value starts to become constant (Table 5.3). These times were also considered for the second and third measurements (orange and red circles in Figure 5.1, respectively). To clean the film after each measurement, NaOH was passed through the donor channel to ensure that there was no more NH₃ diffusing. Also, a flux of dry nitrogen (N₂) with a pressure of 0.2 bar was turned on to allow the desorption of the NH₃ molecules from the nanotubes. N₂ was used as the cleaning gas because it is inert and does not react with carbon nanotubes [68]. The recovery time was taken at the instant when the sensor film reached its initial resistance for the three measurements (Table 5.4).

From Table 5.3, it can be observed that the response time increases with increasing gas concentration. In [67], it was reported that with an increase of gas concentration, the interaction between CNTs and NH₃ molecules increase as well. This may lead to the adsorption of some molecules on the CNTs wall, while "other molecules must diffuse into the CNT film to find available sites". This process may be responsible for the increase of the response time with increasing gas concentration. The maximum response time obtained was 1680 s (28 min), which can be considered a high time when compared to the systems reported in the literature. However, in many investigations, a specific time cycle for measuring the CNTs-based sensor response to the NH₃ molecules is defined. In [70], three 10 min cycles are used for evaluating the gas sensing mechanism of a vertically aligned MWCNTs-based sensor. Ma [50] also uses periods of 10 min to characterize the response of a resistive MWCNTs-based sensor when exposed to a 100 mg/l of NH₃.

Table 5.3 – Response time of the 4L-film for the ammonium concentration range of 1-5 mg/l.

Ammonium concentration (mg/l)	Response time (s)
1	240
2	600
3	960
4	1320
5	1680

Similarly, it can be observed in Table 5.4 that the recovery time also increases with the NH_4^+ concentration in each measurement. It is the kinetic energy of the N_2 that removes the NH_3 molecules adsorbed in the carbon nanotubes. It is reported in [48] that the adsorption energy of NH_3 within a SWCNT is very low (<0.2 eV) allowing that the cleaning of the developed prototype could be made based on this information. However, for higher NH_3 concentrations, the recovery time is high having a maximum value of 1200 s (20 min). In [71], it is also verified a slow recovery time of the developed resistive MWCNTs-based film sensor when exposed to NH_3 . The researchers attribute this result to the “excellent adsorption capacitance on the surface of MWCNT” contributing to the slower release of the gas. To overcome this issue, they recommend to increase the temperature as a process for improving the desorption of the NH_3 molecules from MWCNTs surface.

It is important to highlight that the recovery time presented is the time when the initial resistance of the sensor film was achieved. However, it was noticed that stopping the flux of N_2 , the resistance continued to increase. This means that the kinetic energy of N_2 is sufficient for causing the desorption of the NH_3 molecules from the MWCNTs but is not enough to push them out of the GDU. It is needed more time for the overall system to be stabilized in the initial resistance value.

Table 5.4 – Recovery time of the 4L-film for the ammonium concentration range of 1-5 mg/l.

Ammonium Concentration (mg/l)	Recovery Time (s)		
	1 st Measurement	2 nd Measurement	3 rd Measurement
1	35	23	10
2	58	60	35
3	170	120	200
4	200	240	371
5	600	1140	1200

5.1.1.3 - Comparison with the Flow Analysis Spectrophotometric Technique

The measurement process developed here is based on the work made by Segundo et al. [30]. In that research, the detection of a NH_3 concentration in the range of 0.1-5.0 mg/l was achieved using a spectrophotometric analysis detection method. To compare the system developed here with that one, the relative variation of the 4L-film's resistance to a NH_4^+ concentration in the same range of 0.1-0.5 mg/l was also measured. These experiments were carried out under the same conditions adopted in the previous measurements where the film's V_R was obtained. However, since the sample volume used in the first tests was too high, it was decided to measure the sensor response in a restrict time of 13 min, the time needed to consume 50 ml of an ammonium sample. This condition is based on the time cycles issue considered in other reports already mentioned.

Figure 5.2 shows the results obtained for the relative variation of the 4L-film's resistance as a function of NH_4^+ concentration. It can be noticed that the resistance variation is not consistent with the concentration.

The first measurement (yellow circles in Figure 5.2) was made after the third measurement made with a NH_4^+ concentration in the 1-5 mg/l range (red circles in Figure 5.1). As it can be seen from Figure 5.2, the V_R in the first measurement is the same for NH_4^+ concentrations of 0.1-0.4 mg/l, differing only for a concentration of 0.5 mg/l. In addition, comparing with the second and third measurements in Figure 5.2, the V_R in the first measurement is higher. This issue can be due to an incomplete cleaning of the system in the previous measurement leaving behind some NH_3 molecules that influenced the first measurement presented in Figure 5.2.

The second and third measurements shown in Figure 5.2 were done in different days. It is observed that the sensor film responds, but there is not a clear relation between the NH_4^+ concentration and the relative variation of the resistance.

The concentrations reported for NH_3 in a healthy individual are in the range of 18.73-206.08 mg/l [70,71]. As concluded in chapter 2, the presence of a pathology is usually associated with high values of urea, and consequently, higher values of the complex $\text{NH}_4^+/\text{NH}_3$. Since the developed sensor film can detect NH_4^+ concentrations as low as 1mg/l, its final application is not compromised.

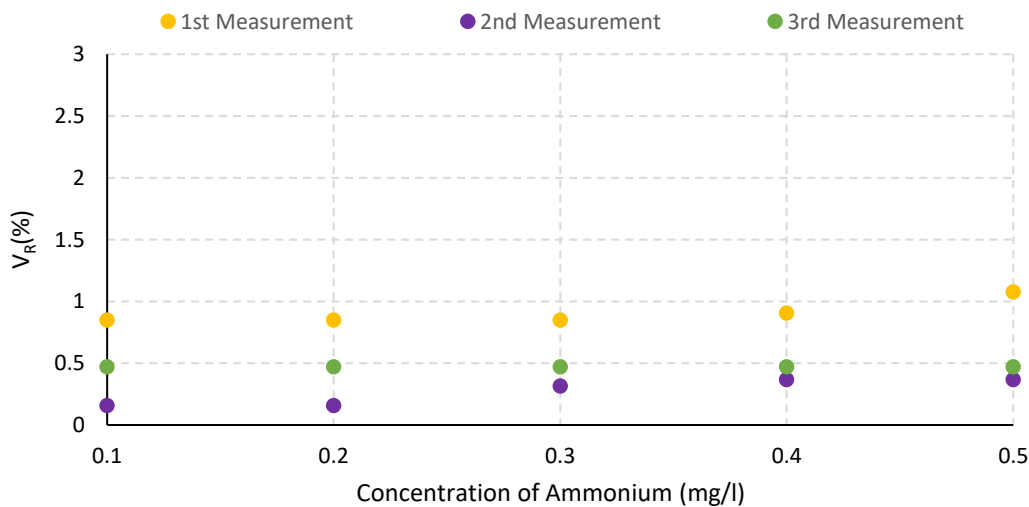


Figure 5.2 - Relative variation of the 4L-film's resistance as a function of various NH_4^+ concentrations (0.1-0.5 mg/l) at room temperature.

5.1.1.4 - Influence of the sensor film's length on the relative variation of its resistance

To see if the length of the sensor film influences its performance when interacting with NH_3 , two more MWCNTs-based sensor films with different lengths were developed: one with 20 mm of length (2L-film) and other with 10 mm of length (1L-film). These trials were done in the same conditions as the previous measurements made to evaluate the relative variation of the 4L-film's resistance in a continuum flux. Once the repeatability of the 4L-film to detect NH_4^+ concentration in the of 1-5mg/l range was proved, only one measurement was performed with these two sensor films. However, their response was recorded for a restrict time of 13 min considering the reason stated in the previous experimental tests.

Because the relative variation of the 4L-film's resistance was recorded with different response times, to evaluate the influence of the film's length on its performance, the comparison of the response of the three films was plotted as a function of the NH_4^+ mass (Figure 5.3). This is possible because the tube caudal where the sample is transported is known (3.25 ml/min).

As it is shown, the V_R of the three sensor films increases with increasing mass of NH_4^+ . This is explained by the same interaction between NH_3 molecules and MWCNTs already detailed. In subsection 5.1.1.1, it was observed that the length influences the absolute value of the resistance. However, when comparing the relative variation of the resistance in the three sensors, their behaviour is the same. 2L-film seems to achieve a higher response than the other two films. Since all the measurements were done in different days, the same issue of the system assemble remains.

The recovery times for 2L-film and 1L-film are presented in Table 5.5. The cleaning of both films was performed in the same way as described for the 4L-film. In both 2L-film and 1L-film, the recovery time increases with the mass of NH_4^+ converted into NH_3 and diffused through the hydrophobic membrane. This relation is the same as the one observed for the 4L-film recovery time.

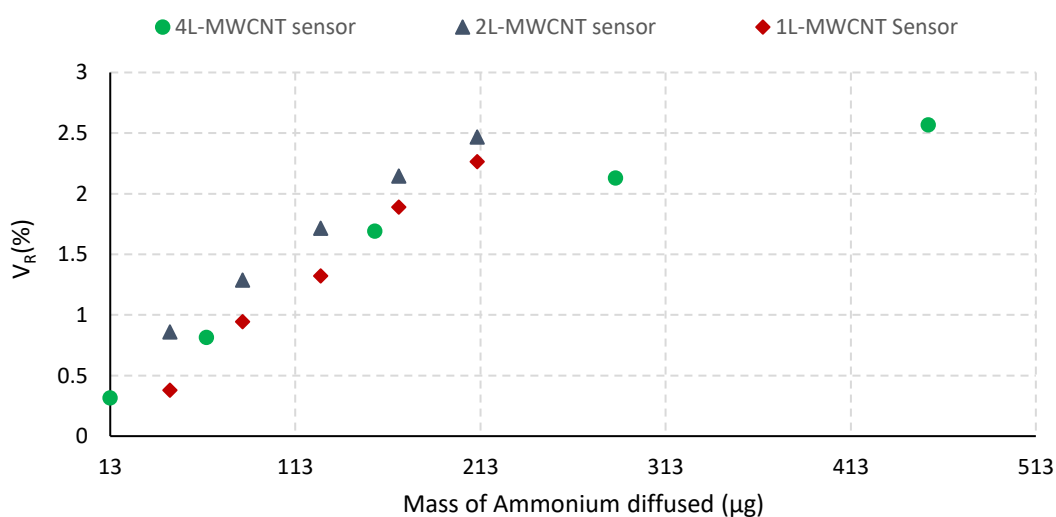


Figure 5.3 - Relative variation of the resistance of the three sensors of different lengths as a function of the mass of NH_4^+ diffused.

Table 5.5 – Recovery time of the 2L-film and 1L-film for the ammonium concentration range of 1-5 mg/l.

Mass of NH_4^+ diffused (μg)	Recovery time (s)	
	2L-film	1L-film
45.25	60	9
84.5	180	170
126.75	340	282
169	600	480
211.25	1100	1020

5.1.1.5 - Performance of the sensor film within a static flux

The volume of the samples used in the previous trials was 50 ml. However, when thinking about collecting saliva, this could be a large volume. The time the mix of the sample with NaOH takes to reach the waste recipient is 36 s. To decrease the sample volume used, it was thought to test the system with a static flux, passing the sample only during the 36 s and waiting until the resistance becomes constant. The cleaning process after each measurement was made in the same way as in the previous trials.

The response of the 4L-film to a NH_4^+ concentration range of 1-5 mg/l for a static flux is shown in Figure 5.4. Now, three sequential measurements were made with the same concentration and the results obtained reflect the average value of the relative variation of the film's resistance for each concentration. It is observed that the sensor film can respond but it cannot distinguish different concentrations. For NH_4^+ concentrations of 1-3 mg/l, the V_R is always the same, increasing when NH_4^+ concentrations of 4 and 5 mg/l are used.

After these measurements, a sample of NH_4^+ with a concentration of 2 mg/l concentration was passed in the donor channel in a continuum flux for 13 min, implying the use of a 50 ml NH_4^+ sample. The concentration used corresponds to 84.5 μg of NH_4^+ converted into NH_3 and diffused through the membrane. The response of the sensor film was 0.94 % for this mass of ammonium,

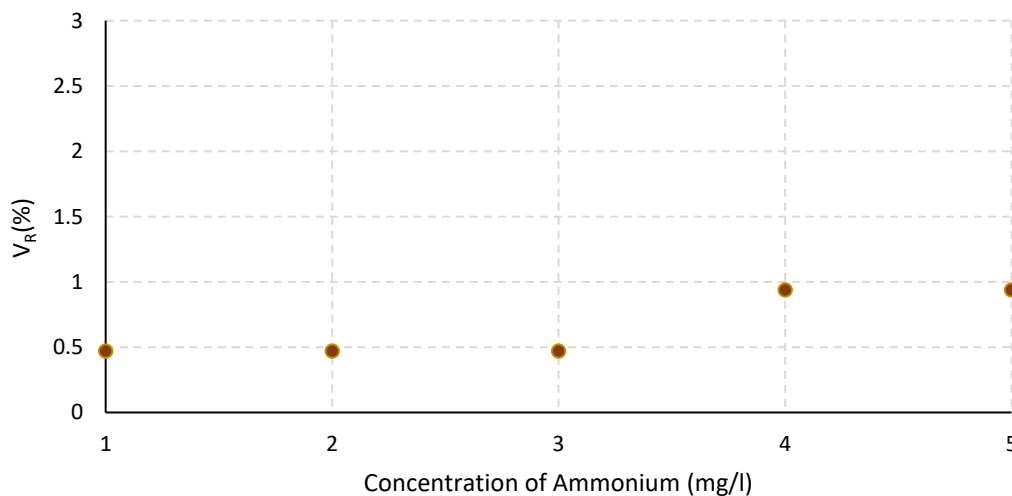


Figure 5.4 - Measured response of the 4L-film to various NH_4^+ concentrations (1-5 mg/l) at room temperature, in a static flux. The relative variation of film's resistance was plotted as a function of NH_4^+ concentration.

which is in agreement with the results obtained for the measurements of the V_R presented in Figure 5.3. This means that a better performance of the system is reached with a continuum flux.

It is believed that the explanation for this can be due to the concentration gradient created between the two sides of the hydrophobic membrane: the donor channel and the gap created by the additional piece for the gas accumulation and interaction with MWCNTs. When the sample flux is continuum, a concentration gradient is created between the two sides of the membrane allowing the continuum NH_3 diffusion from the sample passing in the donor channel to the gap. Stopping this sample's flux, an equilibrium between the concentrations of the both sides of the membrane will be achieved earlier and the NH_3 diffusion will stop, decreasing the system response.

It was also tried to reduce the sample volume to 25 ml passing in a continuum flux, but the sensor film response was also lower when compared with that observed with 50 ml sample.

5.1.2 - Capacitive sensor film

5.1.2.1 - Initial capacitance measurement

In the literature, it was reported that the capacitance of CNTs based sensors could also change when these nanostructures are exposed to NH_3 molecules [50,55,72]. A capacitive sensor film was also developed to investigate whether a CNTs based capacitive sensor presents better detection capabilities.

The capacitance measurements were done using an impedance meter IX 3131 from Metrix. The capacitive sensor film presented an initial capacitance of 0.26 nF at a frequency of 1 kHz. The instrumentation used for the capacitance measurements only allows two frequencies: 120 Hz and 1 kHz. At a 120 Hz frequency, the capacitance value of the sensor film could not be read. This is because the initial capacitance presented by the sensor at 1 kHz is a low value and for these type of capacitors, higher frequencies are suggested [75].

5.1.2.2 - Relative variation of capacitance and recovery time

In the experiments relative to the chemiresistive sensor film, it was demonstrated that the system could operate with a NH_4^+ concentration in the 1-5mg/l range, having a good performance with measurement times of 13 min for each concentration in a sample continuum flux. Due to these reasons, the capacitive sensor film response was studied in the same NH_4^+ concentration range and the measurements were performed under the same conditions. The cleaning process of the film was made in the same way as for the chemiresistive sensor film, passing NaOH in the donor channel after each measurement and then, N_2 with a pressure of 0.2 bar for the molecules desorption.

The relative variation of the film's capacitance (V_C) was calculated using equation (5.3):

$$V_C(\%) = \frac{C_{\text{NH}_3} - C_{\text{CNT}}}{C_{\text{CNT}}} \times 100, \quad (5.3)$$

where C_{NH_3} corresponds to the sensor film capacitance in the presence of ammonia and C_{CNT} is relative to its initial capacitance.

Figure 5.5 shows the relative variation of the film's capacitance plotted as a function of the NH_4^+ concentration for a frequency of 1 kHz. The results for each concentration are the average value of three consecutive measurements made for each one. All measurements were made in the same day.

Observing the obtained results, it can be verified that the capacitive sensor film has a higher capacitance variation when compared with the response obtained for chemiresistive sensor film. Indeed, the capacitive film shows a maximum variation of its capacitance value of 13.8% (at a NH_4^+ concentration of 5 mg/l), while the chemiresistive sensor film only can reach a maximum variation of 2.56% in its resistance (Figure 5.3). Sánchez et al. [55] also verified that the capacitance variation in the ammonia sensor based on SWCNTs developed by them was higher than the resistance variation.

To ensure that the capacitance variation obtained for the developed sensor film is due to the interaction of NH_3 molecules with MWCNTs, deionized water was passed through the donor channel and no capacitance change was observed.

Although the film's V_C is high when expose to NH_3 molecules, it seems that there is no specific relation with the NH_4^+ concentration. With 1 and 2 mg/l of NH_4^+ , the film response seems to be the same. Also, there is an increase followed by a decrease when the NH_4^+ concentration of 3 mg/l changes to 4 mg/l. The value of R^2 shows that there is no perfect linear fit between the linear fitting curve and the relation obtained for the capacitance values as a function of the NH_4^+ concentration. Because of this, nothing can be concluded form the behavior of the capacitive sensor film developed in this work. In the literature, it is reported that the capacitance of sensors made with carbon nanotubes increases with their exposure to NH_3 . The authors of [74] developed a vertically aligned carbon nanotubes-based ammonia and formic acid sensor. In this research, they detect the gradual increase of the capacitance when NH_3 reacts with CNTs, obtaining a response of 2% for 1 mg/l of NH_3 and 10% when using a NH_3 concentration of 15 mg/l. Also, in [50,74], the same behavior of CNTs capacitance was observed when interacting with NH_3 gaseous molecules.

The recovery time was also measured for each concentration. The values presented in Table 5.6 are the average values of the three times taken for each three measurements of the same

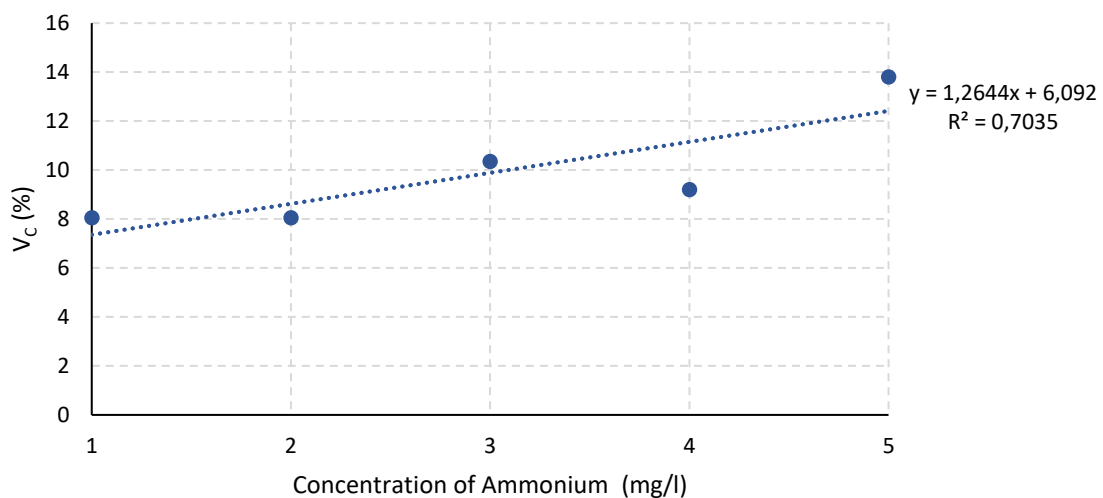


Figure 5.5 - Relative variation of the film's capacitance to various NH_4^+ concentrations (1-5 mg/l) at room temperature for a frequency of 1 kHz. The linear fitting curve is also presented as well as the R^2 value.

concentration. As it can be observed, there is also no specific relation between the recovery time with the NH_4^+ concentration. Between 1-3 mg/l of NH_4^+ , the time increases followed by a decrease when using a sample with 4 mg/l of NH_4^+ . With 5 mg/l, it is observed an increasing of the recovery time, again. These observations reinforce the inexistence of final conclusions that can be taken with these measurements, pointing to the need of further studies with the capacitive sensor film.

Table 5.6 – Recovery time of the capacitive sensor film with ammonium concentration in the range of 1-5 mg/l.

Ammonium concentration (mg/l)	Recovery time (s)
1	240
2	720
3	900
4	840
5	1020

5.2 - Measurements with the Impedance Measurement Circuit

5.2.1 - Chemiresistive sensor film

To evaluate the performance of the overall prototype in the detection of NH_3 , in this point of the project, experimental trials were performed with the developed impedance measurement circuit.

The sensor prototype was first tested with the 4L-film. However, after the measurements it was detected that the hydrophobic membrane was damaged. This lets the fluid pass to the gap and wet the film. Since CNTs are also sensible to water molecules in a way that their resistance increases in the presence of water [75,76], this sensor film could not be reused. This empathizes again the importance of a correct assemble of the GDU.

As demonstrated previously, the sensor films' length does not interfere in the relative variation of the resistance. Thus, the 2L-film was used for the trials.

The experiment was done with the same time cycle and flux conditions for each measurement: periods of 13 min for each one and a continuum flux of NH_4^+ samples (50 ml). The cleaning process was the same as in the previous tests.

To evaluate if the IMC gives a reliable reading of the sensor film response, firstly the measurements were taken with the Protek 506 digital multimeter, as in the previous tests, and then with the IMC. The results are shown in Figure 5.6. The calibration of the system was made with an R_{FB} value of 100 Ω . Since the IMC measurement process includes a frequency sweep, as explained in chapter 4, the values presented for each concentration are the average value obtained for a frequency sweep of 10-100 kHz. The frequency range is not relevant, because resistance does not vary with frequency, nevertheless this averaging allows reducing the measurement noise.

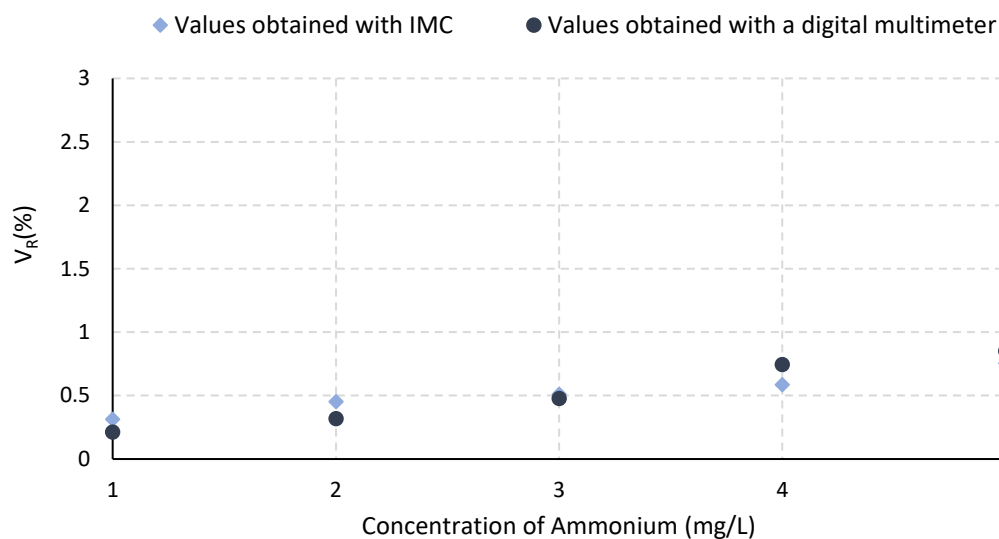


Figure 5.6 - Comparison of 2L-film response using a digital multimeter and the developed IMC.

As it can be observed, the response obtained with the IMC is similar to the one obtained with the multimeter. It is observed an increase of the resistance with the NH_4^+ concentration in both measurements. However, comparing these results with the ones obtained in the Figure 5.3, one can notice a decrease of the relative variation of film's resistance. Here, the maximum response of the sensor film only reaches 0.8% for a concentration of 5 mg/l while in the previous measurements it reached 2.5% for the same concentration. After these trials, when the GDU was disassemble it was verified that some of the nanotubes fallout from the sensor film (Figure 5.7). This implies a decrease of the number active sites available for the adsorption of NH_3 molecules and, consequently a decrease of the V_R [69]. It is believed that this problem could be related to two issues: the adhesion of the MWCNTs at the substrate that may imply a better optimization of the ink used in the development of the sensor film, or the pressure of N_2 flux in the cleaning process that may be too strong and causes the desegregation of the nanostructures from the substrate. Further studies are needed to better understand this question and optimize this feature.

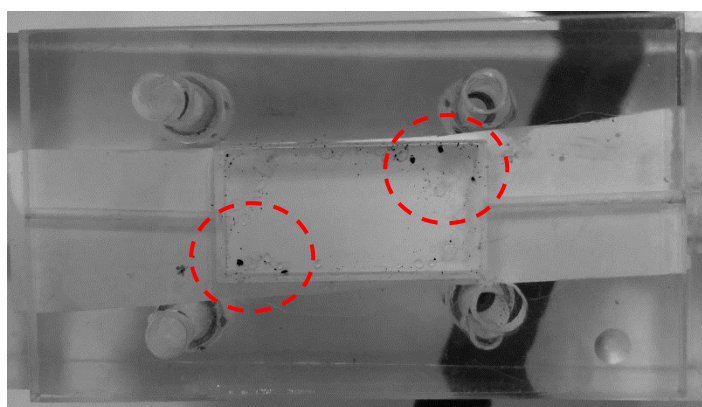


Figure 5.7 - Carbon nanotubes deposited in the membrane (red circles) after the disassemble of the GDU.

5.2.2 - Capacitive sensor film

Although the results obtained for the capacitive sensor film in subsection 5.1.2.2 were not conclusive, it was tried to measure the impedance variation of the film using also the IMC.

Having as reference value the initial capacitance of the film measured with the impedance meter (C) and knowing its resistance (R=1.435 kΩ), it is possible to calculate the initial impedance (Z) of the sensor film at frequency (f) of 1 kHz. Using equations (5.4) and (5.5), the value of the calculated impedance is around 612 kΩ.

$$X_C = \frac{1}{2\pi f C} \quad (5.4)$$

$$Z = \sqrt{(X_C)^2 + (R)^2}. \quad (5.5)$$

Knowing the initial impedance value, the system was calibrated with a R_{FB} value of 30 kΩ at a frequency of 1 kHz. However, the obtained impedance was 868.68 kΩ, a very different value compared with the one calculated from equation 5.5. In [79], it was reported that for frequencies lower than 5 kHz, there is a problem with the sampling time of the ADC in the reception stage of AD5933 leading to wrong measurements. This was verified when a resistor of 560 kΩ was measured with the IMC at a 1 kHz-10 kHz frequency range, with a calibration resistor of 30 kΩ (Figure 5.8). Indeed, considering the values obtained for a frequency range of 1 kHz-4 kHz, the average error is 36 %, while for a frequency range of 5 kHz-10 kHz the average error is around 3 %. This compromises the impedance measurements using samples with different NH_4^+ concentrations at a 1 kHz frequency.

Once more, further studies are needed for a better understanding of the capacitive sensor film response when exposed to NH_3 molecules. These could include the measurements of capacitance and impedance at different frequencies to obtain a conclusive relation between the film's response and the concentration of NH_4^+ .

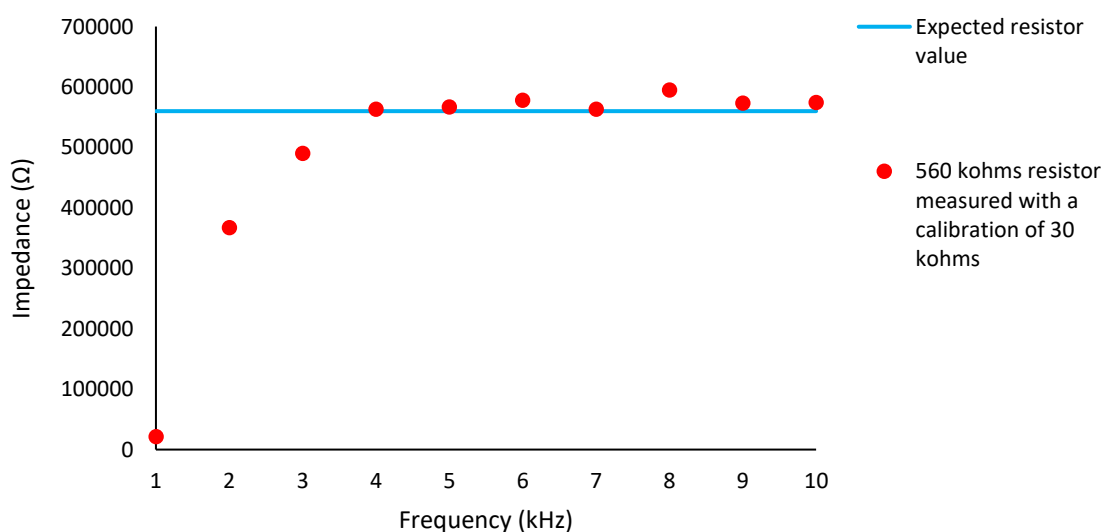


Figure 5.8 - Impedance as a function of frequency for a resistance of 560 kΩ with a $R_{FB}=33$ kΩ.

5.3 - Sensor Prototype Operation with Synthetic Saliva

Because no conclusion could be taken from the behaviour of the capacitive sensor film, the operation of the developed prototype with synthetic saliva was studied only using the chemiresistive sensor film.

The film used for this purpose was the 2L-film, because also the 1L-film was wet due to the same reasons reported before for the 4L-film. These measurements were performed in the same day with the same conditions of the trials presented in subsection 5.2.1. The results obtained for the prototype operation with synthetic saliva are presented in Figure 5.9.

The results presented show that the sensor prototype follows the same behavior when considering synthetic saliva samples and deionized water samples, both with different concentrations of ammonium. Indeed, when using synthetic saliva, the variation of the resistance increases with NH_4^+ concentration. This is explained by the interaction between the NH_3 gas molecules (formed when NaOH is mixing with the sample) and the MWCNTs, as already reported in subsection 5.1.1.2. However, when compared with the values obtained previously for deionized water samples (light blue lozenges in Figure 5.9), the response of the prototype is higher with synthetic saliva. Between these two measurements, the GDU was disassembled and this may explain the obtained result. It was observed before that the placement of the sensor film influences the active sites of MWCNTS exposed to the gaseous molecules. In the synthetic saliva sample measurements, the sensor film could have been better placed leading to better results. The decreased of the relative variation of resistance when compare with the first results presented in Figure 5.3 was already explained in the subsection 5.2.1.

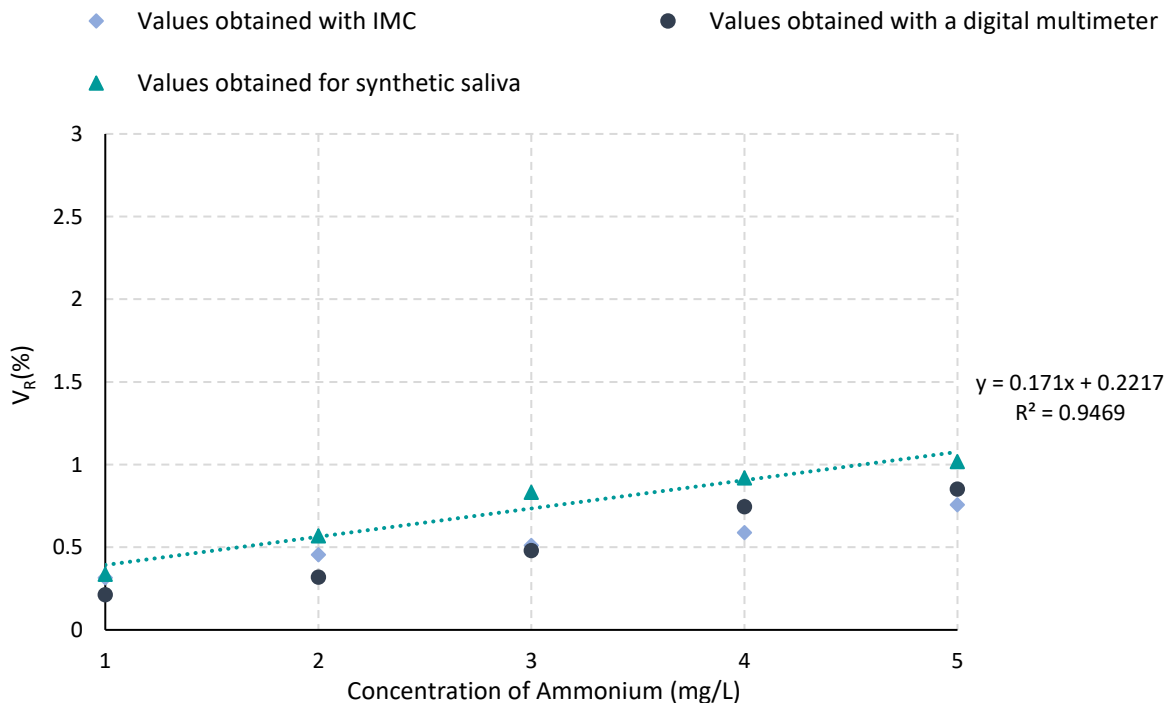
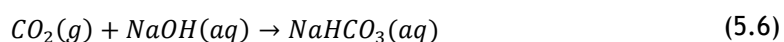


Figure 5.9 - Comparison of 2L-film response using deionized water and synthetic saliva standard samples, both with different NH_4^+ concentrations (1-5 mg/l). The linear fitting curve for the measurements of the synthetic saliva standards (light green dash line) is represented as well.

The obtained fitting curve of the prototype response to synthetic saliva standards is also shown on Figure 5.9. However, the issue reported previously about the fallout of the nanotubes from the film's substrate prevent the use of this curve in further studies to estimate the concentration of NH_4^+ in a real human saliva sample. A new sensor film should be used for this measurement for obtaining a better curve in order to correctly estimate the NH_4^+ concentration.

It was also mentioned the issue of the sample volume when considering saliva. The prototype presents a good performance with samples of 50 ml. The amount of saliva that can be collected is lower than this value. The higher volume of collected saliva read in the literature was 3 ml [5]. Nevertheless, this is not an obstacle for the developed prototype if the saliva dilution is considered. In fact, this dilution will be advantageous for the device performance because the interferents present in saliva will also be diluted (e.g. proteins) having a lower significance in the results. The average ammonia concentration for a healthy subject is around 18.73-206.08 mg/l, much higher values than 1-5 mg/l. But, with the proper saliva dilution, the estimation of the concentration of $\text{NH}_3/\text{NH}_4^+$ can be done with curves obtained in this work because the concentration of the complex $\text{NH}_3/\text{NH}_4^+$ will also be diluted.

Besides NH_4^+ , CO_2 is also a product from urea hydrolysis (equation 3.1). It was reported that carbon nanotubes are sensible to CO_2 which is also an electron donor [50,70,78]. However, this does not represent a problem for the developed prototype since the mixture of the sample with NaOH converts the gaseous CO_2 into aqueous sodium bicarbonate (NaHCO_3) (equation 5.6):



Saliva has also in its constitution some volatile organic compounds (VOCs), but these are present at low levels in human saliva and so, when thinking in the final application of this prototype, the influence of these compounds in the sensor behavior can be discarded [81].

5.4 - Conclusions

The performance of the prototype developed in this work was described in this chapter. The first feature studied was the behaviour of the developed MWCNTs-based sensor films in the presence of NH_3 molecules.

For the chemiresistive sensor film, it was firstly concluded that, the absolute value of the film's resistance can be influenced by the mass of the MWCNTs deposited in the films surface and its length. Regarding the film response to different concentrations of NH_4^+ , it was seen that the relative variation of sensor film's resistance increases with the NH_4^+ concentration. This relation is influenced by the electrons donated by NH_3 to the valence band of MWCNTs. This increase of the MWCNTs resistance when exposed to NH_3 molecules also leads to the conclusion that the chemiresistive sensor film presents a p-type semiconductor behaviour. In addition, the increase of the recovery time of the sensor film with the increase of NH_4^+ concentration was attributed to the good adsorption capacitance on the MWCNTs' surface. Compared with the spectrophotometric technique, the method developed here does not present a low detection limit as the one reported for that technique. However, the final application of the developed prototype is not compromised since the achieved resolution of 1 mg/l is a lower value than the NH_3 concentrations considered for healthy subjects. It was also observed, that the system performed correctly considering a sample volume of 50 ml with time-cycles of 13 min for each measurement. With lower sample volumes, an equilibrium of the concentrations in both side

of the membrane is verified leading to stopping the NH_3 diffusion. For chemiresistive sensor films it was also concluded that the film's length does not influence the relative response of the system when exposed to different concentrations of NH_4^+ . What actually can compromise the relative variation of the film's resistance is the GDU assemble since an incorrect placement of the sensor film in the additional piece may reduce the available sites of MWCNTs exposed to NH_3 molecules affecting the performance of the prototype. A bad assemble of the GDU also includes the damage of the hydrophobic membrane as well as its incorrect placement in the donor channel. This may lead to the passage of fluid to the gap formed by the additional piece where the sensor film is placed. Wetting the film makes it not reusable since water can influence its response. Thus, it is very important to ensure the correct GDU assembling and the good condition of the membrane to guarantee the reliability of the results and the good performance of the prototype.

A capacitive sensor was also developed to understand which one of the electrical characteristics, resistance and capacitance, present a higher variation when exposed to the target gas. Although the capacitive sensor presents a maximum response of 13.8 %, nothing could be concluded because there was a no clear relation between the capacitive variation and NH_4^+ concentration. It was also tried to measure the impedance of the sensor film, but the problem detected in the AD5933 IC at a frequency of 1 kHz limited the measurements. Further studies are needed to understand the capacitance and impedance variation of the MWCNTs when they interact with NH_3 molecules.

When using the impedance measurement circuit as the measurement instrument, it was seen that the result was similar with that obtained with a standard instrumentation. However, the response of the sensor film was lower in both cases when compared with the first obtained results. This was associated to the fall out of the carbon nanotubes from the sensor film surface, which indicates that maybe the ink composition should be optimized or the pressure of the N_2 sensor cleaning flux is so strong that promotes this problem. This observation leads to the conclusion that the chemiresistive sensor film may have a limited life time and, for future applications, it should be replaced after a defined number of measurements.

The results obtained for the prototype when using the chemiresistive sensor film and synthetic saliva samples were encouraging since it presented the same relation between the MWCNTs resistance variation and NH_4^+ concentration. However, new measurements should be made with a new film to obtain a better fitting curve for the future estimation of the NH_4^+ concentration present in a real human saliva sample.

The fact of using sample volumes of 50 ml leads to the need of diluting saliva samples, what is an advantage for reducing the interferences influence in the system and to fit the results in the curves obtained for the estimation of NH_4^+ concentration as a function of the sensor response. Also, it was demonstrated that the CO_2 produced from urea hydrolysis is not a problem for the developed prototype since it is transformed in NaHCO_3 due to the mixing of the sample with NaOH that happens before the sample enters in the donor channel.

In conclusion, the prototype developed here provides a good approach for NH_3 detection. It is sensitive to low concentrations of NH_4^+ (1 mg/l) and simple to use. The incorporation of the IMC allows for a simple and portable data recording and analysis procedure. As it was observed, at this point of the project the chemiresistive sensor film presents a better choice because it promotes a better understanding of the results considering the estimation of NH_4^+ concentration as a function of the resistance variation and a good operation of the IMC. There are some features that need to be optimized, but it is believed that the development of this

prototype is a good starting point for constructing a completely automatic and reliable diagnostics method for detecting pathologies after the analysis of saliva.

Chapter 6

Conclusions and Future Work

6.1 - Conclusions

Because of the many disadvantages associated to the diagnostics means usually employed for detecting pathologies, the analysis of human saliva has arisen as an alternative diagnostics methodology. This is due to the presence of biomarkers in the constitution of this oral fluid. One of these biomarkers is urea, whose increased concentration in saliva was verified to be correlated with some pathologies. That is not the case with dental caries which are associated with a low concentration of this compound.

The fact that a standard method for saliva analysis and collection does not still exist, allied to the fact that the constitution of human saliva depend from patient to patient, are the main reasons why salivary tests are not yet able to replace the traditional diagnostics methods. Nevertheless, it is believed that, in situations where early diagnostics is a critical factor, saliva analysis could become a great alternative. Even when the diagnosis is not conclusive, saliva analysis could help in the correct analysis of the disease.

A NH_3 sensor prototype capable of being used for saliva analysis was developed in this dissertation work. It is based on the urea hydrolysis process. Salivary urea is hydrolyzed in CO_2 and NH_4^+ , which, depending on the pH level, can be converted in its volatile molecular form NH_3 . The developed sensing system comprises carbon nanotubes used as the sensing material for NH_3 molecules together with a flow system, a GDU and an impedance measuring circuit connected to a portable computer. The flow system promotes the mixing of the NH_4^+ sample with a solution of NaOH, responsible for converting NH_4^+ into NH_3 , and the continuum flux through the donor channel which was verified to be a determinant factor for the good operation of the prototype. The adaptations made in GDU allowed the incorporation of the MWCNTs-based sensor film.

Two types of MWCNTs-based films were developed: a chemiresistive sensor film and a capacitive sensor film. At the current time of the project, the chemiresistive film appears to be a better choice than the capacitive film. Although the response of the capacitive film was higher than the obtained for the chemiresistive, no conclusions could be drawn regarding the relation between the capacity variation and the NH_4^+ concentration. With the chemiresistive

films, it was possible to observe the increase of resistance with increasing target analytes, a result that is in agreement with other found in the literature. In addition, when using IMC and synthetic saliva samples, the results obtained with the chemiresistive sensor film were in agreement with those taken with a digital multimeter, encouraging the possibility of a good performance of the prototype with real human saliva samples. Also, it was demonstrated that the sensor films' length does not influence the relative variation of the films' resistance allowing the use of smaller films, what will be an advantage for making cheaper devices. The major issues related to this work are the GDU assemble, membrane condition and limited lifetime of the film.

It is concluded that the prototype developed here is an encouraging starting point for the construction of an automatized and reliable diagnostics device based on the analysis of saliva. The fact that all prototype components can be assemble in a single structure gives it the possibility of making it portable. This enables the utilization of this method in other environments rather than only in the laboratory, favouring the use of this process as a point-of-care in places where the conditions required by the usual diagnostic methods are not provided (e.g. developing countries). It is true that further studies are needed to optimize the developed prototype and to better understand some questions related to the overall process, but it constitutes a step forward in the chance of using saliva analysis as an alternative diagnostic procedure.

6.2 - Suggestions for Future Work

One of the adaptations made in GDU was the incorporation of an additional piece which has a thickness of 3.5 mm. The gap created by this piece allows the accumulation of the gas. However, it remains the doubt that if the piece was thinner there would be a better interaction of the target gas with the carbon nanotubes. Thus, it would be important to study if this parameter has some influence in the interaction of the diffused NH_3 molecules with carbon nanotubes by developing other additional pieces with different thicknesses.

The idea behind the prototype operation is the diffusion of NH_3 which is formed due to the mixing of the NH_4^+ sample and NaOH solution. However, it is not known the exact quantity of NH_3 that is diffused through the hydrophobic membrane. Further studies are needed to better understand the NH_3 diffusion rate allowed by flow system because it could influence the sensor film response.

It was observed that the chemiresistive sensor film reached to a maximum response of 2.56 % for the NH_4^+ concentration of 5 mg/l. It should be investigated if the functionalization of MWCNTs could improve its response. Other issue related to the performance of the prototype is its high recovery time. Studies made with increased sensor cleaning temperatures should be made to evaluate if this parameter could be reduced. In addition, it was also mentioned that to completely clean the system, it takes more time than the one reported in subsection 5.1.1.2. To overcome this problem, an optimization of the cleaning system is needed. This optimization can be based on developing a mechanism that can pull out the target gas at the moment that N_2 is passing through the sensor.

Further research is also needed to better evaluate the capacitive sensor film response, making measurements at different frequencies. The measurements taken with the IMC to measure the impedance variation of the capacitive sensor were compromised by the IMC operation at a frequency of 1 kHz. The AD5933 IC allows measuring also the impedance phase. However, this is a very complex process because of the additional calculation that should be done. Besides, the additional analogue circuit also affects the phase value of the impedance. A study of the

frequency response of the additional analogue circuit it will also be important to better understand the average errors associated to each measurement.

Besides CNTs-based chemiresistive and capacitive sensors, FETs are another sensor configuration that can be used when carbon nanotubes are considered as sensing material. One of the possible future investigations should be the development of this type of sensor and the study of its response in the developed prototype.

Another interesting feature to develop in future investigations includes an interface that allows an immediate perception of the NH_4^+ values present in the analyzed sample and that could automatically give the condition of the patient based on the NH_4^+ obtained values. This would make the diagnostics system even more automatized and simple for users.

Finally, the prototype response should be studied using real human saliva samples taken from healthy and unhealthy subjects.

Appendix A

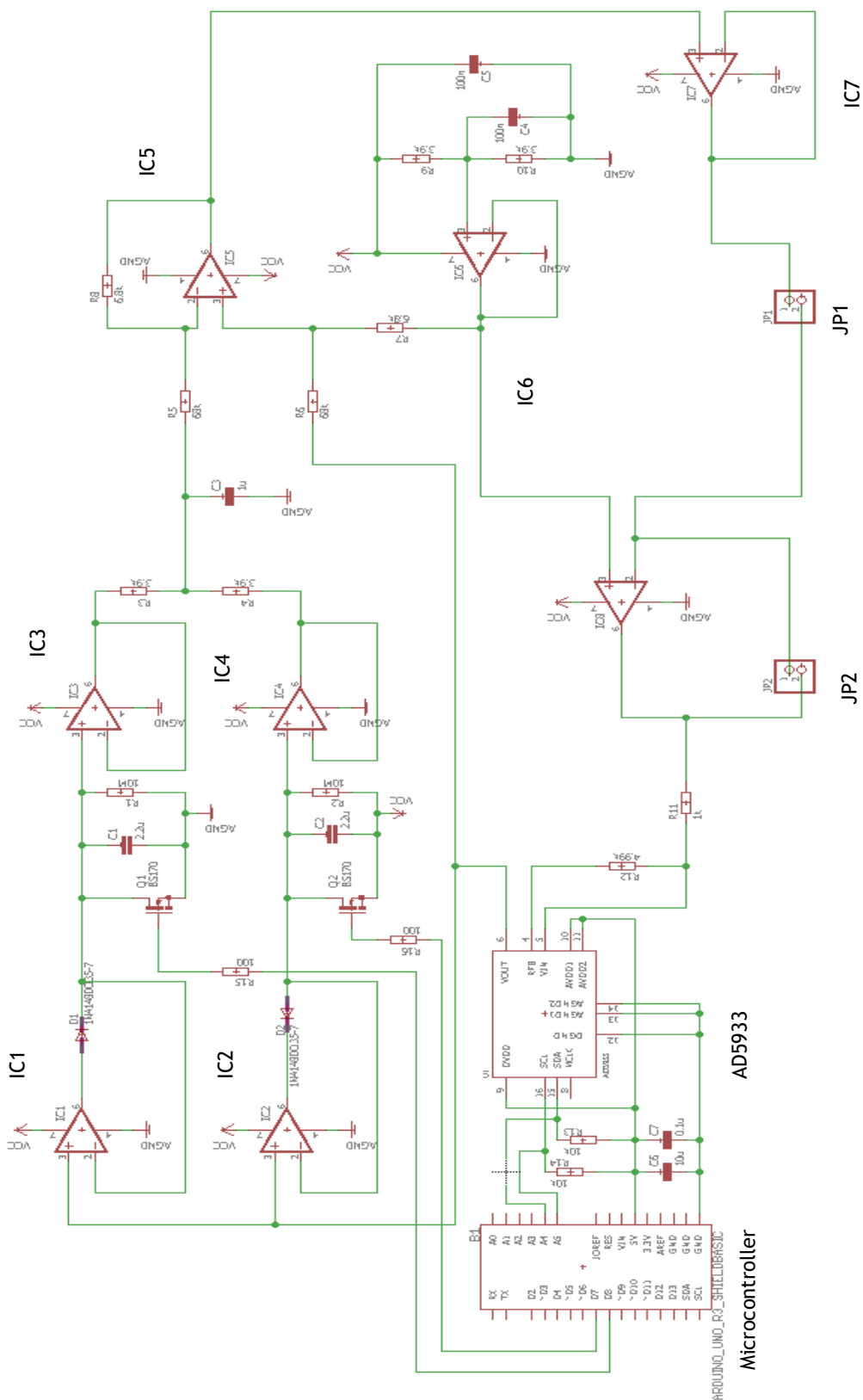


Figure A.1 - Additional analogue circuit connected to AD5933 IC (scheme design on Eagle).

References

- [1] P. Bruno, "The importance of diagnostic test parameters in the interpretation of clinical test findings: The Prone Hip Extension Test as an example.," *J. Can. Chiropr. Assoc.*, vol. 55, no. 2, pp. 69-75, 2011.
- [2] J. Murphy, "A correct Diagnosis is of Increasing Importance," *Irish Medical Journal*, 2016. [Online]. Available: <http://imj.ie/a-correct-diagnosis-is-of-increasing-importance-2/>. Accessed at 18th december, 2017.
- [3] J. K. M. Aps and L. C. Martens, "Review: The physiology of saliva and transfer of drugs into saliva," *Forensic Sci. Int.*, vol. 150, no. 2-3, pp. 119-131, 2005.
- [4] S. Chiappin, G. Antonelli, R. Gatti, and E. F. De Palo, "Saliva specimen: A new laboratory tool for diagnostic and basic investigation," *Clin. Chim. Acta*, vol. 383, no. 1-2, pp. 30-40, 2007.
- [5] T. Lasisi, Y. Raji, and B. L. Salako, "Salivary creatinine and urea analysis in patients with chronic kidney disease: a case control study," *BMC Nephrol.*, pp. 1-6, 2016.
- [6] B. Lisowska, "Role of Uremic Compounds in Organ Injury," *J. Nephrol. Ther.*, vol. 05, no. 03, pp. 3-6, 2014.
- [7] W. Chen *et al.*, "Biochemical pathways of breath ammonia (NH₃) generation in patients with end-stage renal disease undergoing hemodialysis," *J. Breath Res.*, vol. 10, p. 36011, 2016.
- [8] R. Evans *et al.*, "Diagnostic Performance of a Saliva Urea Nitrogen Dipstick to Detect Kidney Disease in Malawi," *Kidney Int. Reports*, vol. 2, no. 2, pp. 219-227, 2017.
- [9] P. Bertocchi, D. Compagnone, and G. Palleschi, "Amperometric ammonium ion and urea determination with enzymebased probes," *Biosens. Bioelectron.*, vol. 11, no. 1-2, pp. 1-10, 1996.
- [10] E. B. Zabokova, A. I. Sotirovska, and V. Ambarkova, "Correlation between Salivary Urea Level and Dental Caries," *Prilozi, Odd. biol. med. Nauk.*, vol. 302, pp. 289-302, 2012.
- [11] M. A. Javaid, A. S. Ahmed, R. Durand, and S. D. Tran, "Saliva as a diagnostic tool for oral and systemic diseases," *J. Oral Biol. Craniofacial Res.*, vol. 6, no. 1, pp. 67-76, 2016.
- [12] Y. Zhang, J. Sun, C. C. Lin, E. Abemayor, M. B. Wang, and D. T. W. Wong, "The emerging landscape of salivary diagnostics," *Periodontol. 2000*, vol. 70, no. 1, pp. 38-52, 2016.
- [13] D. Malamud, I. R. Rodrigues-Chavez, B. J. Janssen, Z. Luo, K. R. Everette, and J. Rees-George, "Saliva as a Diagnostic Fluid," *Dent Clin North Am.*, pp. 159-178, 2011.
- [14] M. Shirzaiy, F. Heidari, Z. Dalirsani, and J. Dehghan, "Estimation of salivary sodium , potassium , calcium , phosphorus and urea in type II diabetic patients," *Diabetes Metab. Syndr. Clin. Res. Rev.*, vol. 9, no. 4, pp. 332-336, 2015.
- [15] F. Khozeimeh, N. Torabinia, S. Shahnaseri, H. Shafaei, and A. Mousavi, "Determination of salivary urea and uric acid of patients with halitosis," *Dent. Res. J. (Isfahan).*, vol. 5, pp. 14-241, 2017.
- [16] C. Carda, N. Mosquera-Lloreda, L. Salom, M. E. Gomez De Ferraris, A. Peydró, and D. C. Carda, "Structural and functional salivary disorders in type 2 diabetic patients," *Med Oral Patol Oral Cir Bucal*, vol. 11, pp. 309-14, 2006.

- [17] K. Ivanovski, V. Naumovski, M. Kostadinova, S. Pesevska, K. Drijanska, and V. Filipce, "Xerostomia and Salivary Levels of Glucose and Urea in Patients with Diabetes," *Contrib. Sec. Biol. Med. Sci.*, MASA, vol. 33, pp. 219-229, 2012.
- [18] W. H. Organization, "Sugars and Dental Caries," [Online]. Available: http://www.who.int/oral_health/publications/sugars-dental-carries-keyfacts/en/. Accessed at 21st january, 2018.
- [19] M. So, Y. A. Ellenikiotis, H. M. Husby, C. L. Paz, B. Seymour, and K. Sokal-Gutierrez, "Early childhood dental caries, mouth pain, and malnutrition in the ecuadorian amazon region," *Int. J. Environ. Res. Public Health*, vol. 14, no. 5, 2017.
- [20] M. R. T. C. Andrade *et al.*, "Role of saliva in the caries experience and calculus formation of young patients undergoing hemodialysis," *Clin. Oral Investig.*, vol. 19, no. 8, pp. 1973-1980, 2015.
- [21] A. Amano, Y. Yoshida, T. Oho, and T. Koga, "Monitoring ammonia to assess halitosis," *Oral Surg. Oral Med. Oral Pathol. Oral Radiol. Endod.*, vol. 94, no. 6, pp. 692-696, 2002.
- [22] Y. Zilberman and S. R. Sonkusale, "Microfluidic optoelectronic sensor for salivary diagnostics of stomach cancer," *Biosens. Bioelectron.*, vol. 67, pp. 465-471, 2015.
- [23] A. M. Giovannozzi, F. Pennechi, P. Muller, P. B. Tivola, S. Roncari, and A. M. Rossi, "An infrared spectroscopy method to detect ammonia in gastric juice," *Anal. Bioanal. Chem.*, vol. 407, no. 28, pp. 8423-8431, 2015.
- [24] E. M. L. Cardoso, A. L. Arregger, O. R. Tumilasci, A. Elbert, and L. N. Contreras, "Assessment of salivary urea as a less invasive alternative to serum determinations," *Scand. J. Clin. Lab. Invest.*, vol. 69, no. 3, pp. 330-334, 2009.
- [25] A. C. Society, "Saliva Samples Offer Pptential Alternative To Blood Testing," *Science Daily*, 2004. [Online]. Available: www.sciencedaily.com/releases/2004/10/041006083824.htm. Accessed at 20th november, 2017.
- [26] B. Timmer, W. Olthuis, and A. Van Den Berg, "Ammonia sensors and their applications - A review," *Sensors Actuators, B Chem.*, vol. 107, no. 2, pp. 666-677, 2005.
- [27] M. Gafare, J. O. Dennis, and M. H. Md Khir, "Detection of Ammonia in Exhaled Breath for Clinical Diagnosis- A Review.," *AIP Conf. Proc.*, vol. 1621, pp. 303-309, 2014.
- [28] L. O. C. Šraj, M. I. G. S. Almeida, S. E. Swearer, S. D. Kolev, and I. D. McKelvie, "Analytical challenges and advantages of using flow-based methodologies for ammonia determination in estuarine and marine waters," *TrAC - Trends Anal. Chem.*, vol. 59, pp. 83-92, 2014.
- [29] V. Cerdà *et al.*, "Flow techniques in water analysis," *Talanta*, vol. 50, pp. 695-705, 1999.
- [30] R. A. Segundo, R. B. R. Mesquita, M. T. S. O. B. Ferreira, C. F. C. P. Teixeira, A. A. Bordalo, and A. O. S. S. Rangel, "Development of a sequential injection gas diffusion system for the determination of ammonium in transational and coastal waters," *Anal. Methods*, vol. 3, pp. 2049-2055, 2011.
- [31] R. B. R. Mesquita and A. O. S. S. Rangel, "Gas diffusion sequential injection system for the spectrophotometric determination of free chlorine with o-dianisidine," *Talanta*, vol. 68, no. 2, pp. 268-273, 2005.
- [32] E. S. Kolesar and R. R. Reston, "Silicon-micromachined gas chromatography system used to separate and detect ammonia and nitrogen dioxide. II. Evaluation, analysis, and theoretical modeling of the gas chromatography system," *Microelectromechanical Syst. J.*, vol. 3, no. 4, pp. 147-154, 1994.
- [33] T. Mathew, P. Pownraj, S. Abdulla, and B. Pullithadathil, "Technologies for Clinical Diagnosis Using Expired Human Breath Analysis," *Diagnostics*, vol. 5, no. 1, pp. 27-60, 2015.
- [34] A. L. Lubrano, B. Andrews, M. Hammond, G. E. Collins, and S. Rose-Pehrsson, "Analysis of ammonium nitrate headspace by on-fiber solid phase microextraction derivatization with gas chromatography mass spectrometry," *J. Chromatogr. A*, vol. 1429, pp. 8-12, 2016.
- [35] A. D. Wilson and M. Baietto, "Applications and Advances in Eelectronic-Nose technologies," *Sensors*, vol. 11, no. 1, pp. 1105-1176, 2011.
- [36] S. W. Chiu and K. T. Tang, "Towards a chemiresistive sensor-integrated electronic nose: A review," *Sensors (Switzerland)*, vol. 13, no. 10, pp. 14214-14247, 2013.

- [37] T. Geerthy, "A Novel Approach To Monitor Ammonia In Exhaled Breath," in *IEE ICCSP*, 2015, pp. 555-558.
- [38] T. Seesaard, P. Lorwongtragool, and T. Kerdcharoen, "Wearable Electronic Nose Based on Embroidered Amine Sensors on the Fabric Substrates," in *the International Conference on Electrical Engineering/Electronics, Computer, Telecommunications and Information Technology, ECTI-CON 2012*, 2012, pp. 3-6.
- [39] L. Rossi, "Transistores Orgânicos de Efeito de Campo em Arquitetura Vertical," Dissertação de Mestrado, Setor de Ciências Exactas, Universidade Federal do Paraná, Curitiba, 2012.
- [40] A. Klug *et al.*, "Organic field-effect transistor based sensors with sensitive gate dielectrics used for low-concentration ammonia detection," *Org. Electron. physics, Mater. Appl.*, vol. 14, no. 2, pp. 500-504, 2013.
- [41] J. Yu, X. Yu, L. Zhang, and H. Zeng, "Ammonia gas sensor based on pentacene organic field-effect transistor," *Sensors Actuators, B Chem.*, vol. 173, pp. 133-138, 2012.
- [42] F. X. Werkmeister, T. Koide, and B. A. Nickel, "Ammonia sensing for enzymatic urea detection using organic field effect transistors and a semipermeable membrane," *J. Mater. Chem. B*, vol. 4, no. 1, pp. 162-168, 2016.
- [43] L. Feng *et al.*, "Unencapsulated Air-stable Organic Field Effect Transistor by All Solution Processes for Low Power Vapor Sensing," *Sci. Rep.*, vol. 6, no. October 2015, pp. 1-9, 2016.
- [44] A. Inaba, K. Yoo, Y. Takei, K. Matsumoto, and I. Shimoyama, "Ammonia gas sensing using a graphene field-effect transistor gated by ionic liquid," *Sensors Actuators, B Chem.*, vol. 195, pp. 15-21, 2014.
- [45] W. Huang, J. Yu, X. Yu, and W. Shi, "Polymer dielectric layer functionality in organic field-effect transistor based ammonia gas sensor," *Org. Electron. physics, Mater. Appl.*, vol. 14, no. 12, pp. 3453-3459, 2013.
- [46] R. S. Andre *et al.*, "Hybrid layer-by-layer (LbL) films of polyaniline, graphene oxide and zinc oxide to detect ammonia," *Sensors Actuators, B Chem.*, vol. 238, pp. 795-801, 2017.
- [47] M. C. Santos, A. G. C. Bianchi, D. M. Ushizima, F. J. Pavinatto, and R. F. Bianchi, "Ammonia gas sensor based on the frequency-dependent impedance characteristics of ultrathin polyaniline films," *Sensors Actuators, A Phys.*, vol. 253, pp. 156-164, 2017.
- [48] J. T. W. Yeow and Y. Wang, "A review of carbon nanotubes-based gas sensors," *J. Sensors*, 2009.
- [49] R. Tang, Y. Shi, Z. Hou, and L. Wei, "Carbon nanotube-based chemiresistive sensors," *Sensors (Switzerland)*, vol. 17, no. 4, 2017.
- [50] N. Ma, "Characterization of carbon nanotubes based resistive and capacitive gas sensors," Ph.D. dissertation, Dept. Electrical and Computer Engineering, University of Kentucky, Lexington, 2007.
- [51] S. Durgamahanty, "Fabrication of MWCNT based gas sensor using site-selective growth of nanotubes on gold patterned silicon oxide substrate," Masters dissertation, Dept. Electrical Engineering, University of Kentucky, Lexington, 2011.
- [52] J. W. Han, B. Kim, J. Li, and M. Meyyappan, "A carbon nanotube based ammonia sensor on cotton textile," *Appl. Phys. Lett.*, vol. 102, no. 19, pp. 2-6, 2013.
- [53] M. Penza *et al.*, "Pt- and Pd-nanoclusters functionalized carbon nanotubes networked films for sub-ppm gas sensors," *Sensors Actuators, B Chem.*, vol. 135, no. 1, pp. 289-297, 2008.
- [54] S. Chopra, A. Pham, J. Gaillard, A. Parker, and A. M. Rao, "Carbon-nanotube-based resonant-circuit sensor for ammonia," *Appl. Phys. Lett.*, vol. 80, no. 24, pp. 4632-4634, 2002.
- [55] M. Sánchez and M. Rincón, "Ammonia Sensor Based on Composites of Carbon Nanotubes and Titanium Dioxide," in *Carbon Nanotubes - Growth and Applications*, 2011.
- [56] E. S. Snow, F. K. Perkins, E. J. Houser, B. S. C., and T. L. Reinecke, "Chemical Detection with a Single-Walled Carbon Nanotube Capacitor," *Science*, vol. 307, no. 2005, pp. 1942-1945, 2005.
- [57] P. Bondavalli, P. Legagneux, and D. Pribat, "Carbon nanotubes based transistors as gas sensors: State of the art and critical review," *Sensors Actuators, B Chem.*, vol. 140, no. 1, pp. 304-318, 2009.

- [58] J. Kong *et al.*, "Nanotube Molecular Wires as Chemical Sensors," *Science* (80-.), vol. 287, no. January, pp. 622-625, 2000.
- [59] Lucite International, "Perspex Design Guide." Lancashire, United Kingdom.
- [60] M. Afonso, J. Morgado, and L. Alcácer, "Inkjet printed organic electrochemical transistors with highly conducting polymer electrolytes," *J. Appl. Phys.*, vol. 120, no. 16, 2016.
- [61] K. Chabowski, T. Piasecki, A. Dzierka, and K. Nitsch, "Simple wide frequency range impedance meter based on AD5933 integrated circuit," *Metrol. Meas. Syst.*, vol. XXII, no. 1, pp. 13-24, 2015.
- [62] Analog Devices, "AD5933 evaluation board datasheet," 2013. [Online]. Available: http://www.analog.com/UploadedFiles/Associated_Docs/%0A537700023EVAL_AD5933EB.pdf.
- [63] K. R. Aroom, M. T. Harting, C. S. Cox, R. S. Radharkrishnan, C. Smith, and B. S. Gill, "Bioimpedance Analysis: A Guide to Simple Design and Implementation," *J. Surg. Res.*, vol. 153, no. 1, pp. 23-30, 2009.
- [64] F. Seoane, J. Ferreira, J. J. Sánchez, and R. Bragós, "An analog front-end enables electrical impedance spectroscopy system on-chip for biomedical applications," *Physiol. Meas.*, vol. 29, no. 6, pp. S267-S278, 2008.
- [65] G. R. Batista, C. R. G. Torres, B. Sener, T. Attin, and A. Wiegand, "Artificial saliva formulations versus human saliva pretreatment in dental erosion experiments," *Caries Res.*, vol. 50, no. 1, pp. 78-86, 2016.
- [66] G. J. Brady, K. R. Jenkins, and M. S. Arnold, "Channel length scaling behavior in transistors based on individual versus dense arrays of carbon nanotubes," *J. Appl. Phys.*, vol. 122, no. 12, 2017.
- [67] L. Q. Nguyen, P. Q. Phan, H. N. Duong, C. D. Nguyen, and L. H. Nguyen, "Enhancement of NH₃ Gas Sensitivity at Room Temperature by Carbon Nanotube-Based Sensor Coated with Co Nanoparticles," *Sensors*, no. 2, pp. 1754-1762, 2013.
- [68] K. Dong, J. Choi, Y. D. Lee, B. H. Kang, Y. Yu, and H. H. Choi, "Detection of a CO and NH₃ gas mixture using carboxylic acid-functionalized single-walled carbon nanotubes," *Nanoscale Res. Lett.*, pp. 8-13, 2013.
- [69] S. G. Bachhav and D. R. Patil, "Preparation and Characterization of Multiwalled Carbon Nanotubes-Polythiophene Nanocomposites and its Gas Sensitivity Study at Room Temperature," *J Nanostruct*, vol. 7, no. 4, pp. 247-257, 2017.
- [70] P. Majzlíková *et al.*, "Sensing Properties of Multiwalled Carbon Nanotubes Grown in MW Plasma Torch: Electronic and Electrochemical Behavior, Gas Sensing, Field Emission, IR Absorption," *Sensors*, vol. 15, pp. 2644-2661, 2015.
- [71] Z. Wang, Z. Chen, J. Zhang, N. Tang, and J. Cai, "Fabrication of sensor based on MWCNT for NO₂ and NH₃ detection," in *13th IEE International Conference on Nanotechnology*, 2013, vol. 2700, no. 2, pp. 686-689.
- [72] J. R. Huizenga, A. Tangerman, and C. H. Gips, "Determination of Ammonia in Biological-Fluids," *Ann. Clin. Biochem.*, vol. 31, pp. 529-543, 1994.
- [73] J. R. H. A. Vissink and E. J. K. C. H. Gips, "Helicobacter pylori and ammonia concentrations of whole , parotid and submandibular / sublingual saliva," *Clin Oral Invest*, pp. 84-87, 1999.
- [74] Y. Chen, F. Meng, M. Li, and J. Liu, "Novel capacitive sensor : Fabrication from carbon nanotube arrays and sensing property characterization," *Sensors Actuators B Chem.*, vol. 140, pp. 396-401, 2009.
- [75] B. K. Precision, "How to Use an LCR Meter." [Online]. Available: http://www.techni-tool.com/site/ARTICLE_LIBRARY/BK%20Precision%20-%20How%20to%20Use%20an%20LCR%20Meter.pdf. Accessed at 30th july, 2018.
- [76] J. Suehiro, G. Zhou, and M. Hara, "Fabrication of a carbon nanotube-based gas sensor using dielectrophoresis and its application for ammonia detection by impedance spectroscopy," *J. Physucs D Appl. Phys.*, vol. 36, no. 03, pp. 109-114, 2003.
- [77] J. Han, B. Kim, J. Li, and M. Meyyappan, "Carbon Nanotube Based Humidity Sensor on Cellulose Paper," *J. Phys. Chem. C*, vol. 116, pp. 22094-22097, 2012.
- [78] J. T. H. Tsai, C. Lu, and J. G. Li, "Fabrication of humidity sensors by multi-walled carbon nanotubes," *J. Exp. Nanosci.*, vol. 5, no. 4, pp. 302-309, 2010.

- [79] B. J. Nordbotten, "Bioimpedance Measurements Using the Integrated Circuit," Masters dissertation, Dept. Physics Electronics and Computer Science, University of Oslo, 2008.
- [80] O. K. Varghese, P. D. Kichambre, D. Gong, K. G. Ong, E. C. Dickey, and C. A. Grimes, "Gas sensing characteristics of multi-wall carbon nanotubes," *Sensors Actuators B Chem.*, vol. 81, pp. 32-41, 2001.
- [81] A. E. Soini *et al.*, "Analysis of Volatile Organic Compounds in Human Saliva by a Static Sorptive Extraction Method and Gas Chromatography-Mass Spectrometry," *J Chem Ecol*, vol. 36, pp. 1035-1042, 2010.